An experimental stellar simulator to study prebiotic chemical reactions under various planetary atmospheres

Tze King Lam

Introduction

We explore the origins of life as a product of prebiotic chemistry subjected to geochemical and astrophysical conditions present during the Archean. By developing experimental apparatus capable of simulating such conditions, we seek to characterise and constrain the timescales over which potential prebiotic chemical reactions would occur on the surface of early Earth.

In this report, we outline the design and developmental work conducted to extend the capabilities of an earlier version of StarLab [1], an experimental stellar simulator set up to simulate the UV light of the faint young Sun on the surface of early Earth.

The top-level goals for the new StarLab are as follows:

(1) Simultaneous broadband illumination (UV, VIS, IR) focused onto either a 10-mm-sided quartz cuvette sample holder or 50-mm-diameter watch glass, with provisions to minimise photon loss from source to sample.

(2) Preparation of simulated planetary atmospheres:
   - (a) Present objective is to simulate an inert gas environment (Ar, N_2, CO_2) mixed with varying amounts of O_2 (0 ppm to 100%).
   - (b) The design will incorporate considerations for the use of reactive gases in the future, such as SO_2, H_2S, CH_4.
   - (c) The environmental chamber, where chemical test samples will be located, should be able to accommodate pressure conditions ranging from 0.5 to 2.0 bar absolute. Purging pressure will be no more than 2 bar absolute. There will be no need for vacuum conditions.
   - (d) Atmospheric temperature modulated near room temperature: 20-30°C

(3) Automated / pre-programmed control of atmospheric pressure and oxygen levels over the course of the experiment, defined as up to several days.

(4) Temperature control for sample over the course of the experiment.

(5) Continuous detection and monitoring of spectral irradiance received by sample and changes after passing through sample.

Design Approach

While the optics subsystem proved to be the most tricky engineering challenge with a myriad of constraints, a number of key parameters required for its design depends on chamber specifications. Therefore, we elected to start with the chamber design, before moving on to the optics subsystem. Mechanical design and system integration followed, before finishing off with a suite of recommendations on the fluidics, as well as control and feedback electronics. The general structure of this document follows roughly the aforementioned design sequence, though we shall introduce the fluidics and electronics design rather early on since they are simpler.

As much as possible, we took into consideration existing equipment and proven designs inherited from StarLab V1. Moreover, for reliability, reputable brands were used for the various components.

A simple python program, StarLab Optics [2], was developed to aid first order optical design work. The program uses simple geometry and basic principles of refraction and reflection to quickly generate a baseline model that can predict how a finite beam of light behaves when manipulated using simple optical devices like lens, windows and mirrors etc, in an ideal world. An optimization module from Scipy is used to solve for the positions of certain pieces of optics while targeting a particular desired parameter.

The results have yet to be confirmed with more sophisticated simulation software such as Zeemax Optics, which is highly recommended. Nevertheless, the practicalities of setting up an optics experiment will inadvertently introduce a number of unpredictable and unmodellable inaccuracies. While a highly sophisticated model might produce predictions with greater accuracy and precision, it is still pertinent to leave ample room for fine-tuning onsite, rather than designing a fixed experimental setup.

The code repository is available on Github:

- SSH: git@github.com:KingLam26/StarLab.git
- HTTPS: https://github.com/KingLam26/StarLab.git

```
.
└── StarLab/
    ├── beamClass.py     # support module, allows for the definition and
    │                      manipulation of light beams
    ├── functions.py     # support module, handles line and circle
    │                      geometry
    ├── main.py          # LSDS
    ├── main4.py         # Horiba
    └── main5.py         # EQ-77
```

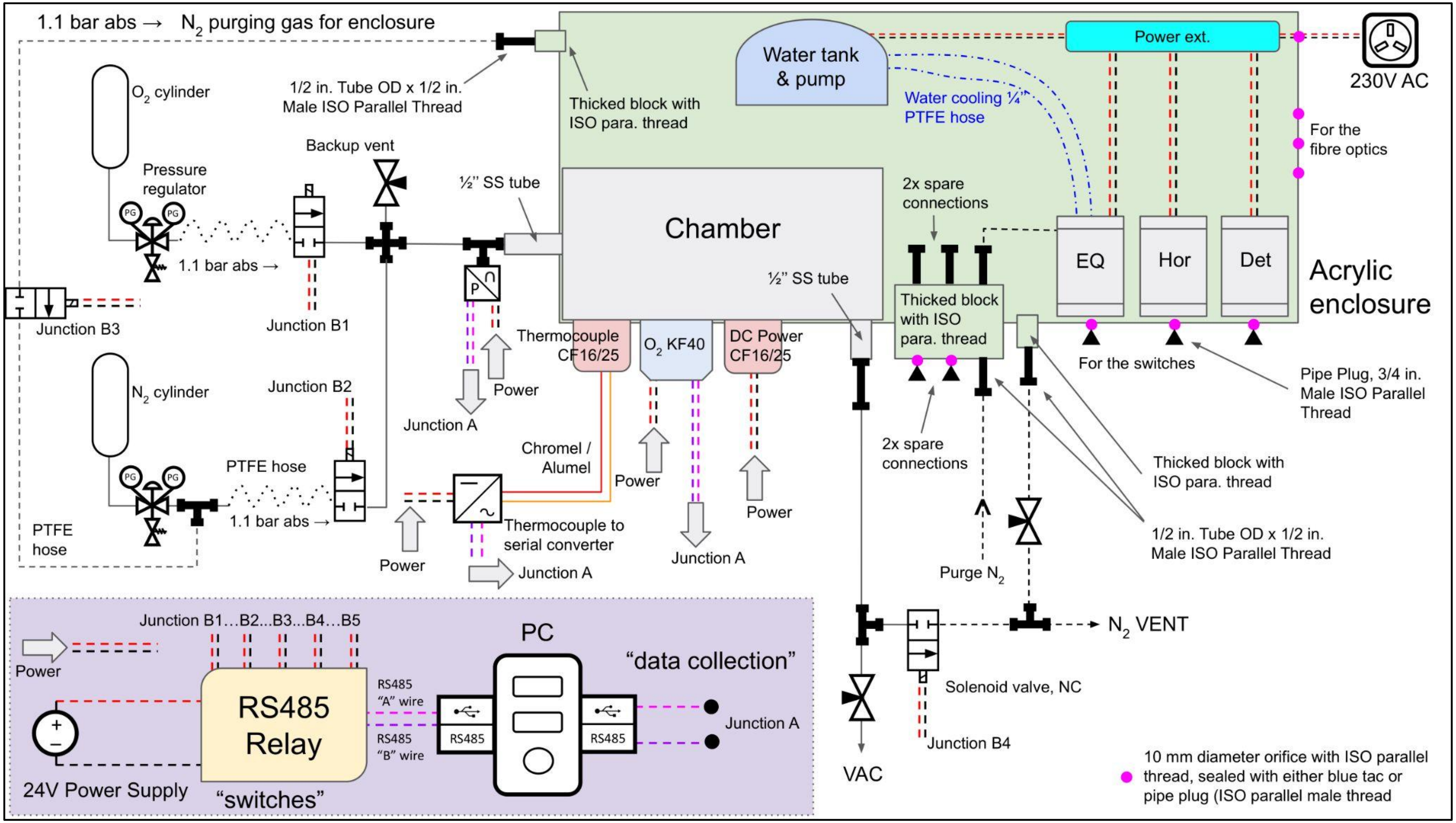

Figure 1: Electronics and fluidics schematic of the overall design for Star Lab V2. In this approach, we propose the use of a secondary enclosure (apart from the primary chamber where the sample will be located) to create a nitrogen rich atmosphere to mitigate the generation of ozone due to the interaction between the UV light source and oxygen in the air. The complexity associated with the secondary enclosure is taken into account, and other options involving beam tubes with active nitrogen purging are considered. Nonetheless, this schematic serves well to introduce the interfaces between the subsystems and the general design philosophy.

Administrative Matters

All relevant documents are saved in a Google Drive folder [3], which has the following file structure:

```
.
└── Star Lab/
    ├── Catalogues and Spec Sheet/
    │   ├── Flanges & Feedthroughs
    │   ├── MODBUS+RS485
    │   ├── Optics
    │   ├── Sensors
    │   ├── Thermoelectric coolers
    │   └── Valves and fittings
    ├── Design Record/
    │   ├── Master Design
    │   ├── Update 1 - 07 JUL 22
    │   ├── Update 2.1 - 15 AUG 22
    │   └── ...
    ├── Part List
    └── Star Lab Report
```

The present document titled "Star Lab Report" documents the latest design as of February 2023, and supersedes previously produced materials in the "Design Record" folder. While key specifications of the various components used will be included in this report, we strongly encourage that the reader refer to the catalogues and specification sheets provided by the manufacturer as the final authority, located in the folder "Catalogues and Spec Sheet".

CAD drawings are saved online in an Onshape folder [4], which has the following file structure:

```
.
└── King Lam/
    ├── StarLabOptics/
    │   ├── DWG-LightPaths-All
    │   ├── ASS-MirrorMount
    │   ├── ASS-LensMount-v1
    │   └── ...
    ├── StarLabFluidics
    ├── Test/
    │   ├── Test-Optics/
    │   └── Test-Fluidics/
    └── StarLabChamberMaster/
        ├── ASS-Full
        ├── Lewvac-HN16CF
        ├── LEWVAC-FHP1-C4-16CF.step
        └── ...
```

Onshape [5] is an online CAD program, which offers a free educational licence. By signing up with a cambridge email, one should be able to start drawing within minutes. Regeneration performance tested on an average Macbook Pro yielded decent results, even up to the full complexity of the entire StarLab experimental setup (Figure 2).

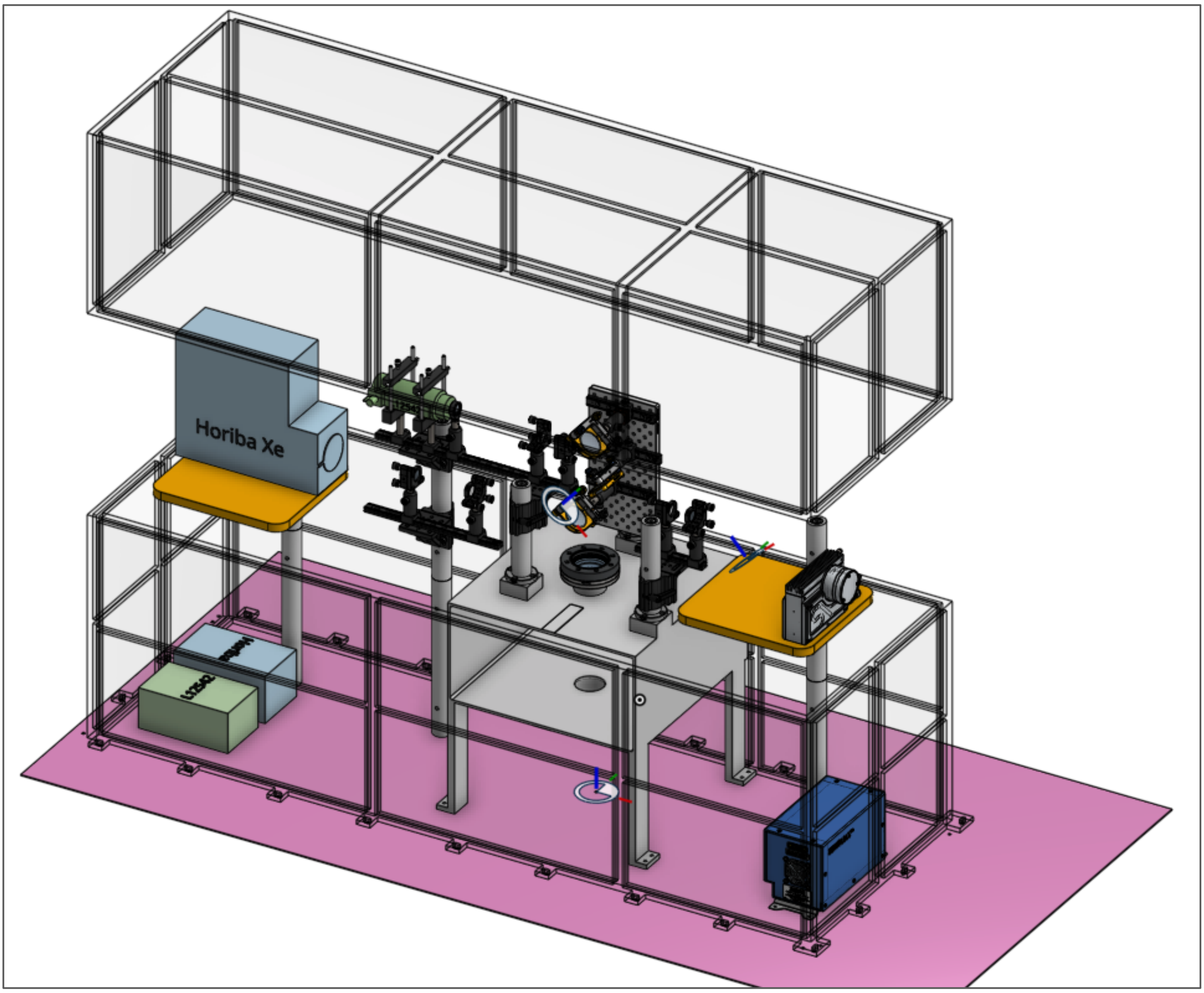

Figure 2: CAD modelling of a potential experimental setup for Star Lab v2 involving the enclosure design, as rendered on OnShape. Machine specifications: Browser - Chrome, Version - 104.0.0.0, Platform - MacOS, GL vendor - Google Inc. (Intel Inc.), GL renderer - ANGLE (Intel Inc., Intel® Iris™ Plus Graphics 640, OpenGL 4.1).

Key features of Onshape:

- Similar drawing and design philosophy as SolidWorks
- Able to import and export STEP files, therefore compatible with AutoCAD
- Ability to create assemblies of multiple part files or even sub-assemblies for overview - critical when designing larger systems such as StarLab
- Google Drive concept for file sharing

Finally, a Part List Google sheet was also created, containing detailed information on individual components, including the supplier, part number, name of specification sheet, and cost.

Subsystem: CHAMBER

General Requirements

ENVIRONMENT

- Atmospheric composition: Ar, N_2, CO_2, O_2
    - Oxygen levels should be adjustable between 0 ppm and 100%.
    - Future: reactive gases (SO_2, H_2S, HCN)

- Operating pressure: **0.5 to 1.2 bar absolute**
    - Vacuum conditions are not needed and generally untenable due to excessive evaporation rates of the aqueous samples. However, to accommodate and maintain a partial pressure difference of up to ca. 0.8 bar (for example, experimental runs with pure oxygenic atmosphere), we require a strong hermetic (“vacuum”) seal.
    - MEOP (1.2 bar absolute) exists because optical windows are not rated for overpressure conditions. We stress the danger of structural failure of the windows, and recommend safety pressure relief valves (more at the fluidics section).
    - Moreover, the optical properties of the windows will be modified in unpredictable ways should pressure-induced deformation occur.

- Temperature control:
    - Atmospheric: modulated near room temperature, around 25^{o}C
    - Sample:
        - Active monitoring achieved using thermocouples
        - Active control (feedback loop) enabled using Thermoelectric coolers (TEC). As an example, consider a 4cm x 4cm thermoelectric Peltier cooler [6] with a centrally located opening for light to pass through.
        - Based on calculations in “Subsystem: OPTICS”, total optical power for the three lamps should not exceed 20 W.
        - The sample is expected to be heated by the light sources, but if additional heating is required, one could consider flexible polyimide heaters.

SAMPLE HOLDER

- Cuvette Holder with Four Light Ports (cuvette need not be in the chamber) [7]
- Borosilicate watch glass: needs to be within box

DIMENSIONS

- Size: 40cm x 40cm x 35cm (height)
- Material: SS 316 (more acid resistant than SS304, though more expensive)
- Expected mass: 50 kg
- General geometry: 5-sided rectangular shell, plus lid on hinge, sealed with O-ring and groove

SENSORS

- Monitoring oxygen:
    - Full range: ppm level, up to 100% O_2
    - O_2 sensors (Cambridge Sensotec) rated for vacuum and up to 5 bar absolute
    - Power supply: 24V DC
    - Output: RS485 + display (ethernet possible too)
    - Process connection: KF40
    - Latest from Cambridge Sensotec:
        - Rated for pressures from vacuum to 5 bar absolute
        - Good with inert gases (Ar, N2), as well as CO2, CO
        - Zirconia based sensor not suitable with combustible and corrosive gases like SO2, H2S, CH4 & VOCs. An electrochemical one might work, which is also offered by the same company.
        - I am checking whether we can simply treat water vapour as another gas that will be invisible to the sensor. Answer: yes.

- Monitoring pressure:
    - Range: 0-5 bar absolute
    - Power supply: 24V DC
    - Output: RS485
    - Process connection: G1/4
    - Note: we do not expect this to be connected directly to the chamber, but in the fluidics upstream of the chamber.

- Monitoring temperature:
    - K-type thermocouple, feedthrough will have provisions for 2 thermocouples
    - Sample: attached to watch glass / cuvette

INTERFACE

- Physical access: hinge door, with O-ring seal
- Windows: located at the top and bottom of the chamber
- Fluidics:
    - Inlet and outlet for purging gas: ½'' SS tube, welded to chamber
- Feedthroughs / flanges:
    - KF40 (x2):
        - Connect to a “weak” vacuum pump to generate an atmosphere with reduced pressure.
        - Oxygen sensor (requires a KF40 blind when oxygen sensor is not used)
    - CF16 (x2):
        - Thermocouple
        - DC Power

OnShape

Before introducing the prototype design for the chamber, we digress to provide a quick overview of OnShape. The key capability of OnShape is forming assemblies, crucial in checking for interface compatibility.

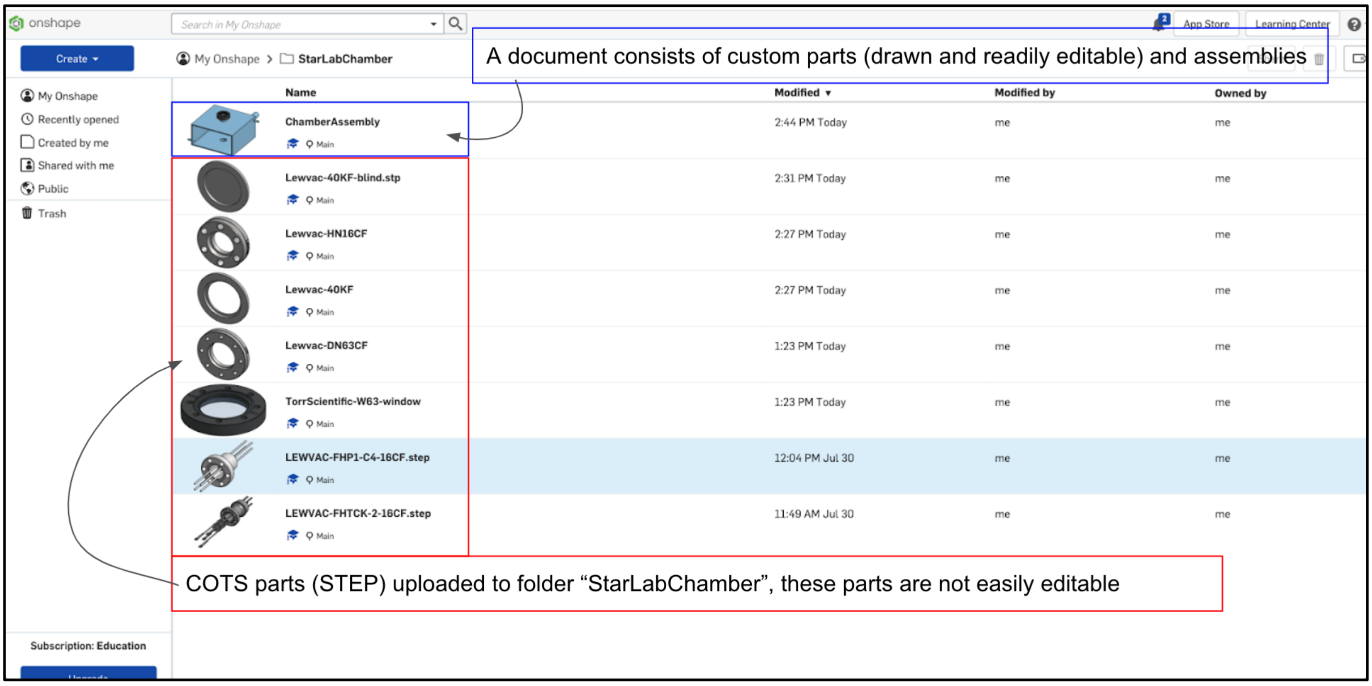

Figure 3: File storage in OnShape is similar to Google Drive. In general, standard commercial off the shelf (COTS) components come with downloadable STEP files, which are uploaded into the repository. Components that need to be designed from scratch, such as the chamber and sample holder, are created using the built-in CAD capability. In concept, all these components are known as PART files.

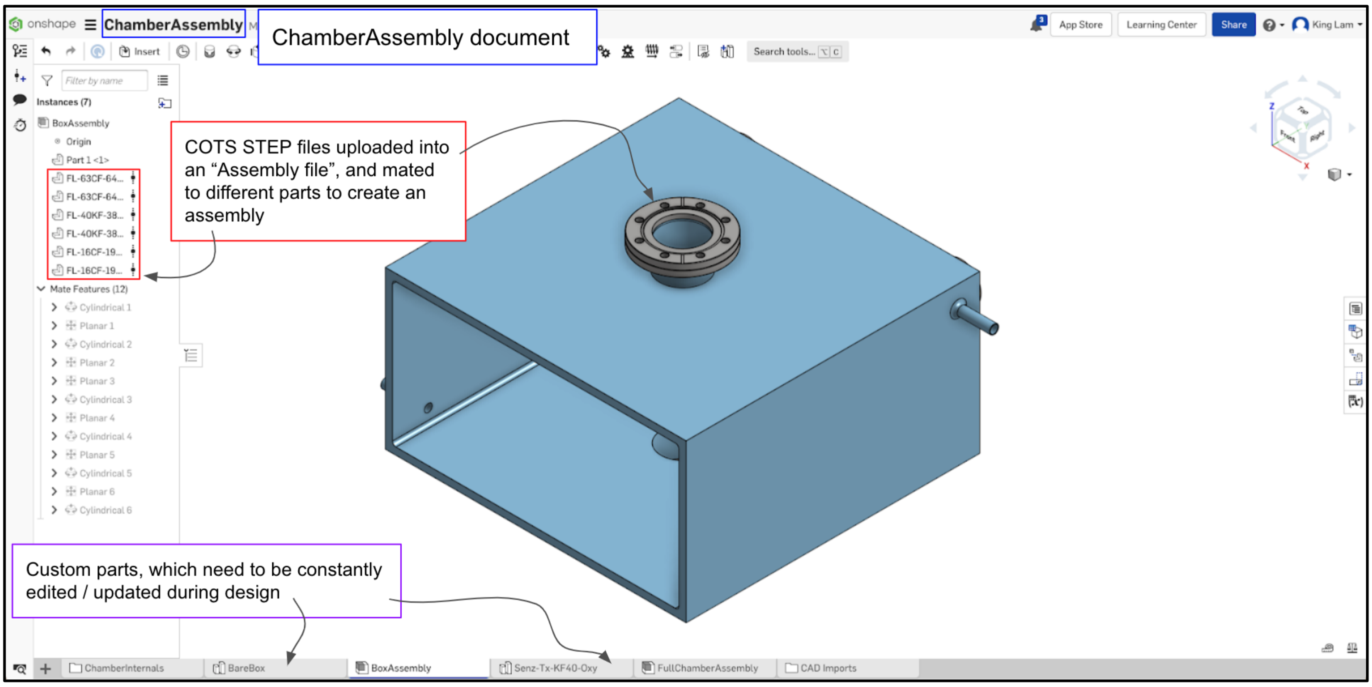

Figure 4: Various PART files can be imported into a new assembly document (ASSEMBLY file) where the mating tool allows one to adjust their spatial configurations and visualise how they can be combined together. In principle, one could form sub-assemblies (still an ASSEMBLY file by extension) that are combined together.

Chamber Design

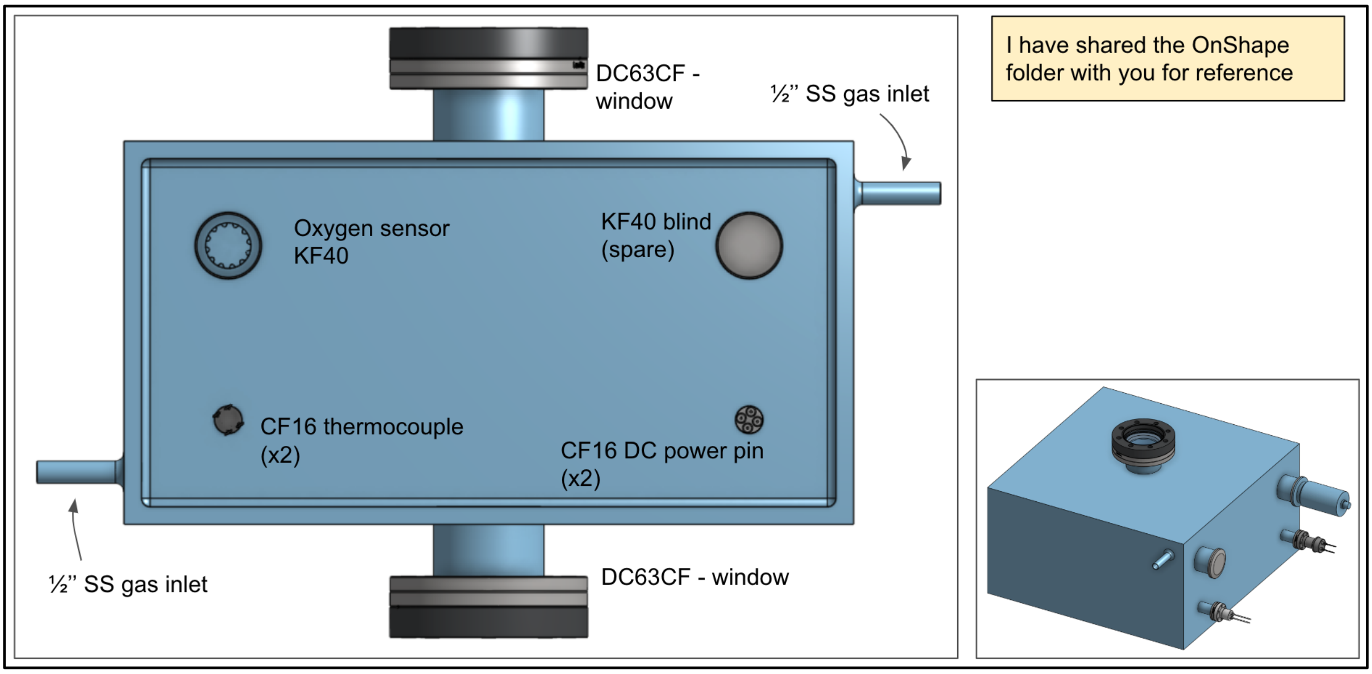

Figure 5: (left) Chamber with lid removed. A hingeless design is shown, which can be easily extended to one with a hinge without introducing spatial interference with other components. (right) Back view.

Both hinged and unhinged doors will employ an O-ring fitted into a groove as the seal, with the latter using fasteners to generate the sealing pressure. Having the windows at the top and bottom pushes the lid to the front, which creates a smaller opening area due to reduced height. In sizing the chamber height, we took into account the width of a fully stretched out human's palm, which should be just under 20 cm. Therefore, the depth of the box is designed to be around 40 cm, about twice the aforementioned width.

As of September 2022, we have received a quote from Rick Tigfusion Ltd for the full chamber. The key specifications are as follows:

- The chamber will be made of SS 304, while the door will be made of Al 5083 (to reduce door weight).
- SS wall thickness will be reduced from 10 mm to 5 mm, since vacuum conditions are not needed. Exception will be the back panel (back of chamber), where thickness will remain 10 mm to accommodate threaded fasteners needed to ensure a seal with the enclosure.
- Depending on whether we proceed with an enclosure based design (see), grooves to accommodate a rubber cord are built into the backplate of the chamber.
- Outer dimensions remain unchanged, so the internal volume of the chamber is increased without having to redesign the external interfaces.
- Together with flanges and sensors, the estimated mass of the chamber is ca. 70 kg. The design includes a hinged door with dimensions of 45 cm (L) x 50 cm (depth) x 35 cm (H).

Design requirements from the manufacturer:

> To supply a custom design welded vacuum box chamber assembly – 220mm high x 420 wide x 410 deep with 10mm thick stainless steel 304 walls. Price includes design for manufacture based on customer provided STEP file and the addition of stainless steel 304 door frame and aluminium alloy 5083 door held with Misumi hinges, lever-action door latch and double claw clamps. Door sealed with fluorocarbon (FKM) O-ring. Chamber will have feet to suit the optical table, with a clearance of 150mm minimum between the bottom flange and the table. General assembly

drawings will be submitted to the customer for approval before manufacturing starts. Total cost for the above chamber including design & producing manufacturing drawing = £7,871.45 – Please find our official quotation attached.

While we have decided not to proceed with this manufacturer since we do not need vacuum conditions, the specifications proposed along the way should guide the general design of the chamber.

Finally, we touch briefly on the pressure conditions in the chamber. At room temperature, water boils when pressure drops below 0.05 bar absolute. Immediately, we see a "vacuum" chamber is not possible, and there is no need to contract a vacuum specialty fabrication service; a standard CNC machine shop with standard welding will suffice.

We take this consideration a step further by estimating the rate of evaporation in a dry atmosphere with 1% relative humidity. This is likely the case when using dry N_2 for purging. We used the Mollier diagram for data on enthalpy of evaporation of water based on temperature, ambient pressure and absolute humidity [8], and a simple model for evaporation [9].

Here are our input parameters and results for chamber pressure of 0.5 bar absolute (worst conditions in terms of pressure), 25ºC and 1% R.H.:

Enthalpy of evaporation	26.1	kJ/kg
Humidity ratio in air (g/kg) (g H2O in kg Dry Air)	0.4	g / kg
Our puddle parameters:		
● Water surface area, at 40 mm diameter	1.26×10^{-3}	m2
● Max. sat. humidity ratio in air (kg/kg) (kg H2O in kg Dry Air)	0.019826	kg / kg
● Corresponding Water Vapor Saturation Pressure	0.0313	bar
● Velocity of air above water surface (m/s)	0	m / s
Results:		
● Evaporated water per hour (kg / h)	0.000612	kg / h
● Change in water height over 24 hours of experiment (mm)	>10	mm

Again, this is clearly untenable. Repeated calculations with other parameters show that the rate of evaporation drops to zero when RH is ~60%. Therefore, for long duration experimental runs with dry nitrogen as the purging gas, it may be worth having a beaker of water in the chamber (best equipped with a heater) to generate water vapour in the atmosphere. For more sophisticated experiments, we recommend a sensor to monitor relative humidity.

Subsystem: FLUIDICS & ELECTRONICS

These two subsystems will prove to be intricately intertwined, and so their design took place in tandem.

Atmosphere Control

Ultimately, the biggest concern we face here is leaks, which will prove to be tricky considering our goal of maintaining O_2 levels down to ~1 ppm for days.

Our strategy is two-fold. For one, we seek to reduce the number of interfaces. For instance, we eliminate the chamber-to-fluidics interface by welding a ¼'' SS tube directly to the chamber. Compression fittings and KF flanges will be used to connect different tubes, sensors and valves, and will be the default interface, as commonly employed in the aerospace industry. Purging gas (N_2) will be transferred from the gas cylinders to the chamber via flexible and acid-resistant Teflon (PTFE) tubing.

With reference to Figure 1, provisions will be made to allow for the mixing of several types of gases before injection into the chamber. For a start, we focus only on two types of gases: nitrogen and oxygen. This brings us to the second strategy, which is active monitoring and control of the oxygen level.

As an introductory example, we envision the following feedback loop for two general cases:

(1) Plummeting O_2 levels (for experimental runs with O_2 rich atmosphere) detected by the oxygen sensor leads to simultaneous activation of two solenoid valves: one guarding the pressurised O_2 line and the other for venting excess pressure from the chamber.

(2) Rising O_2 levels (due to in gassing leaks from the more O_2 rich external environment) detected by the oxygen sensor leads to simultaneous activation of two solenoid valves: one guarding the pressurised N_2 line and the other for venting excess pressure from the chamber.

Our requirements suggest the need for fast-acting control electronics capable of reading signal inputs from several sensors and sending out commands to actuate a number of valves. A Microcontroller (MCU) could do the job, but a more readily available option is a simple laptop with several USB ports. We propose the use of a common standard, RS485 to connect the network. RS485 is a standard serial communications protocol with readily available and vast documentation. Moreover, most suppliers will have this option available.

In a standard 2-wire RS485 configuration, data is encoded in binary and transmitted by rapidly alternating the voltage difference between the two wires, the so-called (A)- and (B)+. Multiple devices (in the hundreds) can be connected together on the same lines because each device can have a reprogrammable address.

In our setup, we shall handle data collection and device control separately, i.e., on two separate circuits. In the data collection circuit, we will adopt a wiring configuration very similar to Figure 6. A RS485-to-USB converter allows the entire network to be connected to a laptop, allowing one to then interact with the entire network using any program on the laptop that can decipher or issue RS485 commands. To that end, we propose the well-tested pySerial module [10] because it can be implemented using Python, which unlocks a wealth of capabilities the general-purpose programming language offers.

For example, with reference to Figure 6, to retrieve sensor data from device 2, we will code a command (using 8 bytes of data) to be sent from the computer via the USB port onto the entire network, such that all devices will receive the same command. Crucially, one of the first few bytes will encode the target device address, e.g., 0x2 for device 2. Therefore, only device 2 will act on the command, typically to perform the "sensing process", and upon retrieving a data point, the device will in turn generate a signal that is sent back onto the entire network. Typically, a certain byte in the data packet will indicate a signal sent from a "slave", so that other "slaves" ignore this command, which will only be picked up by the "master". A typical data collection loop for one device will take around 100 milliseconds. In this manner, one could code up a loop in Python to survey each device in sequence. It will only take one second to obtain data points from ten devices, a cadence that well suits our needs.

Finally, we point that two additional wires are needed for each device to provide DC power, as well as for the RS485-to-USB converter. Considering the fact that standard RS485 transceivers operate over a limited common mode voltage range that extends from –7V to 12 V, one might be wary of any electrical interference that might cause a voltage surge. Based on our experiences, this should not be a problem since our transceiving distance is rather short, just a couple of metres.

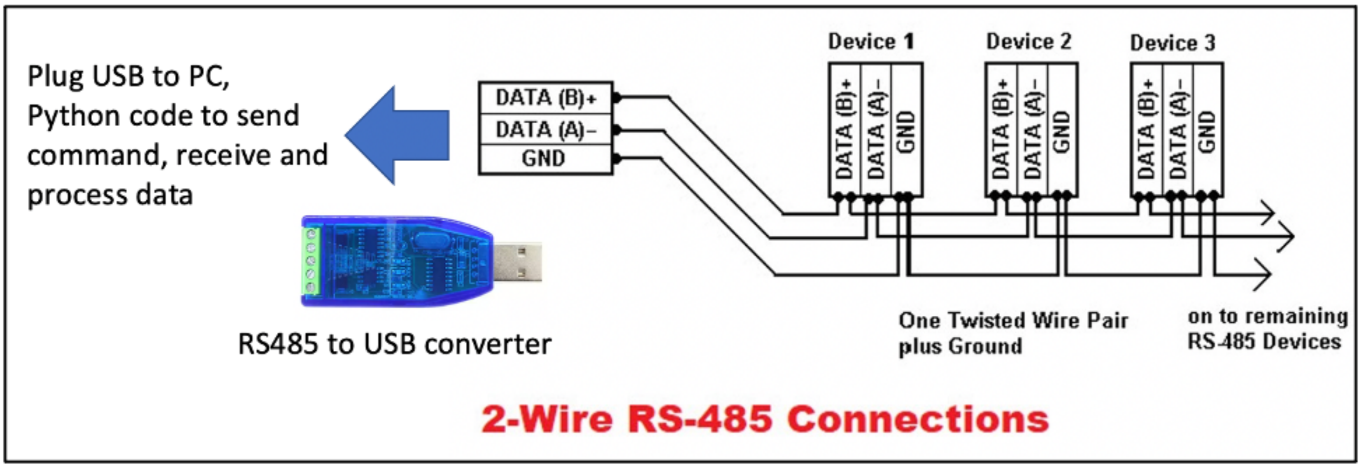

Figure 6: Standard 2-wire RS485 network, with an additional ground line (optional). The controlled devices (Device 1, 2, 3…) are often called "slaves" while the controlling CPU (typically a MCU, but in our case we elect to use a readily available laptop since we do not face spatial constraints) is called the "host" or "master". This is the configuration we will adopt for data collection from our sensors (temperature, pressure, O_2 level).

As for device command and control, we will adopt a slightly different configuration, though not at all due to the fault of the RS485 protocol. Quite simply, a normally closed solenoid valve typically requires a DC source of 24 V to open, which cannot sufficiently be delivered by the RS485 A- and B+ wires. Our solution is to employ a relay bus, which might contain a number of channels, 8 for example, with each connected to its target device, solenoid valves, TEC and heaters in our case. Again, each channel will have its own address, and the entire relay bus will be controlled using a laptop via RS485. In other words, the relay bus acts as a single device, albeit with a number of channels or switches. Activating one channel amounts to switching on the voltage to a particular device. The relay bus will contain its own MCU chip. Each of the downstream devices is therefore separately powered by each of the channels in the relay bus, which really is just a box of switches. We turn on / off a switch using RS485.

At this point, the reader is advised to re-consult Figure 1, which should make a lot more sense now.

Miscellaneous Pointers

(1) The Python program can be easily developed, though the exact parameters, e.g., time delay, actuation sequence etc. will require further consultation on the requirements of a particular experiment. Undoubtedly, a number of tests will be needed to fine tune such a system, we are rather confident on its successful implementation, since we have prior experience.

(2) A number of tools will be needed for the assembly of the fluidics, for example, metric / imperial spanners, tube cutters etc.

(3) Considering flow rate and pressures, propose using 1/2’’ as the standard outer diameter for SS and teflon tubes.

(4) We suggest using Ham-let (now known as UCT) or Swagelok for the fluidics fittings. Proposed pressure sensors, thermocouples, and fluidics part numbers are detailed in the “Part List” document.

Subsystem: OPTICS

Light Source

To cover the broadband UV-VIS-IR spectrum, three separate light sources will be used for beam generation. Their part numbers and key specifications are shown below:

(1) D2 L12542 [11]
- Spectral range: 120 - 170 nm

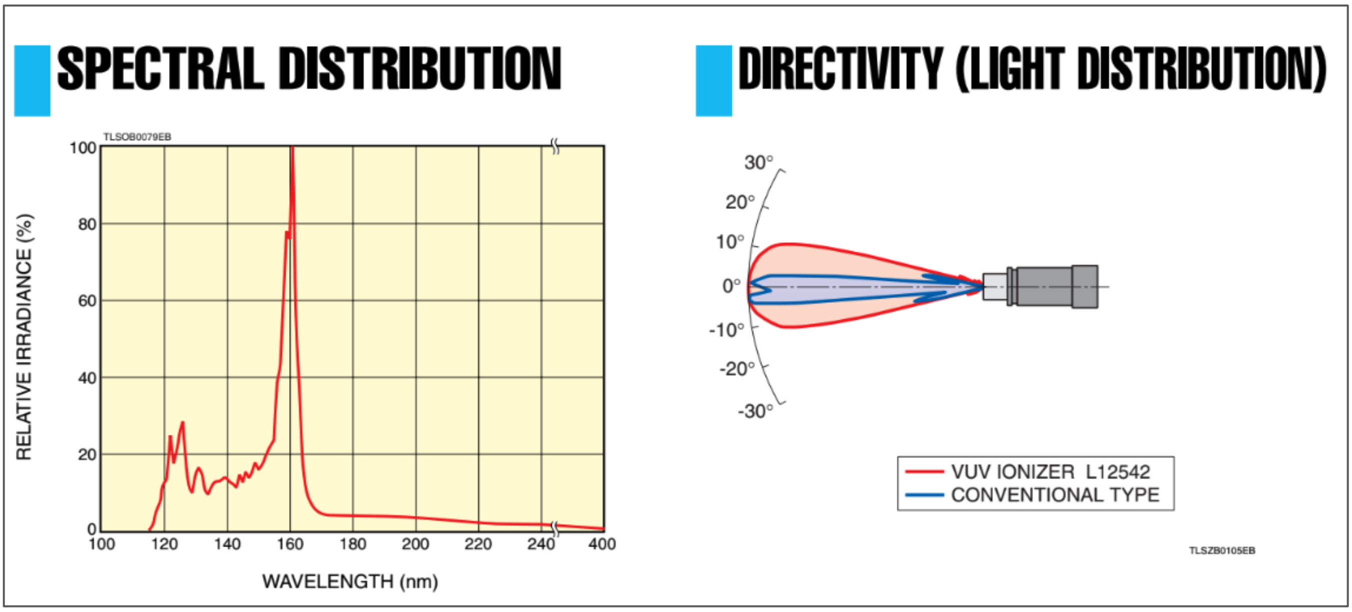

SPECIFICATIONS

●GENERAL RATINGS

Parameter	Description / Value	Unit
Spectral distribution	115 to 400	nm
Window material	MgF_2	—
Cooling method	Forced air cooling by fan	—
Operating temperature range	+10 to +40	°C
Storage temperature range	0 to +60	°C
Operating humidity range	Below 80 % (no condensation)	—
Storage humidity range	Below 85 % (no condensation)	—

●RECOMMENDED OPERATING CONDITIONS AND CHARACTERISTICS (at 25 °C)

Parameter	Description / Value	Unit
Warm-up time	25 ± 5	s
Light source guaranteed life ①	2000	h
Input voltage (AC)	100 V to 240 V (100 V/200 V auto switching), single phase 50 Hz / 60 Hz	—
Power consumption (Max.)	90	VA

①End of life is defined as the time when light output at 230 nm falls below 50 % of its initial value. Note that the light output attenuation depends greatly on the environment of the vacuum equipment.
* When replacing the light source, please specify the type No. L12565.

We estimate power output based on a reference deuterium lamp spectral irradiance data [12], in which we only considered power output from 200-400 nm. Based on the irradiance ($mWm^{-2}nm^{-1}$) at 0.5 m versus wavelength (nm) curve provided in the reference, we obtained the following data points, to which a curve was fitted.

In the table below, the dimensionless numbers have units $mWm^{-2}nm^{-1}$.

200 nm	1.0	275 nm	0.32	350 nm	0.1
225 nm	0.8	300 nm	0.21	375 nm	0.08
250 nm	0.5	325 nm	0.14	400 nm	0.065

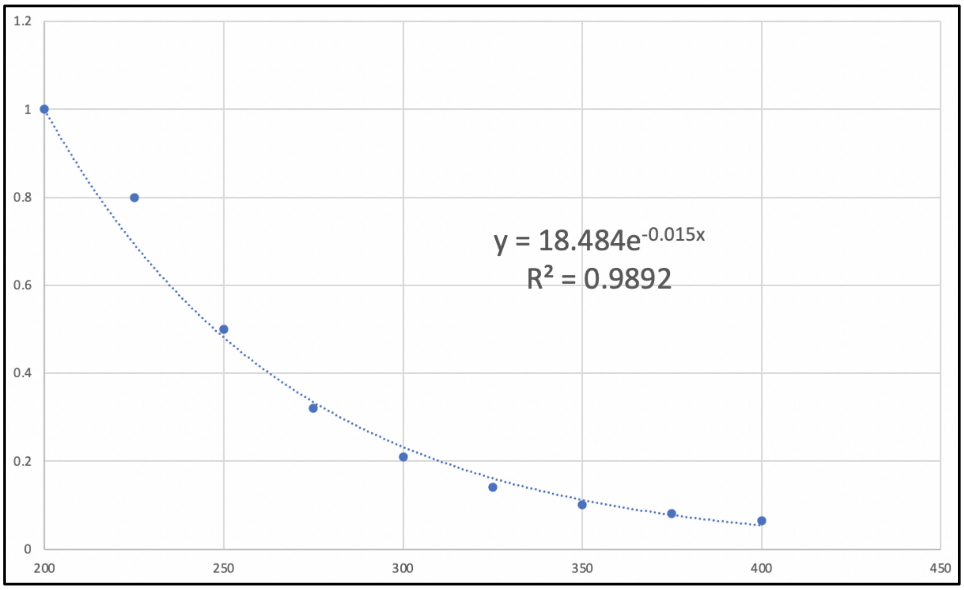

$$\int_{200}^{400} 18.484\, e^{-0.015x} dx = 3641 \text{ mWm}^{-2}$$

The aforementioned intensity corresponds to a distance of 0.5 m, so the total power collected by a hypothetical sphere of that radius is given by

$$P = 3.641 \cdot 4\pi \cdot 0.5^2 = 11 \text{ W}$$

We shall take this as the upper bound power output (**please confirm**), which appears reasonable considering the maximum power consumption of the lamp is 90 W.

(2) LDLS EQ77 [13]

- Spectral range: 200 - 2500 nm

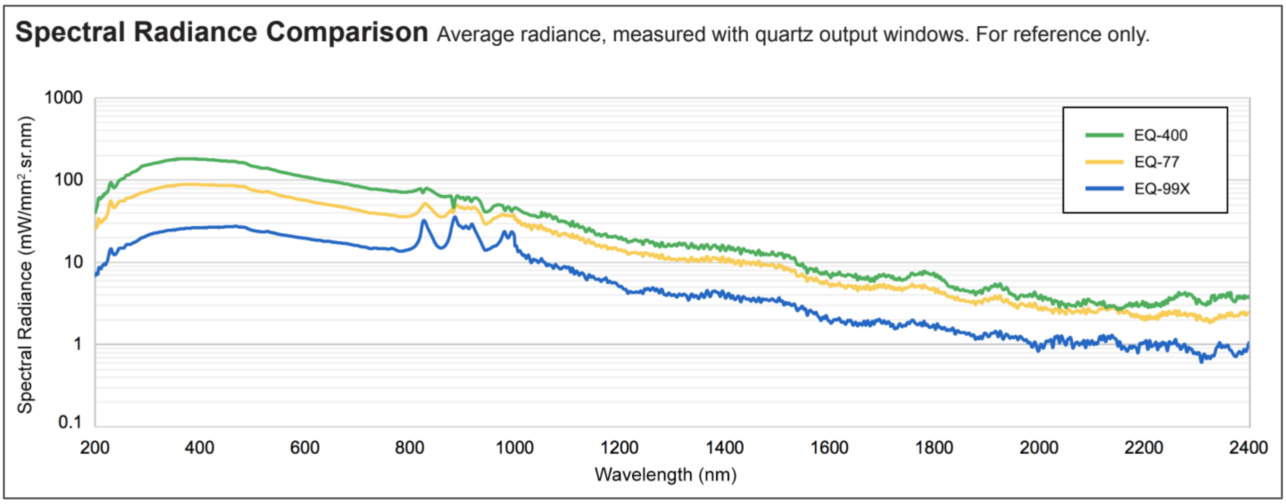

Typical Performance

Spectral Radiance at 500 nm	75 mW/mm^2.sr.nm
Broadband Optical Power*	2.75 W

*Measured with thermopile

Power output for this lamp shall be taken as **3 W**.

(3) Horiba PowerArc [14]

- Spectral range: 200 - 1000 nm (IR water filter is expected to truncate the IR range)

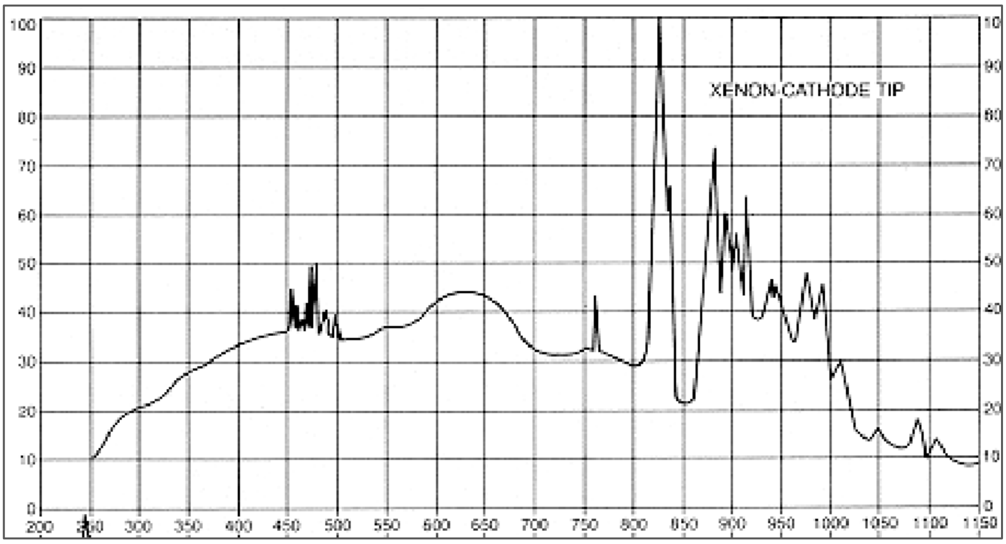

Xenon Arc Lamp Intensity Chart

Wavelength	% output	Wavelength	% output	Wavelength	% output	Wavelength	% output
250-300	2.489	750-800	4.682	1250-1300	0.896	1750-1800	0.345
300-350	3.540	800-850	8.914	1300-1350	0.705	1800-1850	0.306
350-400	4.577	850-900	6.284	1350-1400	0.931	1850-1900	0.306
400-450	5.245	900-950	6.788	1400-1450	0.919	1900-1950	0.306
450-500	5.626	950-1000	5.848	1450-1500	1.118	1950-2000	0.268
500-550	5.214	1000-1050	2.871	1500-1550	0.701	2000-2050	0.345
550-600	5.729	1050-1100	1.953	1550-1600	0.513	2050-2100	0.230
600-650	6.472	1100-1150	1.402	1600-1650	0.515	2100-2150	0.230
650-700	5.649	1150-1200	1.593	1650-1700	0.552	2150-2200	0.230
700-750	4.862	1200-1250	0.846	1700-1750	0.428	TOTAL	100.000

Therefore, the total power output is expected to be given by 7.5 W (full spectrum) x 85% = ca. **6 W**.

Without considering power loss due to beam propagation through the atmosphere and optical components, we are certain total heating experienced by the aqueous sample due to the light sources will not exceed **20 W**.

~ ~ ~

Cursory comment: it might be useful to think about UV LEDs, ask Corinna Kufner what she uses.

Manipulating Incident Beam

We rule out the possibility of coupling fibre optics from the light source to the chamber, due to insufficient beam intensity provided by a single fibre optic. On the other hand, it makes sense to use fibre optics to direct the transmitted light to a spectrometer, via a collimating lens to fibre.

Since our target sample is located in a borosilicate glass watch, it is clear the transmitted light will have to emerge from the bottom of the chamber, thereby ruling out a sideways incident and transmission setup. Therefore, our design involves directing the incident light beams into the chamber from its top. To that end, two options are available.

In the first instance, the three incident broadband beams (UV, VIS, IR) are to be separated and focused onto the sample, each offset at an angle. This will require the use of a series of lenses to first collimate the beam from the light source, and then focus it onto the sample. Thereafter, provisions will be made to allow the collimating lens to fibre at the bottom of the chamber be angled accordingly for alignment with the corresponding beam of interest. In any case, each incident beam will most likely be scattered and refracted to some extent by the sample and watch glass, so some flexibility must be injected into the positioning of the receiving lens.

Alternatively, we could attempt to combine all three collimated beams using several beam splitters before directing the combined beam into the sample at an orthogonal angle to the window. Properly collimated beams with sufficiently small beam waist will negate the need for any focusing lens.

The broadband nature of our light requirement rules out the second option, as the beam splitters have limited wavelength range; for example, it would be impossible to combine UV and IR light without significant attenuation in either ranges. Therefore, we proceed with the first option.

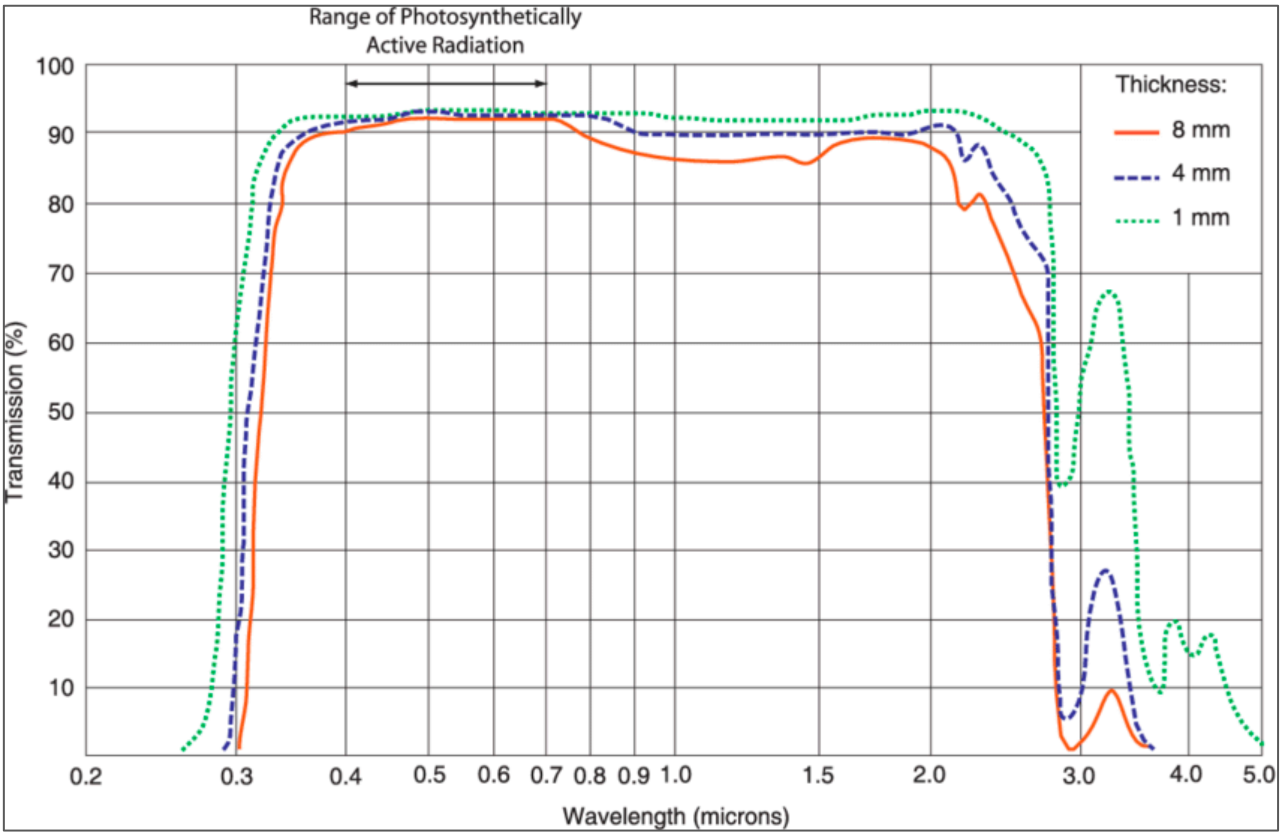

Figure 7: Transmission properties of borosilicate, as a function of wavelength. In particular, note the lack of transparency below 300 nm.

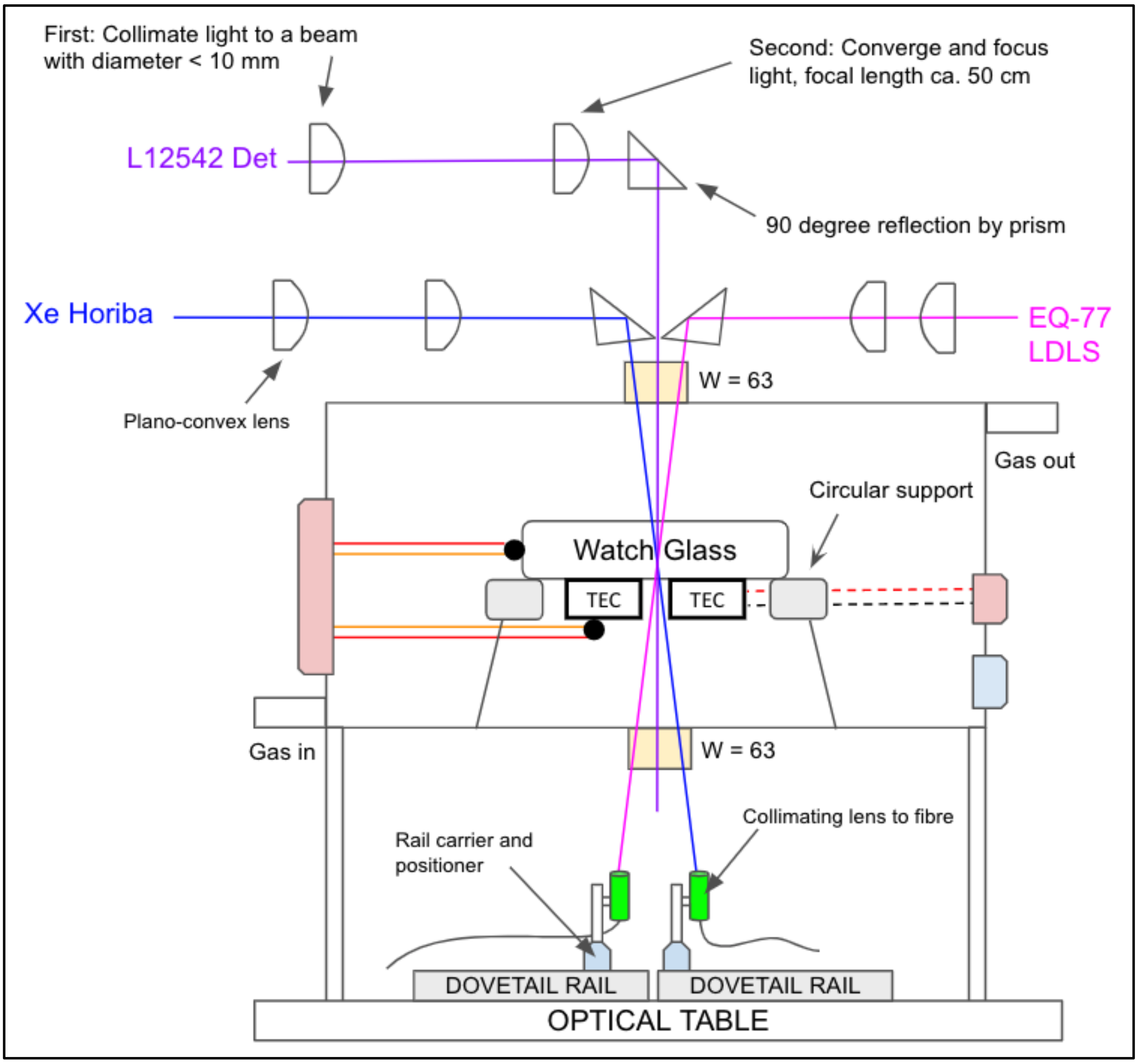

Figure 8: First order design concept. W = circular window (diameter 63 mm); TEC = thermoelectric coolers. A number of hermetically sealed feedthroughs act as the interface for external DC power supply and sensor feedback systems for temperature and pressure monitoring.

Since the light sources are designed to operate while positioned upright, we envision the use of a number of plano-convex lenses to collimate and focus the horizontal light beams, before directing them vertically downwards using several prisms. By rotating the prism through a small angle, the direction of each beam can be adjusted while avoiding overlaps.

In the first instance, we proceeded with a design involving prisms, due to considerations concerning the reflectance bandwidths of mirrors. A thorough comparison and recommendation will be made later, but this does not affect the general design and analysis. The key takeaway is that engineering solutions exist for both designs, one involving prisms and the other mirrors, as we show below, thereby introducing a degree of flexibility in the choice of that particular component without major overall design modifications.

For the optics-box interface, we propose using windows built into vacuum flanges (CF standard) to provide an air-tight seal. Simple trigonometry shows that the height of the box, or more specifically the vertical distance traversed by the beam from the prism to the collimating lens to fibre, constrains the size of the window.

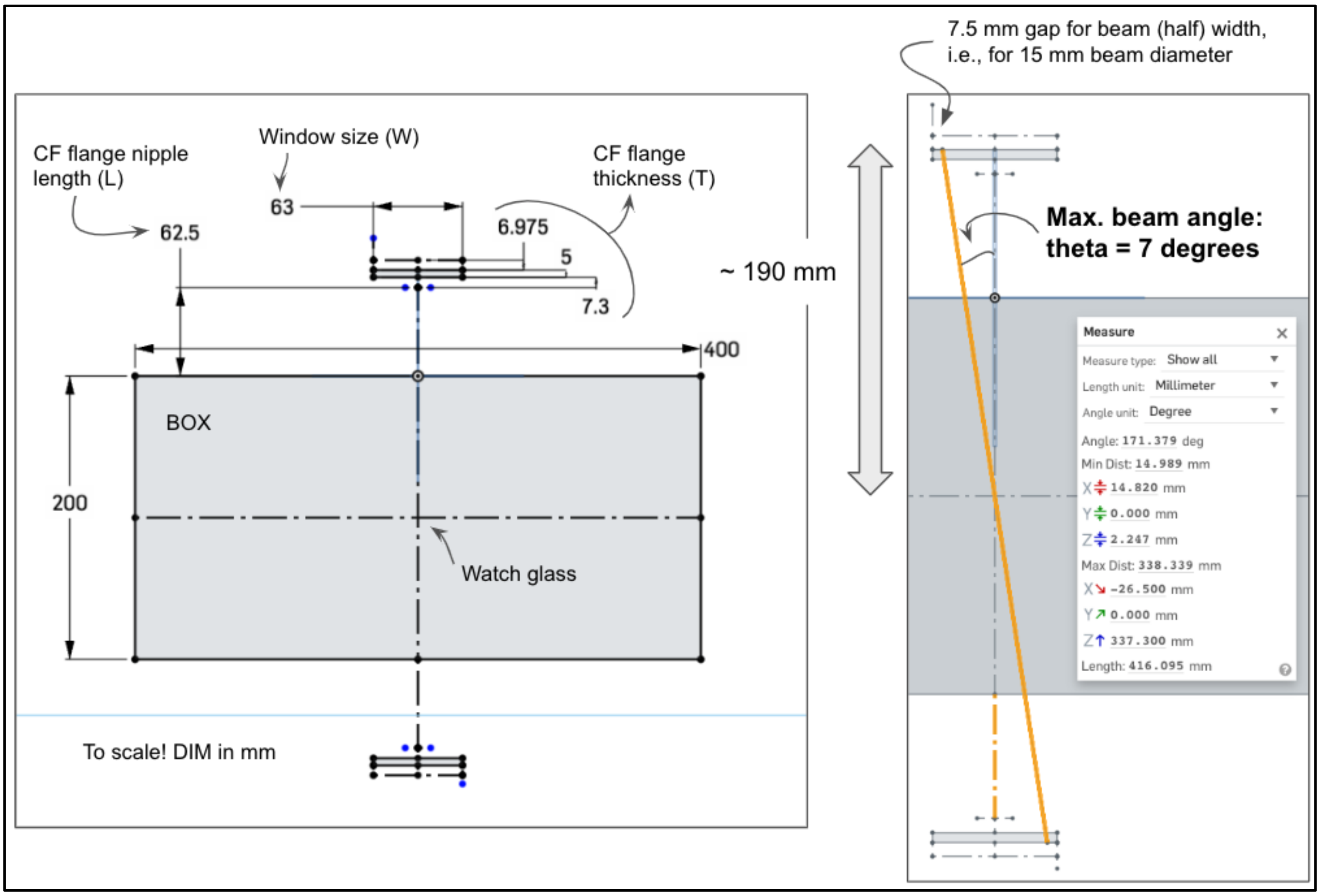

Figure 9: We consider key components contributing to the vertical distance: (1) flange with built-in window, (2) flange half nipple (adaptor to box) and (3) box height. The crucial parameter is the maximum allowed beam angle, which in turn affects the vertical positioning of the prisms. We assume a maximum beam size of 15 mm.

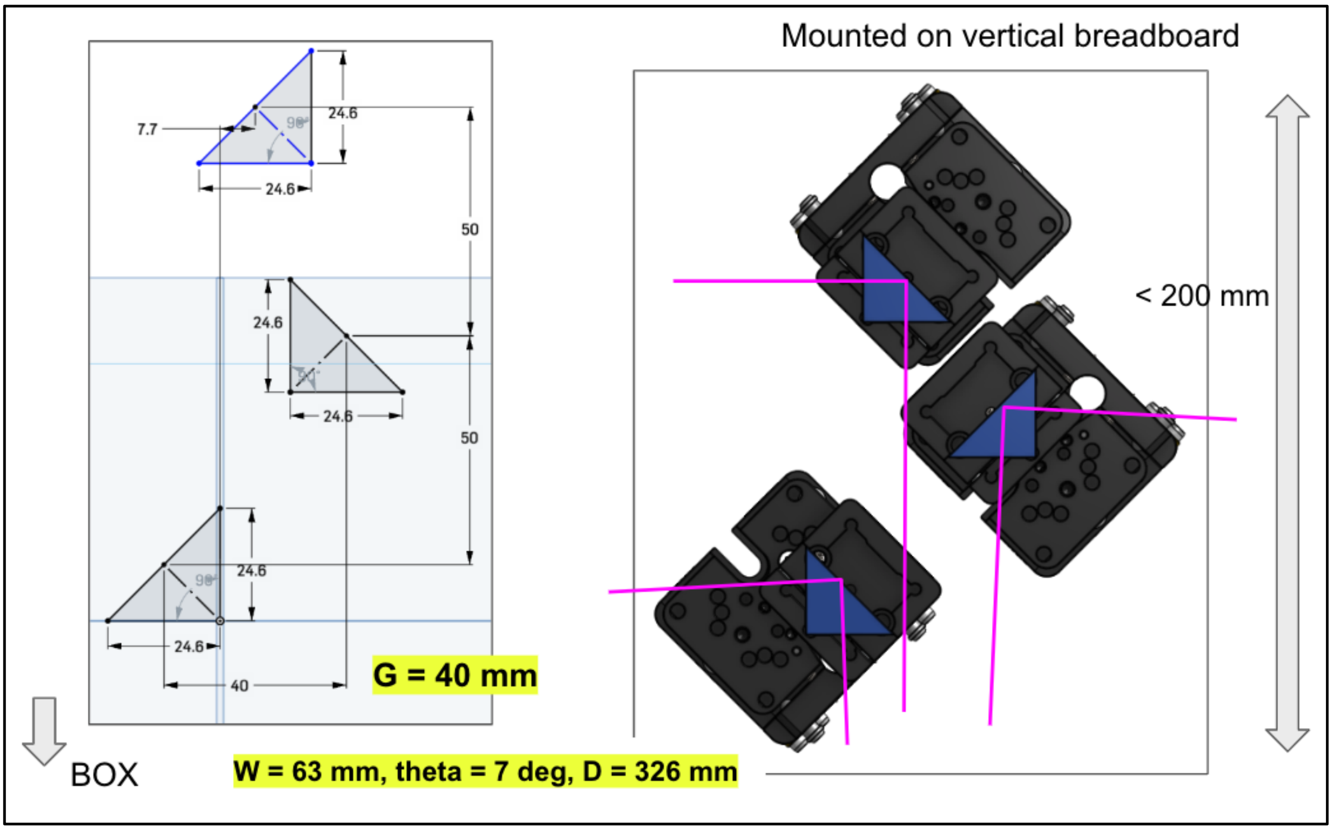

Figure 10: The ThorLabs Compact 5-Axis Stage [PY005(/M)] has been chosen to secure the three prisms, with vertical and horizontal offsets due to spatial constraints.

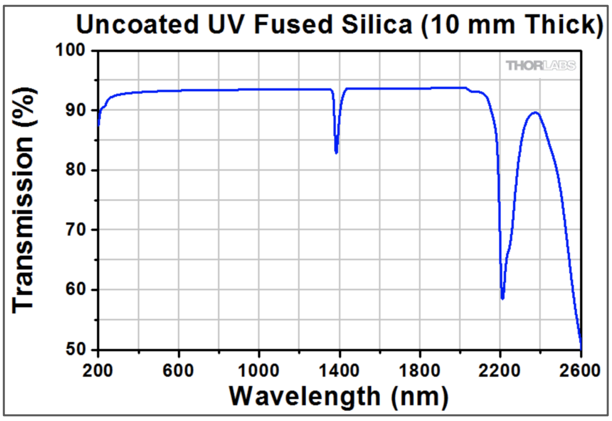
Uncoated UV Fused Silica (10 mm Thick)
Transmission (%)
Wavelength (nm)
THORLABS

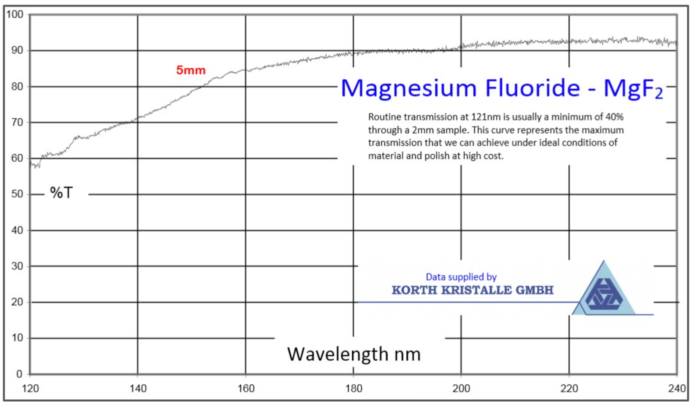
Magnesium Fluoride - MgF_2
5mm
Routine transmission at 121nm is usually a minimum of 40% through a 2mm sample. This curve represents the maximum transmission that we can achieve under ideal conditions of material and polish at high cost.
%T
Wavelength nm
Data supplied by
KORTH KRISTALLE GMBH

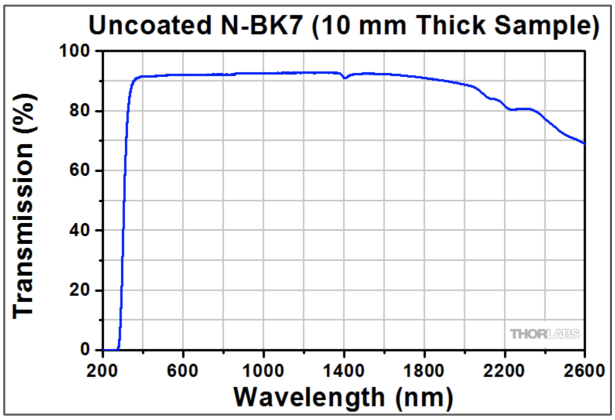
Uncoated N-BK7 (10 mm Thick Sample)
Transmission (%)
Wavelength (nm)
THORLABS

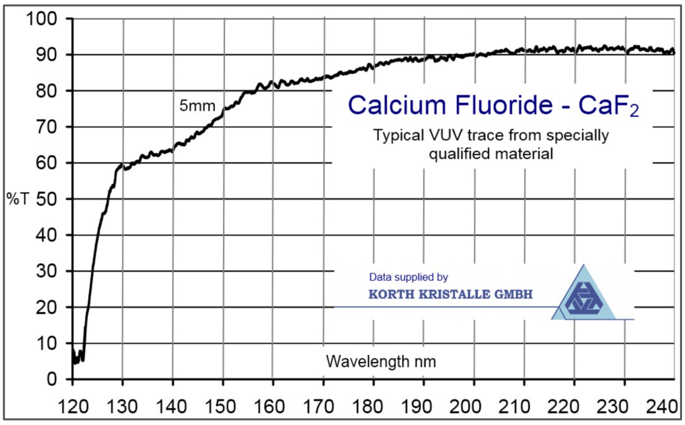
Calcium Fluoride - CaF_2
Typical VUV trace from specially qualified material
5mm
%T
Wavelength nm
Data supplied by
KORTH KRISTALLE GMBH

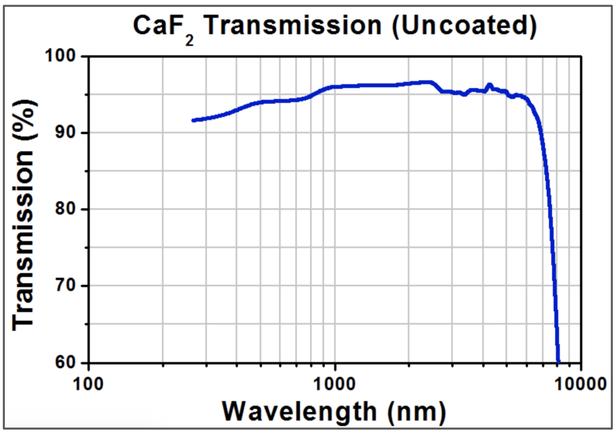

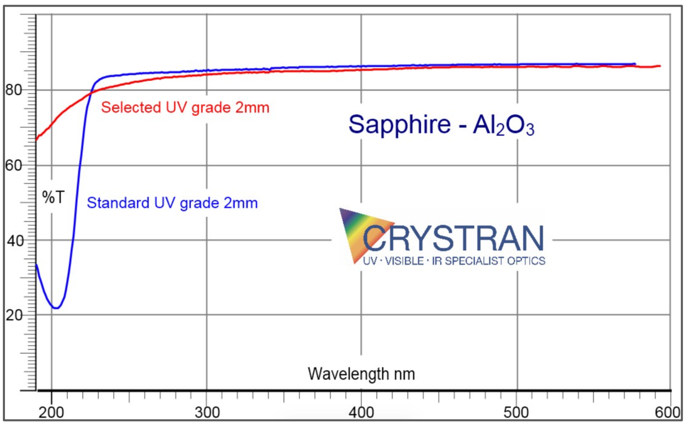

Figure 11: Concerning the choice of prisms, based on transmittance data from ThorLabs (data exists only down to 200 nm) and Crystran, we recommend either MgF_2 or CaF_2.

We then used the StarLab optics python module developed in-house (StarBeam) to propagate a beam with finite width through the prism, using refractive index data by Malitson (1963) to show that total internal reflection does occur as expected with negligible beam divergence induced by refraction for a perfectly collimated input beam. However, chances are the incoming beam is not perfectly collimated already, which will result in a bigger error than that introduced by the prism.

Mirrors versus Prisms

Concerning the choice of mirrors and prisms, we now elucidate our latest understanding on the matter, as of February 2023. The initial decision to proceed with prisms was based on the poor reflectance performance of ThorLabs mirrors, especially in the lower wavelengths (< 200 nm) [15], which is remedied by the high transmittance prisms offer. The only downside with prisms is potential significant chromatic aberration and dispersion. While this is worth noting, we have not verified the extent of these effects either with StarBeam, let alone Zeemax Optics, which is recommended.
Concurrently, new offerings by Edmund Optics [16] on mirrors with special coating, (VUV, DUV, UV) Enhanced Aluminium, provide a decent 80% reflectance down to 120 nm. In this regard, we recommend using mirrors with diameter 50 mm (taking into account that in the original design, prisms with 25 mm length, or > 35 mm hypotenuse sufficed, with clear aperture 90%).

Typical Reflectance Curve for Metallic Mirror Coatings NIR - IR Range

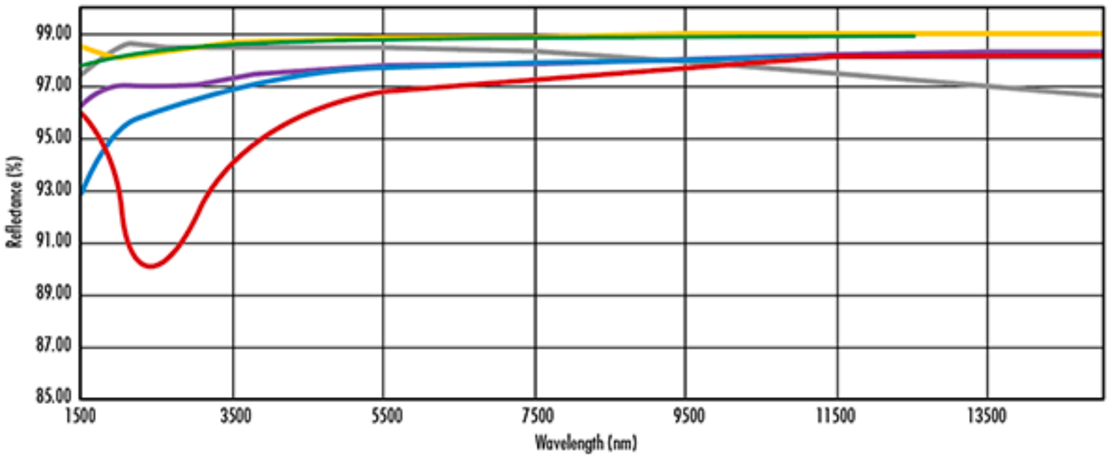

Typical Reflectance Curve for Metallic Mirror Coatings UV - NIR Range

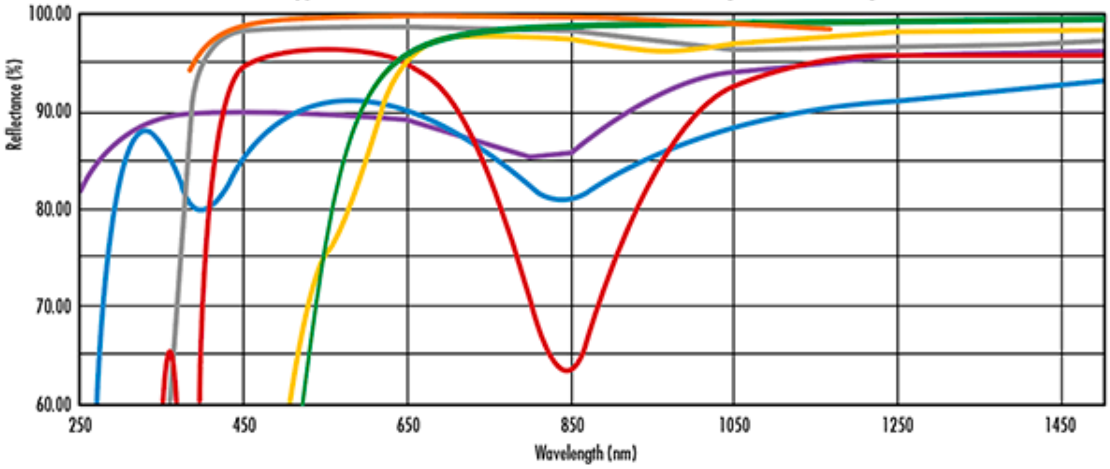

Protected Aluminum		Enhanced Aluminum		UV Ehanced Aluminum		Protected Gold		Bare Gold		Protected Silver		Ultrafast Enhanced Silver	
Range (μm)	% Reflection	Range (μm)	% Reflection	Range (μm)	% Reflection	Range (μm)	% Reflection	Range (μm)	% Reflection	Range (μm)	% Reflection	Range (μm)	% Reflection
0.4 - 0.7	85	0.45 - 0.65	95	0.25 - 0.45	89	0.7 - 2.0	96	0.7 - 0.8	94	0.45 - 2.0	98	0.6 - 1.0	99
0.4 - 2.0	90	–	–	0.25 - 0.70	85	2.0 - 10.0	96	0.8 - 2.0	97	2.0 - 10.0	98		
								2.0 - 12.0	98				

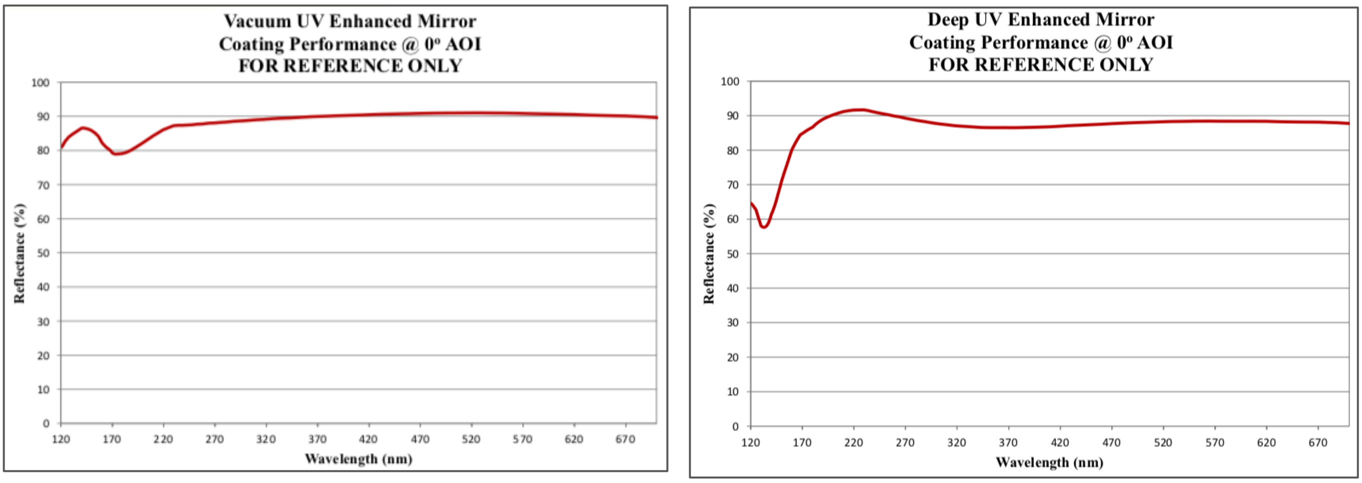

Figure 12: Reflectance data on mirrors with special coating from Edmund optics [17].

At this juncture, we highlight that for the VUV mirrors, the coating has been rated to survive operating temperatures of 0-50^{o}C, and the damage threshold value of the coating is roughly 0.5 J / cm^2 at 193 nm. The full exchange of the email with a technical staff from Edmund Optics can be found on slide 16 of “Update 3 - 12 SEP 2022”.

Even considering the EQ-77, which has one of the lowest beam powers, we are looking at ~3 W over a circular cross-section with diameter 10 mm on the mirror, the intensity amounts to ~ 2.5 J / cm^2, which is significantly higher than the rated LIDT of 0.5 J / cm^2. We believe the mirrors are designed for the manipulation of low power lasers rather than high throughput light sources with an uptime of hours to days.

Therefore, we strongly recommend revisiting the following:

(1) Checking that beam power calculations for the light sources are correct
(2) Characterising the extent of chromatic aberration and dispersion for prisms

That said, the rest of the design surrounds the use of mirrors, which we stress again, does not impact the general design approach significantly.

Windows

With considerations for cost and versatility, we recommend Torr Scientific vacuum optics for CF flanges with built-in windows. While a vacuum flange can afford a sufficiently strong seal that would sustain a stable atmosphere (down to ~1 ppm O_2 for example) over extended periods of time, we stress the danger of chamber overpressure resulting in structural failure of the windows. Unavoidably, this results in a maximum expected operating pressure (MEOP) rating for the chamber, which will be further elaborated in Sub-system: Chamber.

Our choice for the window material is based on transmission performance at different wavelengths of light, with size constrained by design considerations for the beam paths identified earlier.

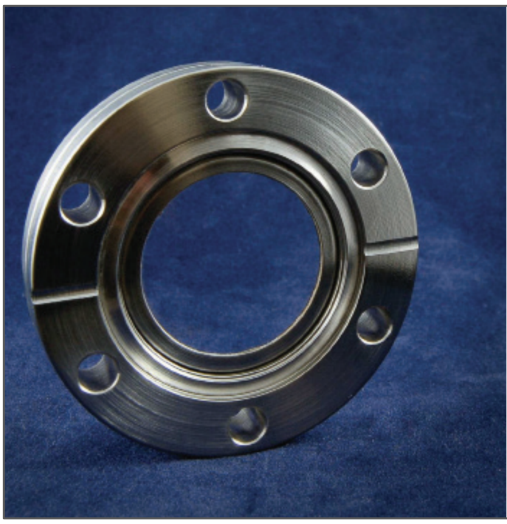

Specification	
Seal Type	Bond
Maximum Temperature	120 °C
Minimum Temperature	minus 45 °C
Maximum Rate of Temperature Change	3 °C per minute
Leak Rate	$<1\times10^{-10}$ atm-cc/sec (He)
Pressure Range	1 bar $<1\times10^{-9}$ mbar
Surface Quality	20/10 scratch/dig
Parallelism	< 3 arc minutes
Flatness	λ/2

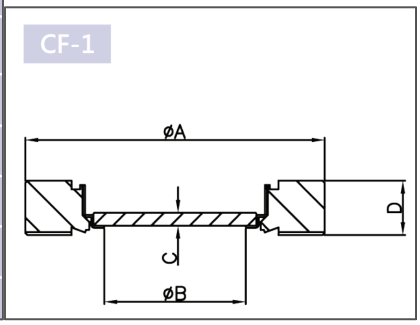

Figure 13: We recommend the CF-1 configuration with the following dimensions in mm: A = 114, B = 63, C = 4.5, D = 17.4. Flange specification: NW63CF. Material: 304L. Part code: BVPZ64NQZ.

Wavelengths (nm) used for comparison (% transmission)				
Material	**150 nm**	**160 nm**	**200 - 400 nm**	**400 - 1000 nm**
CaF_2	38	58	80 to 95	95
MgF_2	53	60	91	91
Sapphire	Just not good enough			
Quartz	48	75	90	91

Silica	40	42	94	94

Table 1: Data extracted from transmission (%) versus wavelength (nm) charts [18]. We suggest using quartz natural Z-cut zero length viewports.

Plano-Convex Lens

This component constitutes the final design phase for manipulating the incoming light beam. We first note that all three lamps involve a diverging beam from a source of finite width. This necessitates the use of converging lenses to first collimate the beam, before focusing the beam onto the sample. To reduce chromatic aberration, we propose using a plano-convex lens (PLC).

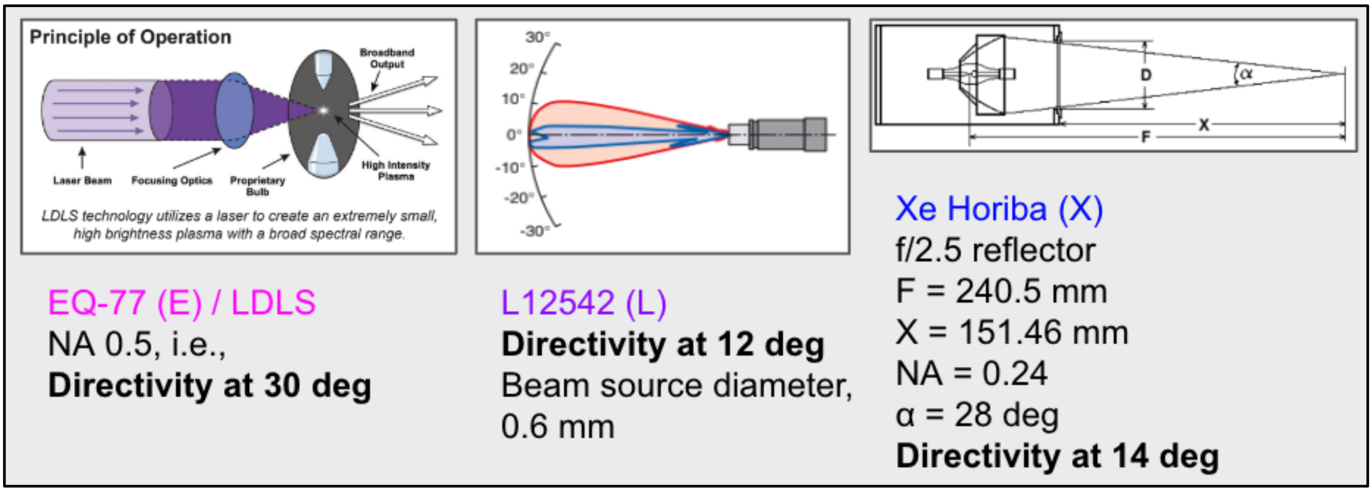

Figure 14: Beam properties for the three light sources.

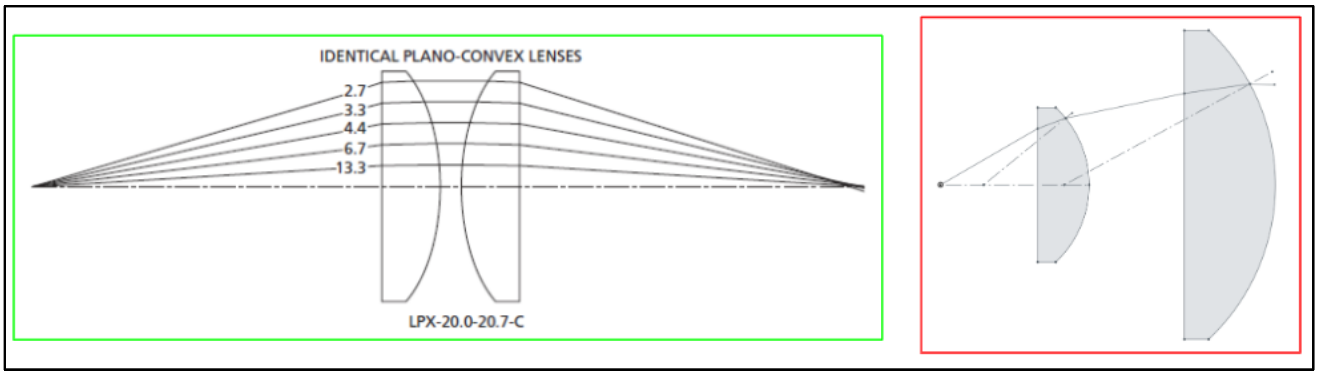

Figure 15: Curved surfaces are the culprit for introducing aberrations, so we shall adopt the green-bordered arrangement.

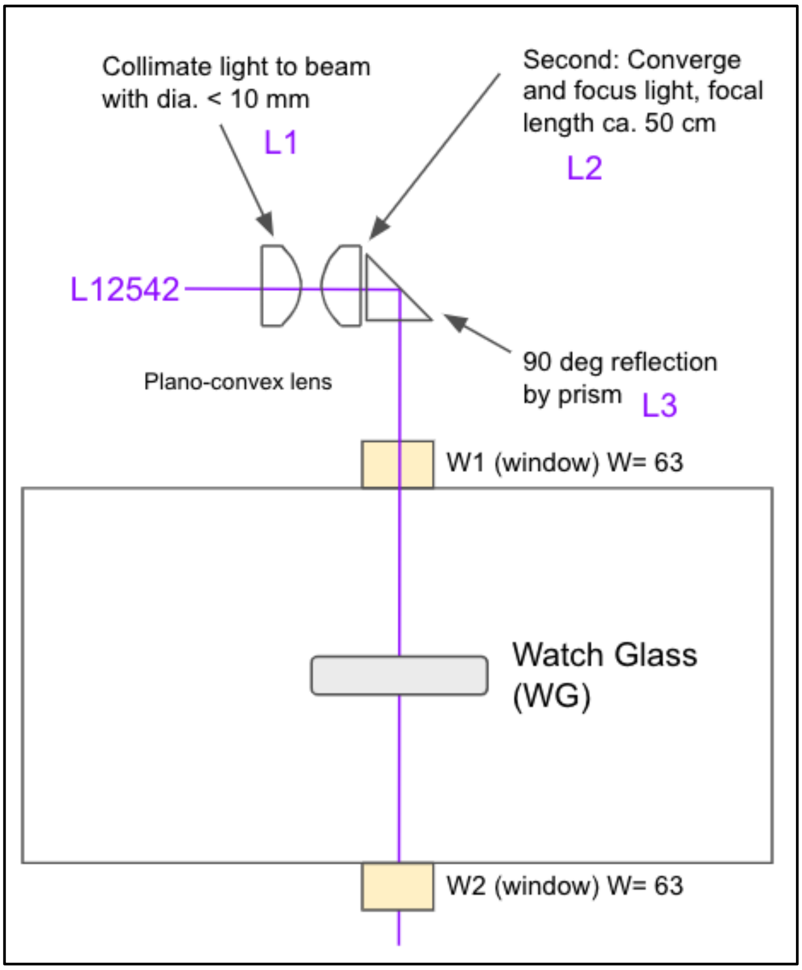

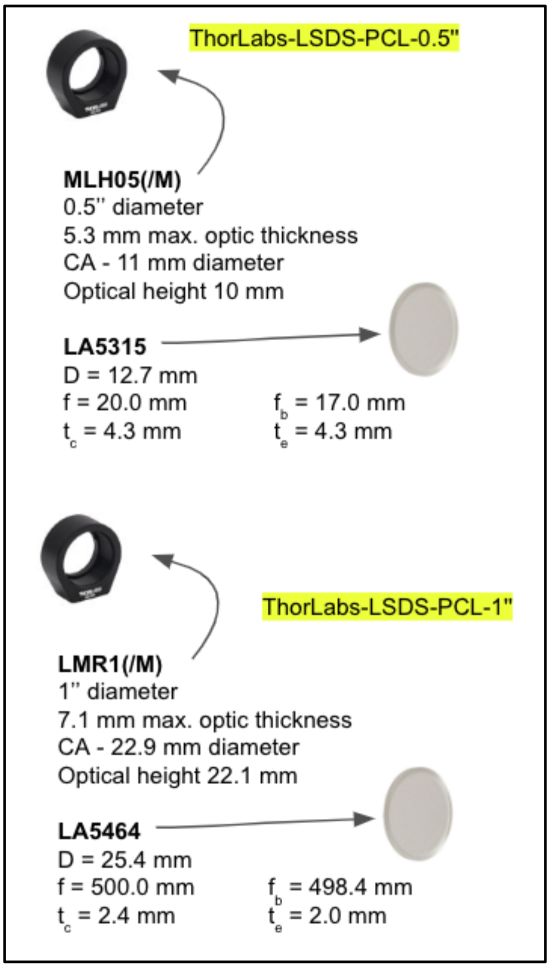

Figure 16: (left) We designate the first PLC for beam collimation as L1, the second PLC as L2 to initial beam convergence, and L3 is the mirror / prism to direct the beam downwards, passing through the window W1 onto the sample. (right) We propose standard ThorLabs mirror mounts and PLCs.

We are constrained by the specifications (notably focal length, thickness and clear aperture size) of commercially available PLCs. Therefore, StarBeam was developed as a simple set of Python codes to generate a light beam, propagate, reflect and refract it, with the goal of focusing the beam to the centre of the watch glass, while ensuring the vertical dimensions of the entire experimental setup is within limits, i.e., engineering feasibility.

This shall serve as a baseline model from which we show that in principle, the aforementioned objective can be achieved, even if in practice, there are a ton of other inaccuracies introduced that will deviate from said ideal model. We mitigate these inaccuracies by introducing sizable manoeuvring buffers into each component.

OnShape was used to draw the ray diagrams for illustration, while the Scipy "minimise function" was used to converge to a solution. We do not delve into the intricacies of the code, but present its concept and general execution, with emphasis on the results and implications.

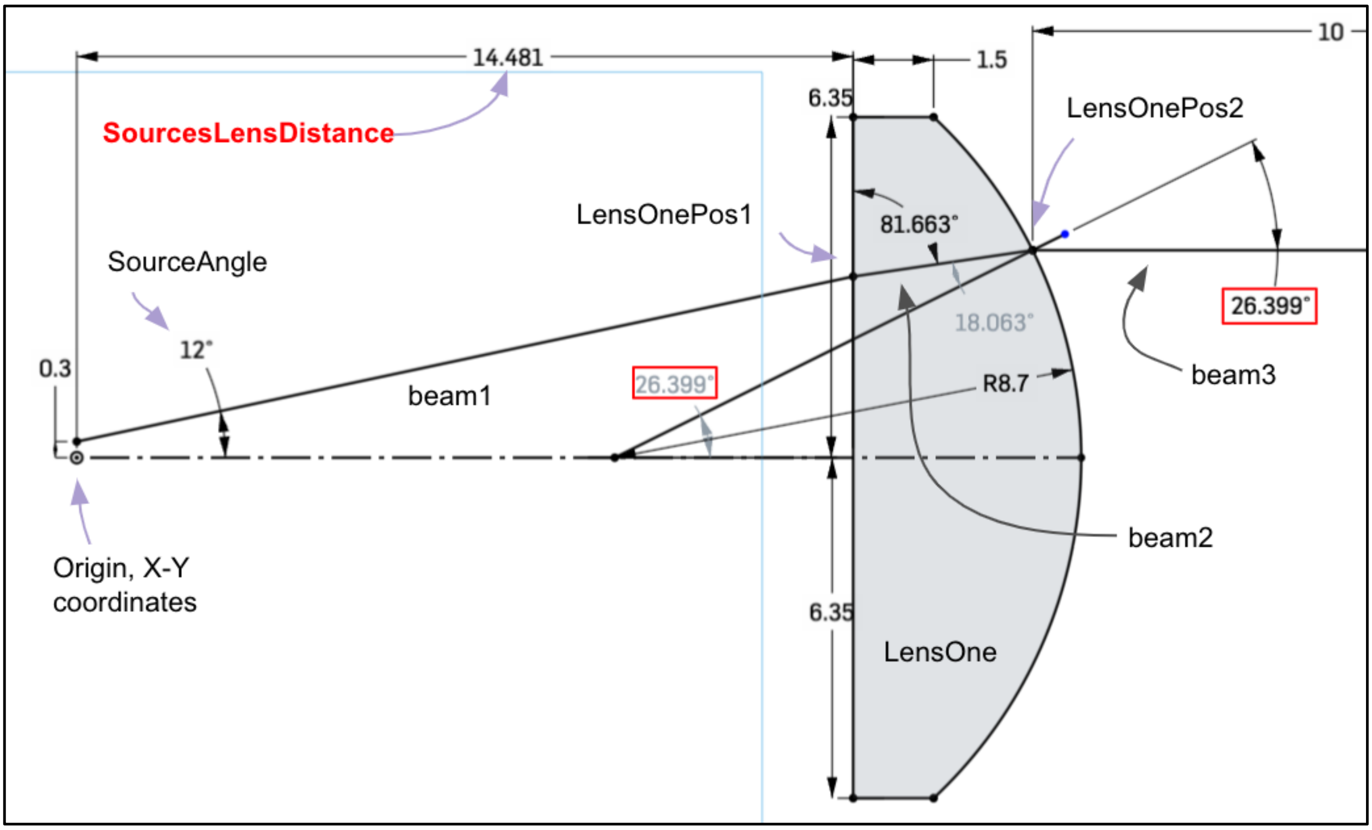

Figure 17: Part 1 of the code seeks to adjust SourcesLensDistance until beam3 is horizontal, judged when the two difference between the two angles in the red boxes is zeroed. In this instance, we have SourcesLensDistance = 14.5 mm.

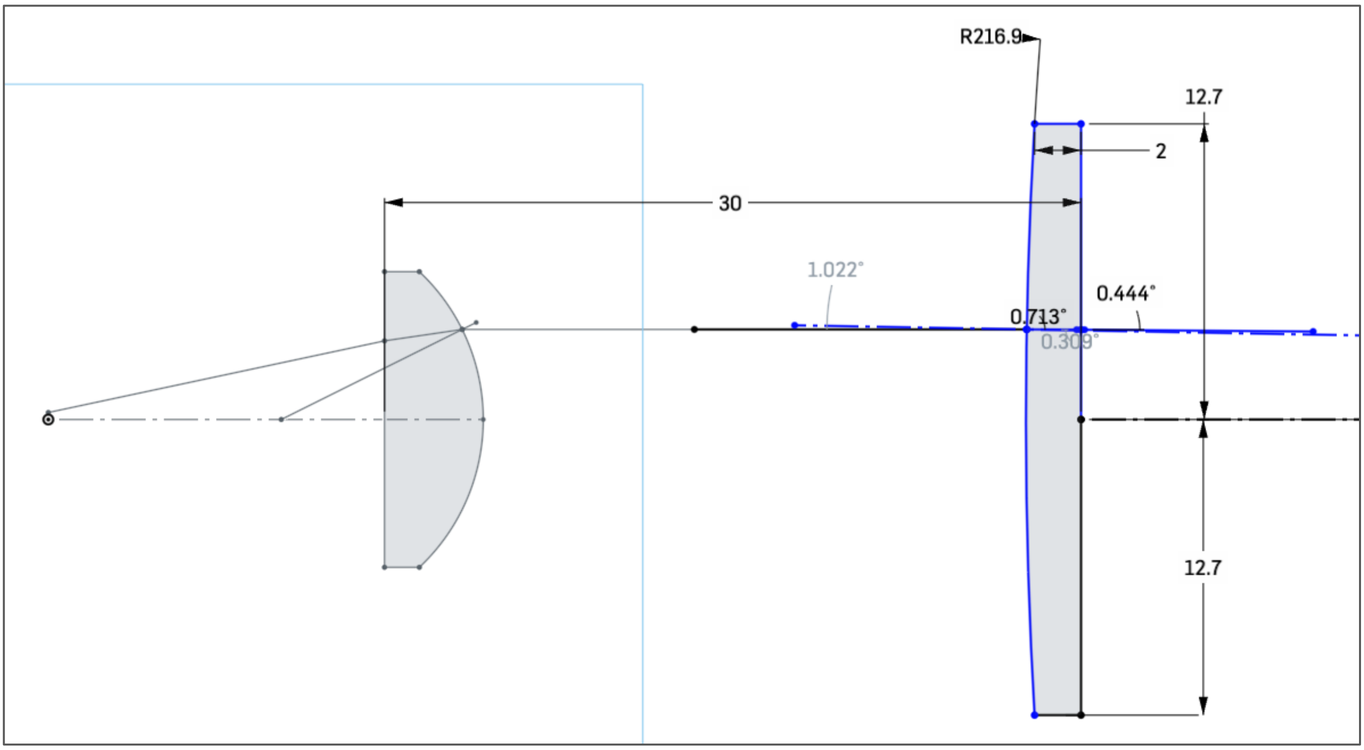

Figure 18: Part 2 of the code propagates the emerging light beam from L1 to L2. In this instance, we fix the distance between L1 and L2 to 30 mm. For a perfectly collimated light beam, this distance is inconsequential. For certain light sources, we increase this distance to accommodate potential additional optical components, such as a water-based IR filter for example.

Part 3 of the code propagates the light beam from L2 to L3 (prism was used for simulation, but results will not differ significantly for mirror), through the window and to the centre. Two beams defining the boundary of the finite beam are required to converge onto the same point at the centre of the glass watch.

With reference to Figure 15, parameters “prismSampleDistance” and “bottomWindowSampleDistance” are fixed. The two degrees of freedom are the distance between L2 and L3 (prism), the so-called “LensTwoPrismDistance” and the tilt angle of the prism. We repeat such calculations for various commercially available L2 specifications.

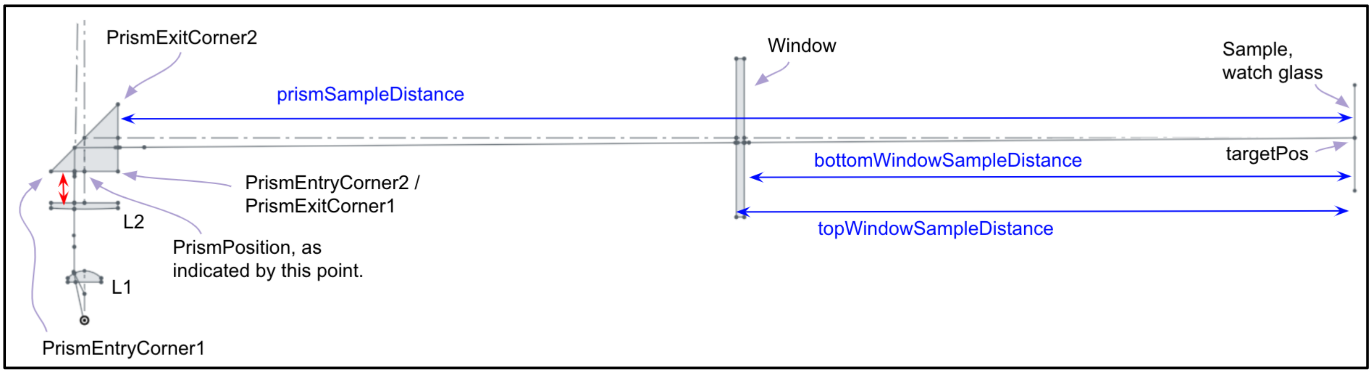

Figure 19: Part 3 of the code. The diagram has been rotated by 90 degrees. In this instance, a solution is obtained for the LSDS lamp, with LensTwoPrismDistance = 11.9 mm.

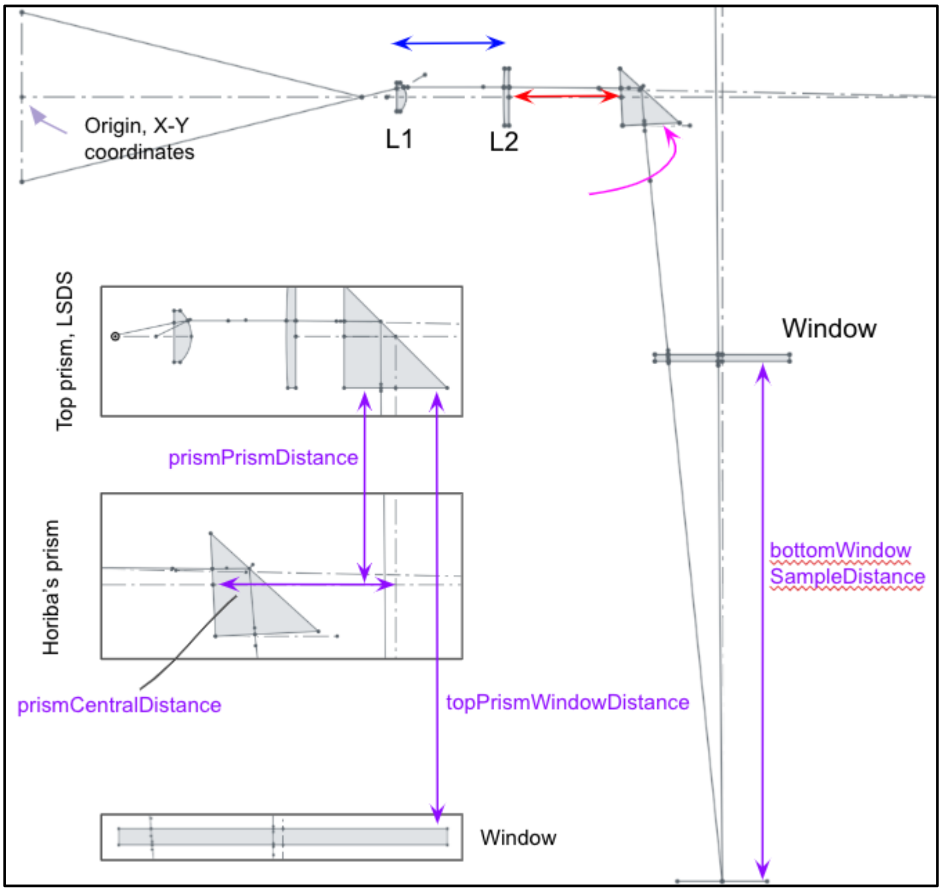

Figure 20: Similar technique applied to the Horiba light source (Xe lamp). We simply wish to draw your attention to the position on the window at which the beam cuts through for a prism that is offset by 50 mm from the central axis. This is to be compared with Figure 15, where the central beam cuts right through the centre of the window. The offset arises from spatial constraints in positioning the prisms / mirrors.

In general, reasonable solutions were obtained for all three lamps using the aforementioned method. We now point out key modifications needed in each case due to individual lamp subtleties.

For the L12542 / Deuterium lamp, beam collimation proved to be trickier as the lamp's arc point is buried a good 42 mm within the cylindrical casing of the light source. To be conservative, we worked with 50 mm from the arc point.

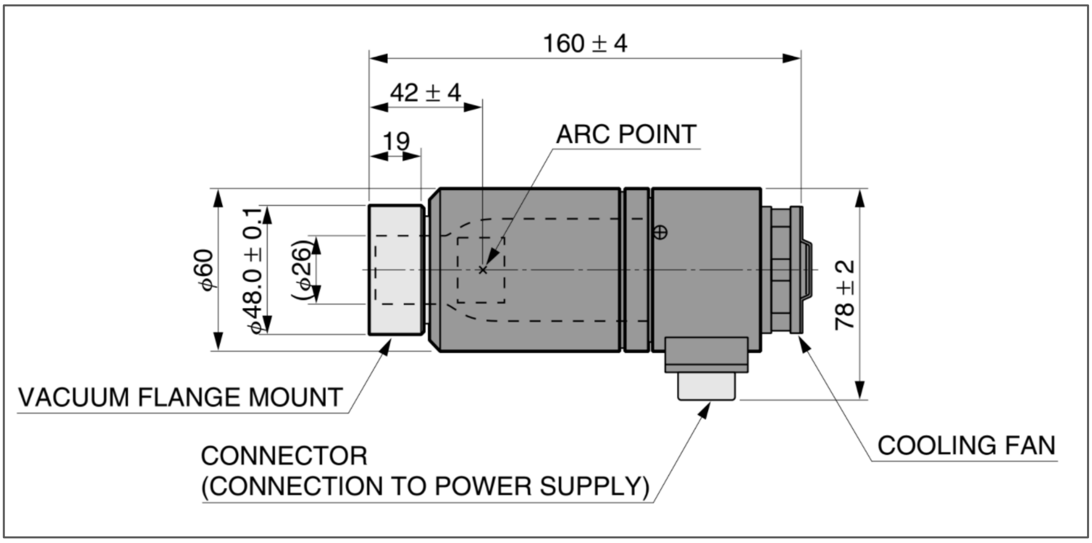

Figure 21: L12532 Deuterium lamp schematic.

The new implications are as follows:

- L1 now needs to be a 1'' wide plano-convex lens instead, with f = 40 mm (part no. Thorlabs LA5370). We could always pick a lens with larger focal length but then, by the distance the beam is collimated, it would have diverged too much, i.e., beam width too large.
- Therefore, by choosing a lens with a shorter focal length, but placing the lens a little to the right (see below) of the focal length, the beam converges.
- A second plano-concave lens, L2 is then used to collimate the beam.
- L3 then focuses the beam onto the watch glass, resulting in a particularly narrow beam.

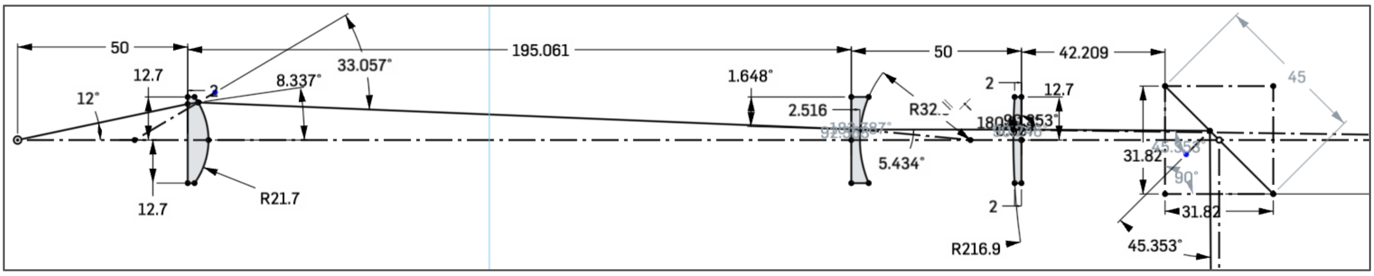

Figure 20: A new optical design involves three lenses instead of two before the mirror / prism.

For the EQ-77 / LSDS, we face a similar problem, and we offer two solutions. In the first instance, we could use the EQ-77-OAP-EFL-6 Off-Axis-Parabolic Assembly - 6" EFL with Tube Extension accessory offered by Energetiq.

16. What OAP configuration is needed for coupling the LDLS into a spectrometer or monochromator?

The EQ-99X and EQ-77 have four different OAP options. Please note that the Numerical Aperture (NA) of the OAP assembly should be slightly less than the entrance NA of the monochromator or spectrometer. Whereas the f/# of the OAP assembly should be slightly larger than the f/# of the entrance to the system, to allow for efficient coupling into the system.

- Use the chart below to match the entrance f/# or NA of your system with the appropriate OAP Mirror Assembly.

	2" EFL OAP	4" EFL OAP	6" EFL OAP	8" EFL OAP
Effective Focal Length (EFL)	2.0" (50.8mm)	4.0" (101.6mm)	6.0" (152.4mm)	8.0" (203.2mm)
Diameter	1.5"	1.5"	1.5"	1.5"
Magnification*	1x	2x	3x	4x
Numerical Aperature	0.375	0.188	0.125	0.094
f/#	1.33	2.67	4.00	5.33

- Magnification is based on an OAP pair with 2" EFL OAP as the collecting mirror and the second OAP (listed above) as the focusing mirror.

Figure 21: Details of various OAP assemblies offered by Energetiq.

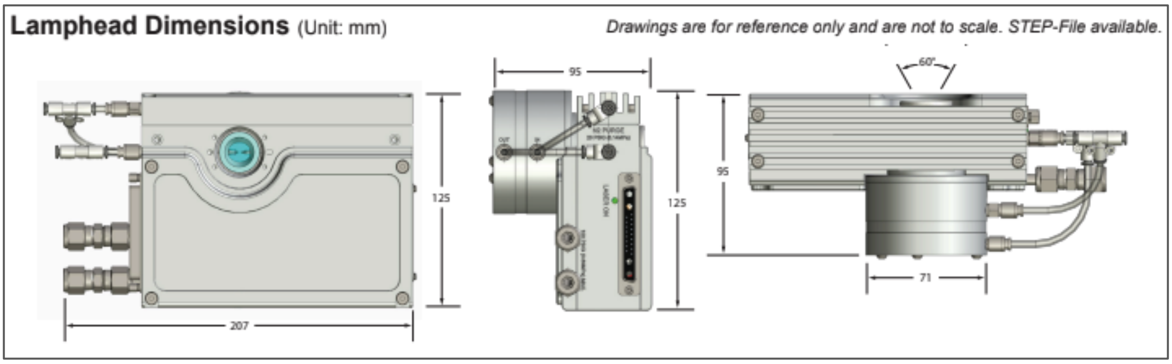

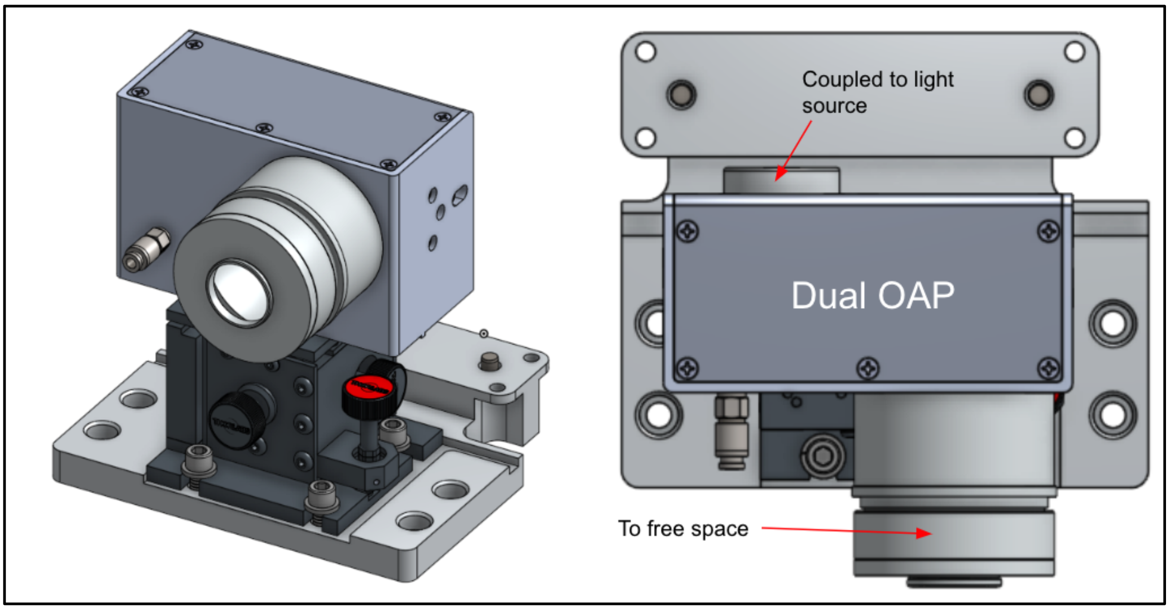

Figure 22: (top) Schematic of the standalone EQ-77. (bottom) Housing for the dual OAP assembly, together with translation stage, and fittings for nitrogen purge (to reduce ozone build up).

To model the light beam, we used information provided by the supplier to deduce that the accessory should consist of two OAPs facing each other to route the beam through two 90 degree turns.

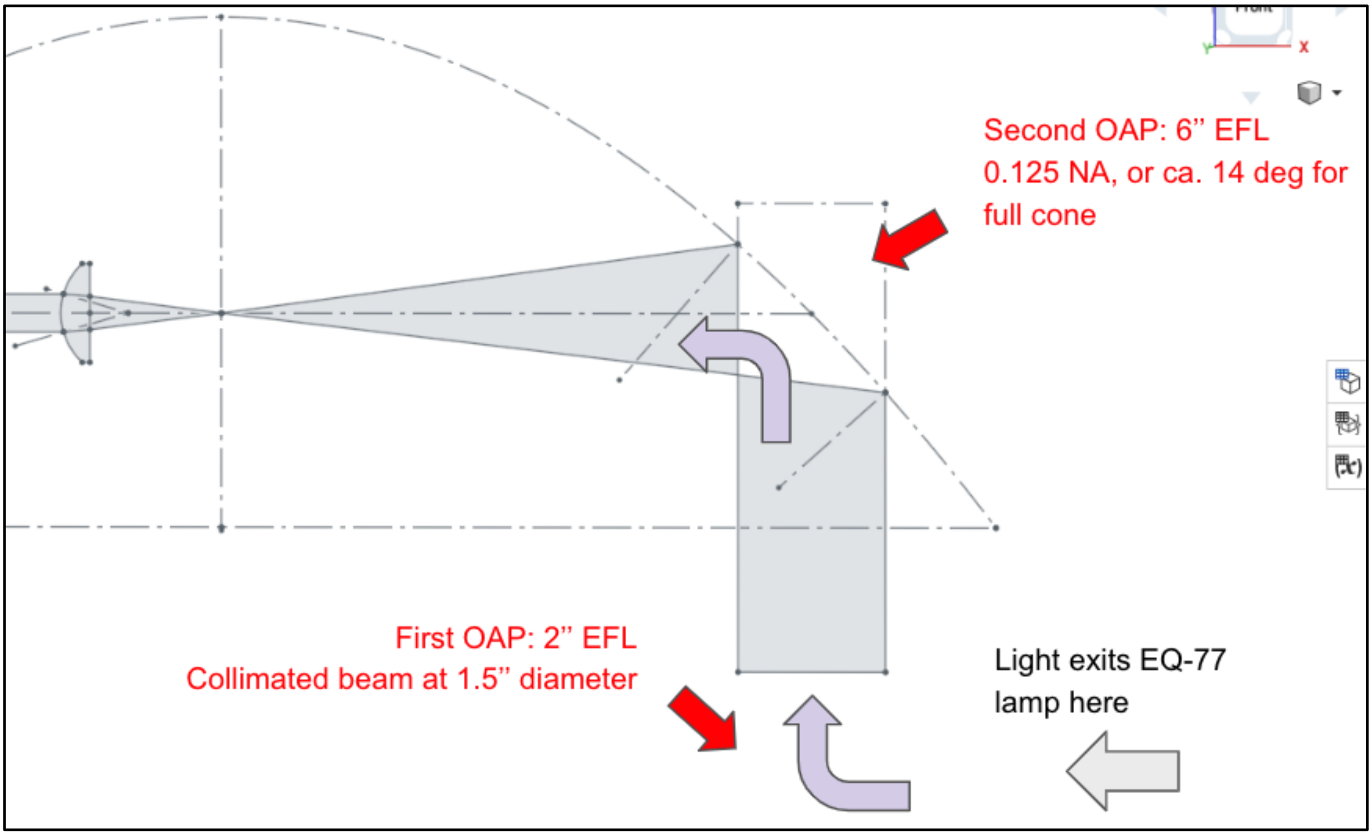

Figure 23: Updated ray diagram following beam manipulation with dual OAP assembly.

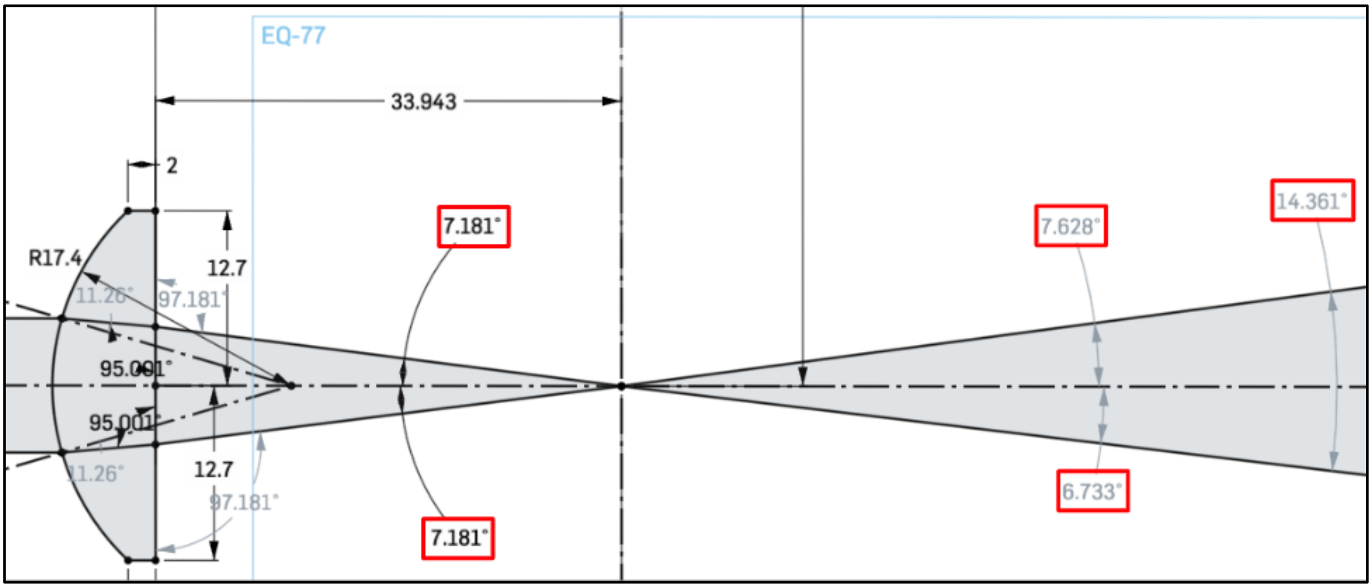

Figure 24: We observe a largely inconsequential intrinsic asymmetry of the outgoing beam from an off-axis parabolic mirror: see red boxes. A symmetric beam, relative to the horizontal axis is used to generate the ray diagram, with the implication that even in the ideal case, the first plano-convex lens needs to be tilted slightly (in real life) to ensure a collimated beam travelling parallel to the horizontal axis. This provides the motivation to replace fixed lens mount with kinematic lens mount.

We mentioned a second solution exists, motivated by the excessive cost and long lead times of the OAP assemblies. A series of plano-convex and plano-concave lenses could do the job (Figures 26-27).

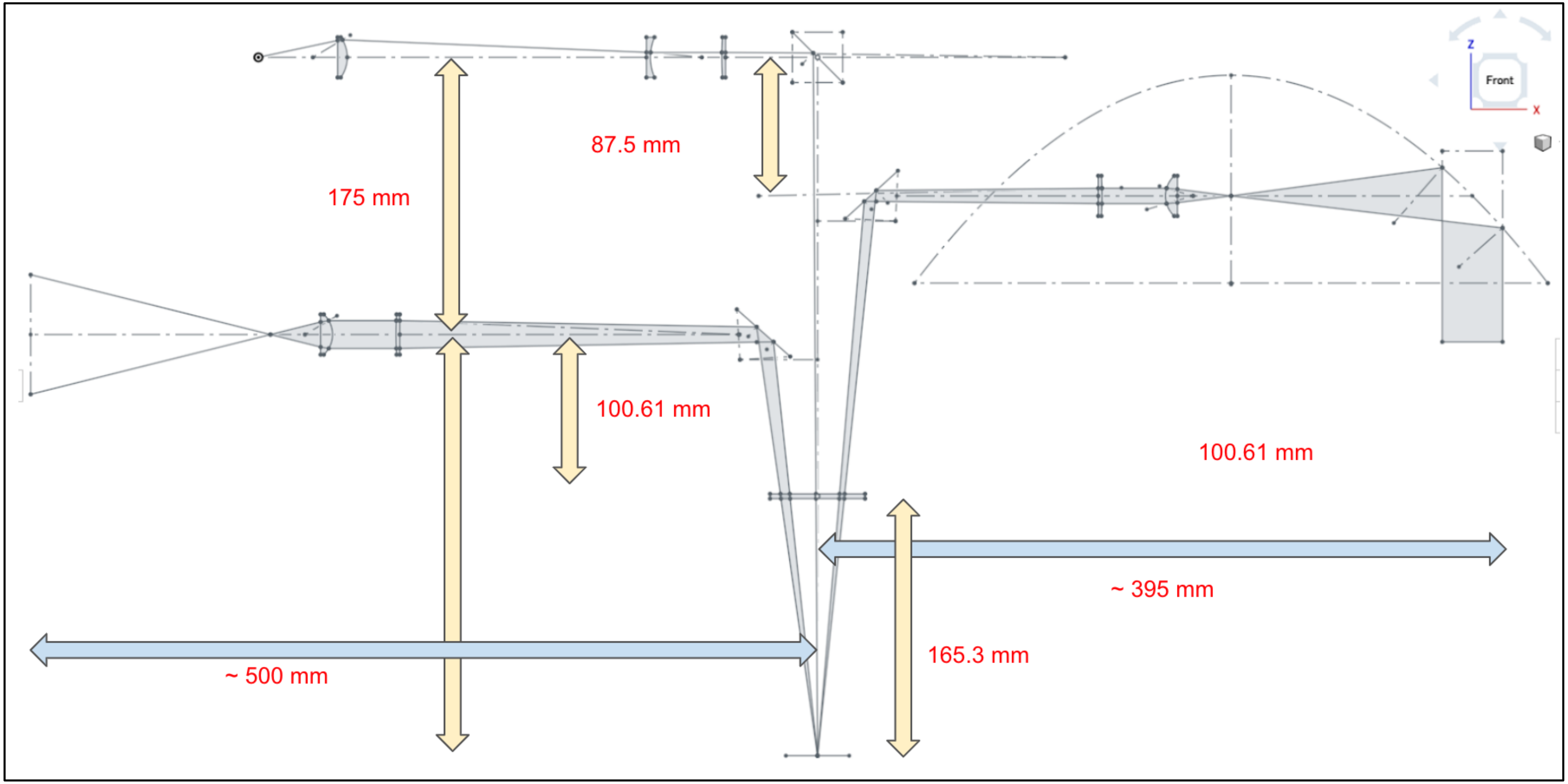

Figure 25: New finite beam diagram with consideration for all three light sources. Note the three lenses needed for the L12542 / Deuterium lamp (top), the use of OAPs for the EQ-77 (middle), and two lenses for the Xe lamp. Crucially, while this ray diagram is far from realistic, it provides a general sense on the dimensions of the setup, and how the lamps are to be spatially positioned.

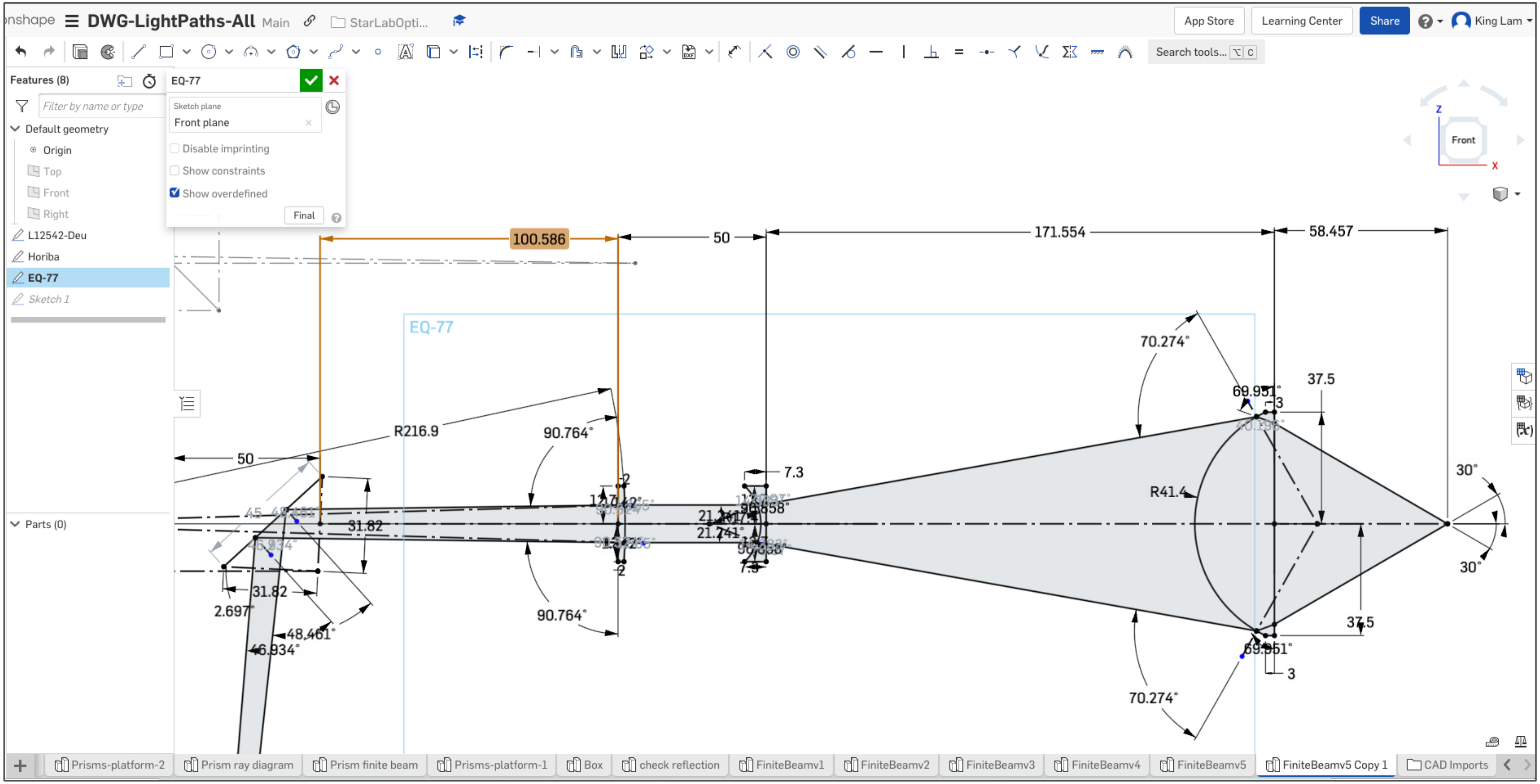

Figure 26: Alternative optical design for EQ-77, forgoing OAP assembly.

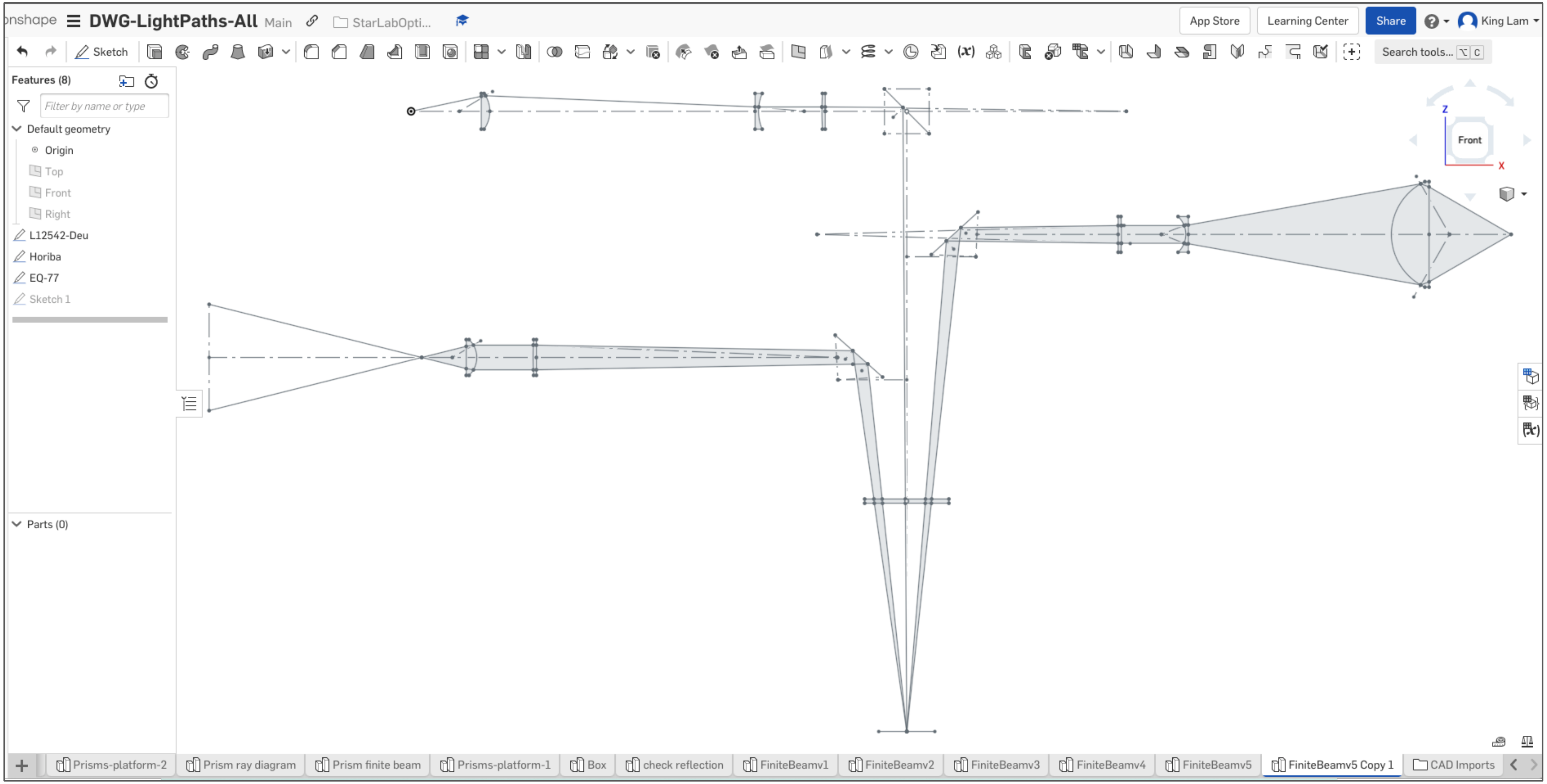

Figure 27: Combined finite beam diagram. Compared to Figure 25, the only difference is the use of three plano-convex and plano-concave lenses for beam manipulation for the EQ-77. We note no significant differences in the spatial arrangement of the setup, see Figure 28.

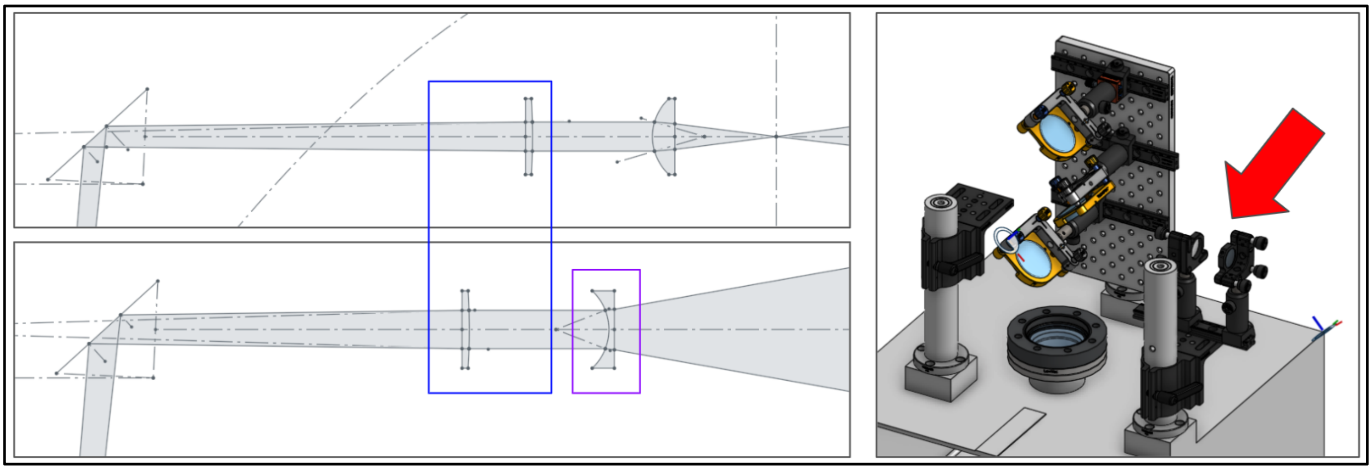

Figure 28: No changes required to parts indicated by red arrow, since the distance between the mirror and the third lens (in blue box) is reduced from ca. 140 mm to ca. 110 mm, and the same lens holder can be used to hold the plano-concave lens, purple box.

Optomechanics: Incident

Based on the optical design so far, we now proceed to list the proposed optical components for manipulating the incident beam from the source up to the top window. We propose the use of mirrors over prisms, pending damage threshold calculations.

L12542 / Deuterium setup

Light source:

• Lamp housing:	160 mm long, 60 mm diameter cylinder	0.53 kg
• Power supply:	200mm x 117mm x 90mm (H)	1.8 kg
• Position of light beam:	277.4 mm above top window of chamber	
• Wavelength range:	125 - 200 nm	

Mirror:

- 50mm Dia., Vacuum UV (VUV) Mirror - STOCK #33-914 (Edmund Optics) [19]
- Mount: 50.0/50.8mm Optic Dia., Kinematic Mount, 3-Screws - STOCK #58-855 [2-]

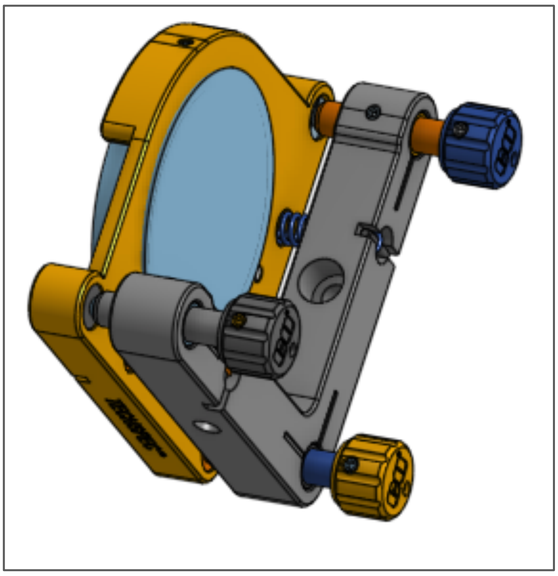

Figure 29: Mirror with mount sub assembly.

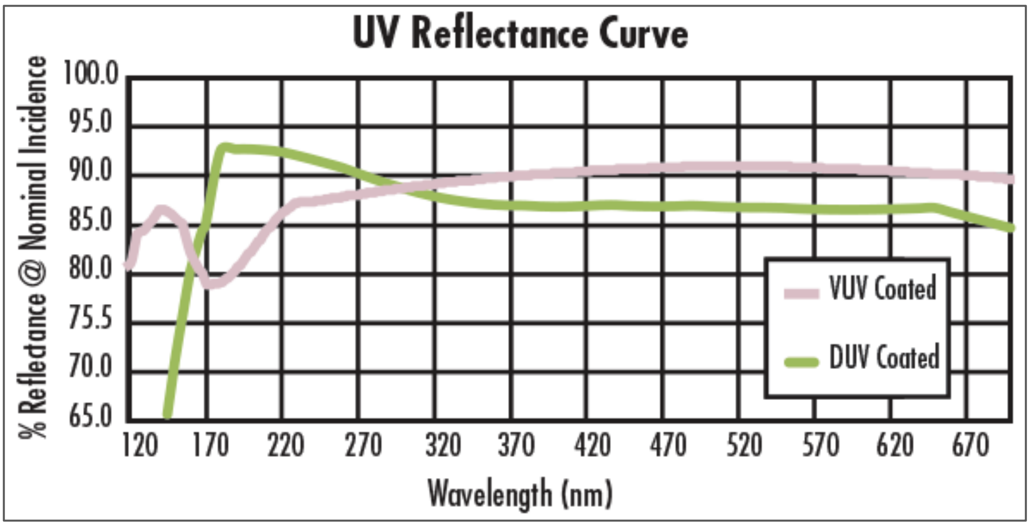

Figure 30: UV reflectance curve for Vacuum UV (VUV) Mirror - STOCK #33-914 (Edmund Optics) [21].

Diameter (mm):	50.00 +0.0/-0.2
Substrate:	Fused Silica (Corning 7980)
Surface Quality:	10-5
Coating:	Enhanced Aluminum (120-600nm)
Angle of Incidence (°):	0
Design Wavelength DWL (nm):	120
Thickness (mm):	10.00 ±0.2
Type:	Flat Mirror
Vacuum Compatibility:	10^{-7} Torr

Surface Flatness:	λ/10
Back Surface:	Ground
Coating Specification:	R_{avg} ≥78% @ 120 - 125nm R_{avg} ≥85% @ 120 - 600nm
Coating Type:	Metal
Clear Aperture (%):	90
Parallelism (arcmin):	<3
Thickness Tolerance (mm):	±0.2
Wavelength Range (nm):	120 - 600

Figure 31: Specifications for Vacuum UV (VUV) Mirror - STOCK #33-914 (Edmund Optics) [19].

Lens assembly: general considerations

- All CaF_2 plano-convex and plano-concave lens will be 1'' in diameter
- Instead of using fixed mounts, we propose using KS1 Ø1" Precision Kinematic Mirror Mount, 3 Adjusters instead.
- Fine control of the pitch and tilt was shown to be necessary if one looks at the ray diagram [22], as well as translation in the Z axis.
    - ±4° of Pitch and Yaw Adjustment
    - Maximum Z translation of 0.25" (6.4 mm) - coarse translation provided by dovetail carriers
- This will be the default design for all lenses, except the first lens for the L12542 / Deuterium lamp, L1, as there will be insufficient spacing between the light source and the lens, taking into account the length of the three knobs. In that case, a fixed mount will be used.

Figure 32: (left) fixed mount. (right) kinematic mount.

Standard post setup: for the lenses and mirrors

- Dovetail Optical Rails [23]
    - RLA150/M Dovetail Optical Rail, 150 mm, Metric
    - RLA300/M Dovetail Optical Rail, 300 mm, Metric
    - RLA450/M Dovetail Optical Rail, 450 mm, Metric

- Optional: 1/2" (12.7 mm) Travel Miniature Dovetail Translation Stages [24]
    - DT12/M 12.7 mm Dovetail Translation Stage, M4 Taps
    - Unlikely to be necessary, considering the kinematic mirror and lens mount already allow for 6.4 mm translation.
    - Nevertheless, post and post holders were designed to accommodate the addition of that if necessary.

- Standard 1/2" Post Holders [25]
    - A variety, height dependent, usually between 40 mm and 75 mm tall
    - E.g., PH50/M Ø12.7 mm Post Holder, Spring-Loaded Hex-Locking Thumbscrew, L=50 mm

- Optical Posts: Ø1/2" and Ø12 mm [26]
    - A variety, height dependent, usually between 30 mm and 75 mm tall
    - E.g., TR30/M Ø12.7 mm Optical Post, SS, M4 Setscrew, M6 Tap, L = 30 mm

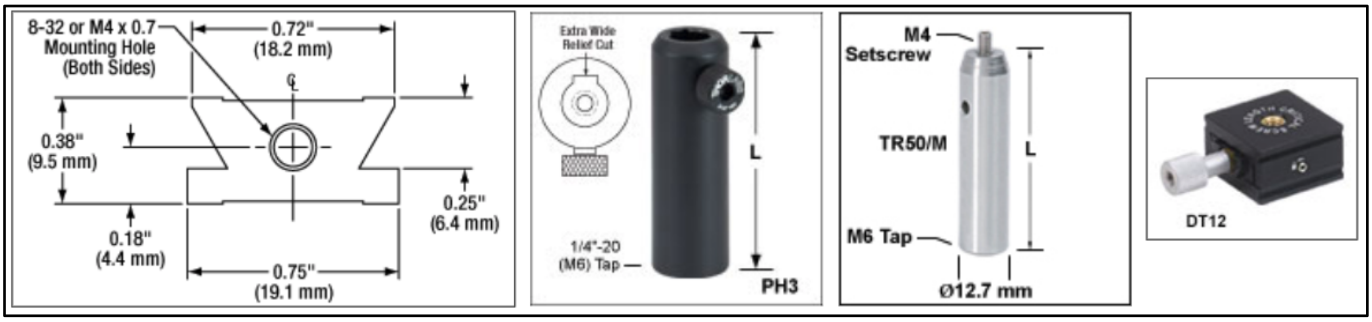

Figure 33: Standard components for post and component (lenses and mirrors) mount.

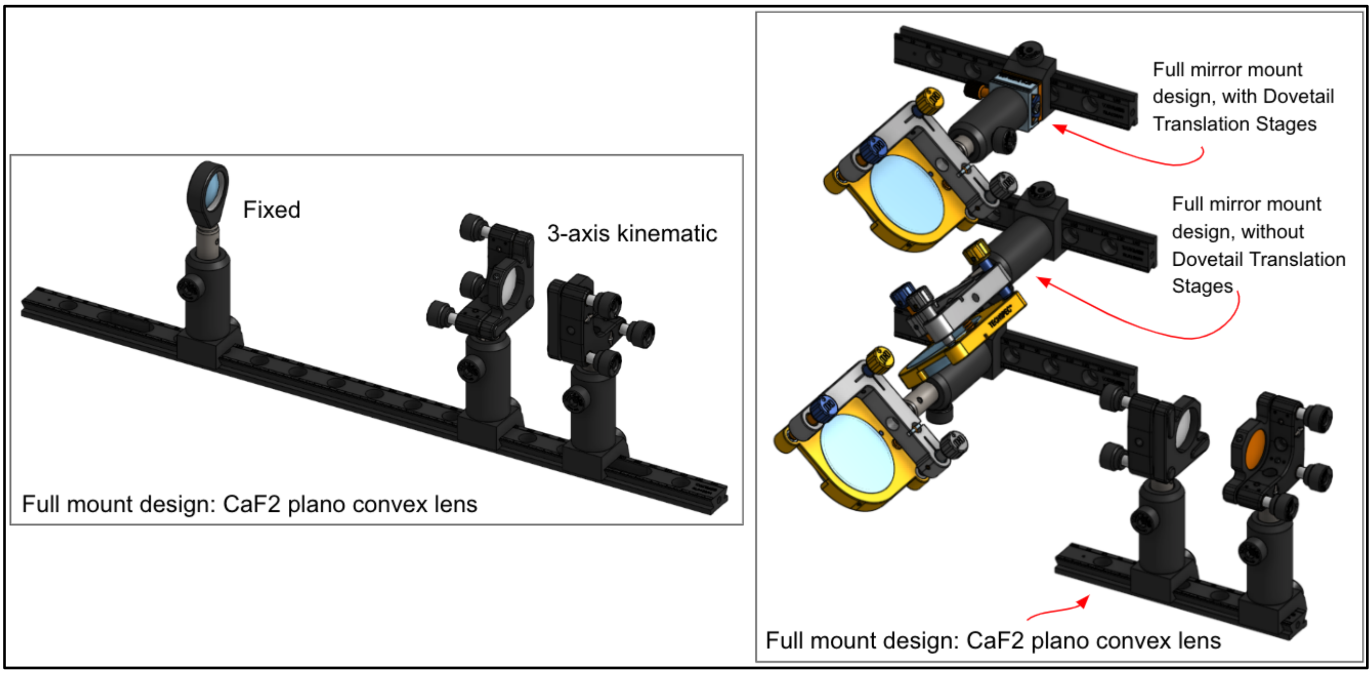

Figure 34: A dovetail rail carrier provides translation for the mounts.

<u>EQ-77 / LDLS</u>

Light source:

- Lamp housing: 128mm x 175 mm x 102 mm 2.2 kg
- Laser Drive Module: 152 mm x 250 mm x 132 mm 2.9 kg
- Position of light beam: 199.7 mm above top window of chamber
- Wavelength range: 200 - 2500 nm

<u>EQ-77 / LDLS</u>

Light source: combined with power supply

- Lamp housing: 115mm (W) x 273mm (L) x 318mm (H) 5.45 kg
- Position of light beam: 114.7 mm above top window of chamber
- Wavelength range: 200 - 1000 nm

For these two other light sources, designs for the mirrors, lenses, mounts, posts etc., are as mentioned above.

We are now finally in a position to integrate the optics (generation of beam only) and the chamber together.

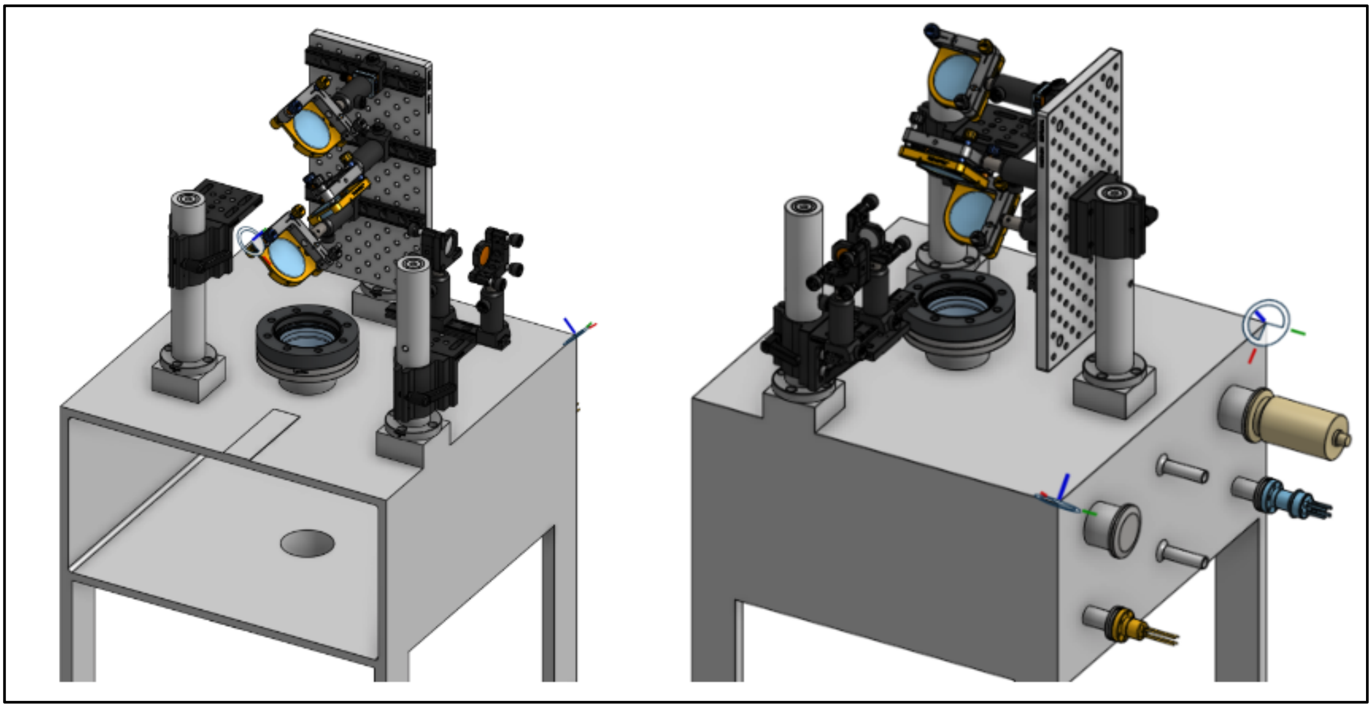

Figure 35: (left) The dovetail rail carriers and their corresponding mounts for the mirrors are attached to a vertical breadboard fixed to the top surface of the chamber. Several posts are erected to facilitate the mounting of a number of focusing lenses. (right) A different angle reveals the process connections (fluidics and electrical interfaces) attached to the back of the chamber.

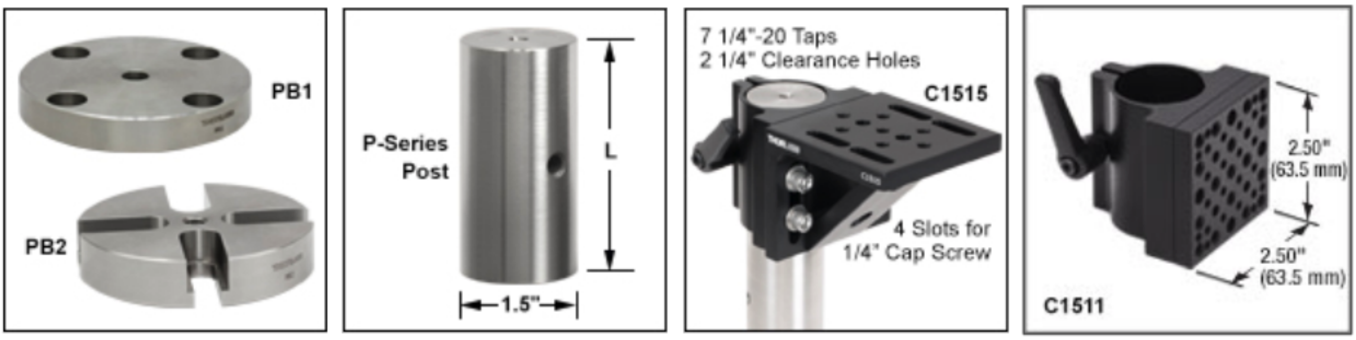

Figure 36: Standard components for mounting the posts.

A list of components used for mounting the posts and vertical breadboard:

- Ø1.5" Post Bases [27]
  - PB1 Mounting Post Base, Ø2.48" x 0.40" Thick
- Ø1.5" Posts [28]
  - P350/M Ø1.5" Mounting Post, M6 Taps, L = 350 mm
  - Twice stackable, up to 700 mm in our setup
- Ø1.5" Mounting Post Bracket [29]
  - C1515/M Ø1.5" Mounting Post Bracket, M6 Taps
- Ø1.5" Post Mounting Clamp [30]
  - C1511/M Ø1.5" Post Mounting Clamp, 63.5 mm x 63.5 mm, Metric
- Aluminum Breadboards, Double-Density Holes, Metric [31]
  - MB1530/M 150 mm x 300 mm x 12.7 mm Aluminum Breadboard, M6 Double-Density Taps

One key component we have yet to discuss thus far is the optical table. We have acquired the ThorLabs T1020Q (with sealed mounting holes) [32]. Key specifications are as follows:

- 1 m x 2 m x 310 mm (full height 91 cm), max. load 2500 kg
- M6 tapped holes 25 mm apart
- Thorlabs quote: “In general, the sealed holes are watertight, but we cannot guarantee they are airtight. I apologise for the inconvenience.” Solution: Keep differential pressure (within enclosure and atmospheric pressure) to be equal.

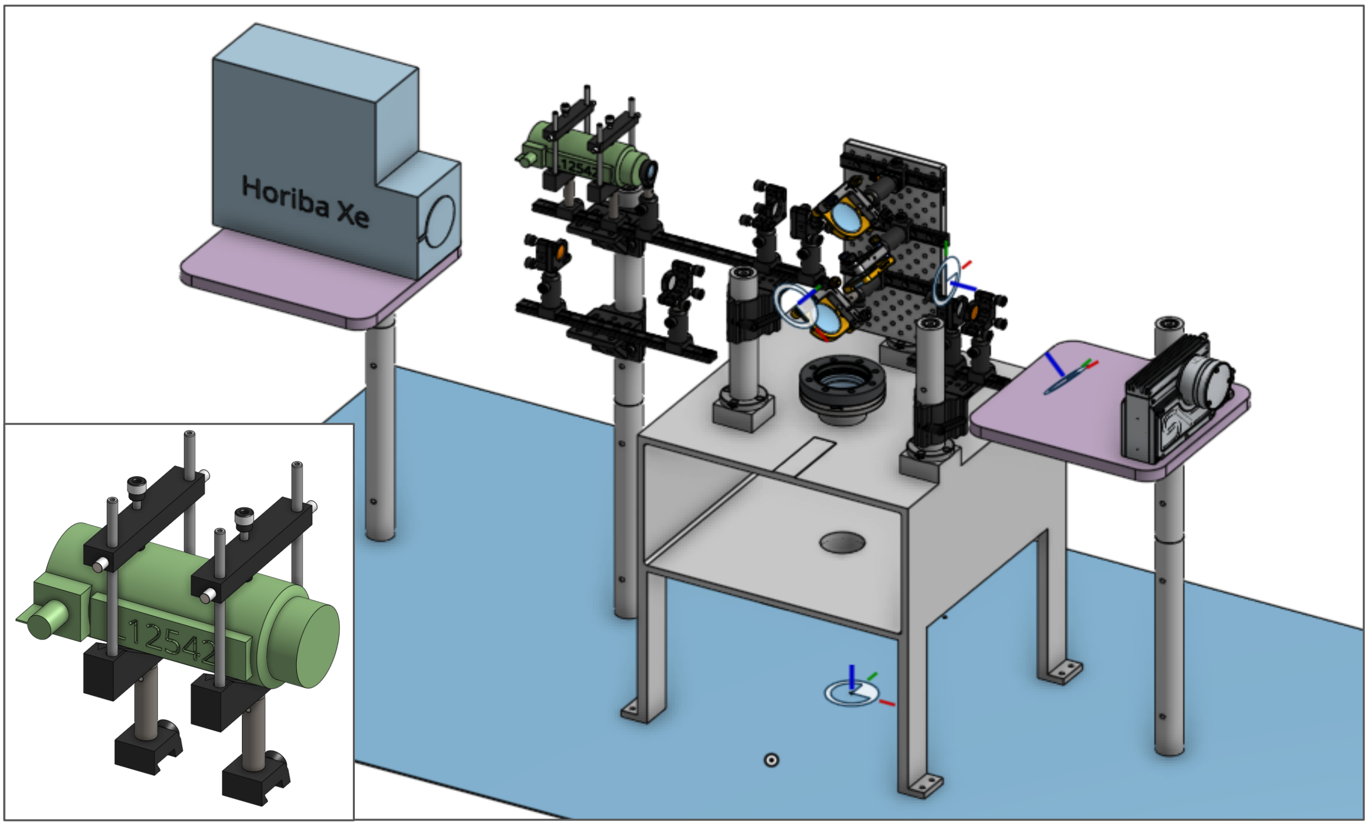

Figure 37: Integrated optics (incident beams) and chamber, together with the optical table.

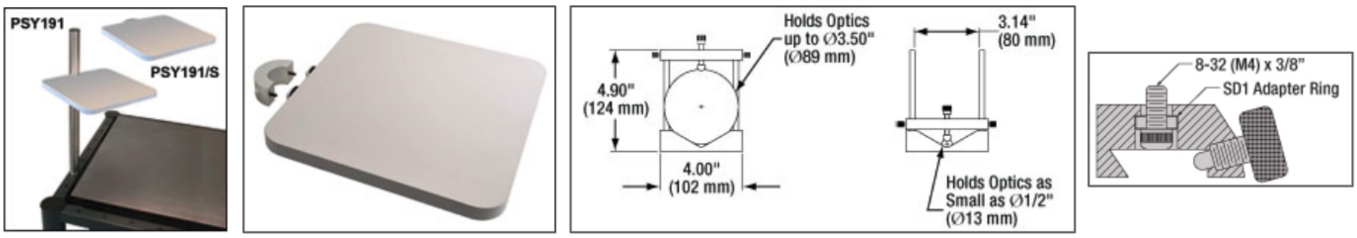

Figure 38: Standard components used for mounting the light sources.

Key components used for mounting the light sources:

- ScienceDesk Instrument Shelves [33]
    - PSY191 300 mm x 278 mm Instrument Shelf with 750 mm High Post
- Same concept for the post (2 x 350 mm tall)

To mount the 60 mm diameter L12542 / Deuterium lamp head, we use:

- Adjustable-Height V-Clamp for Optics [34]
    - VG100/M Adjustable-Height Optics Clamp, Metric

- Standard combination of post + Dovetail Rail Carriers:
    - Dovetail Rail Carrier, 1/4" (M6) Counterbore [35]
        - RC1 Dovetail Rail Carrier, 1.00" x 1.00" (25.4 mm x 25.4 mm), 1/4" (M6) Counterbore

Integrated systems drawing (CAD models) can be filed in the OnShape folder. The key files are:

(1) StarLabChamberMaster > ASS-Full.assembly

This file contains a number of sub-assemblies that are then combined to form the full assembly, which is the latest design we have for StarLab V2.

(2) StarLabOptics > DWG-LightPaths-All.part

This file contains a number of ray diagrams portraying how we envision the optical components we proposed earlier would manipulate the light beams from source to the target sample. The latest iteration is shown in “FiniteBeam v5”.

Manipulating Transmitted Beam

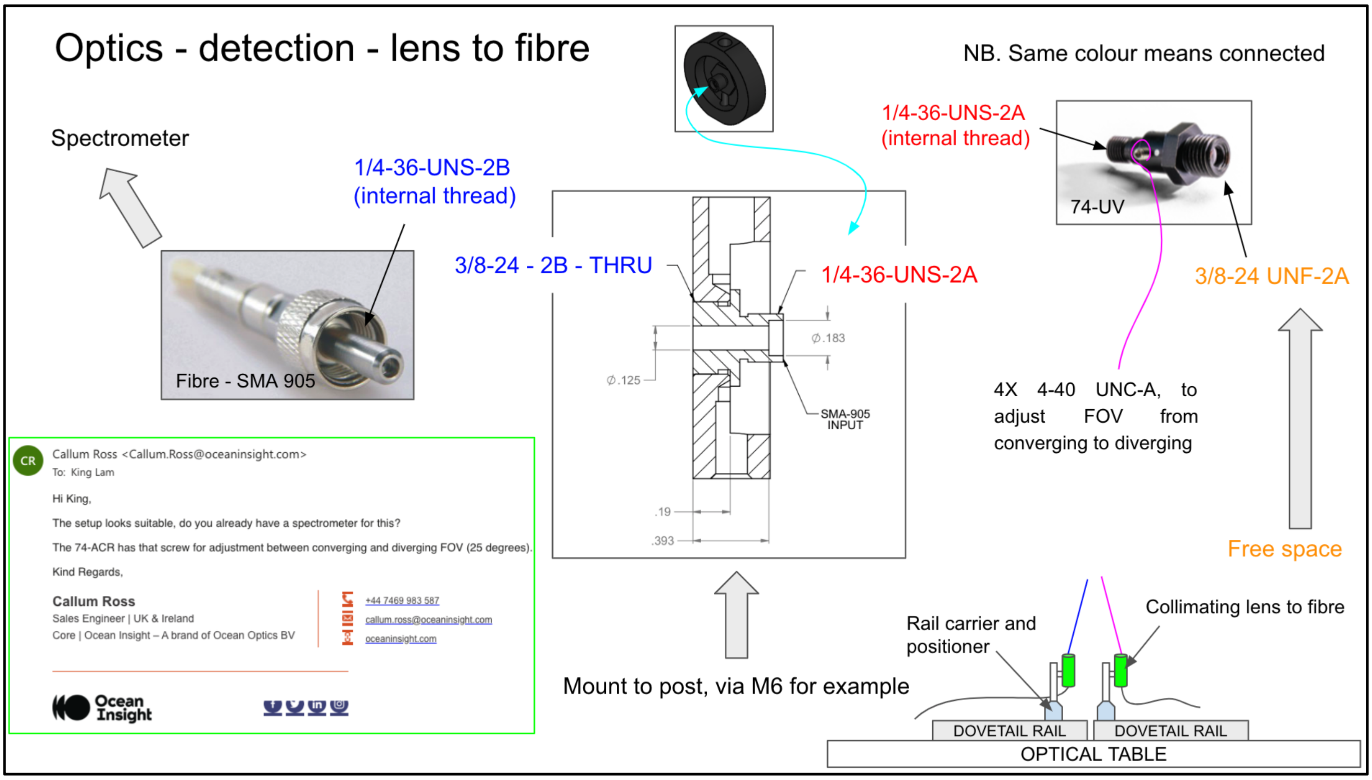

Figure 39: Transmitted light from the sample passes through the bottom window (Free space), before being collected by a collimating lens to fibre (Ocean Insight’s 74-UV). Same colour indicates those parts are directly connected to each other.

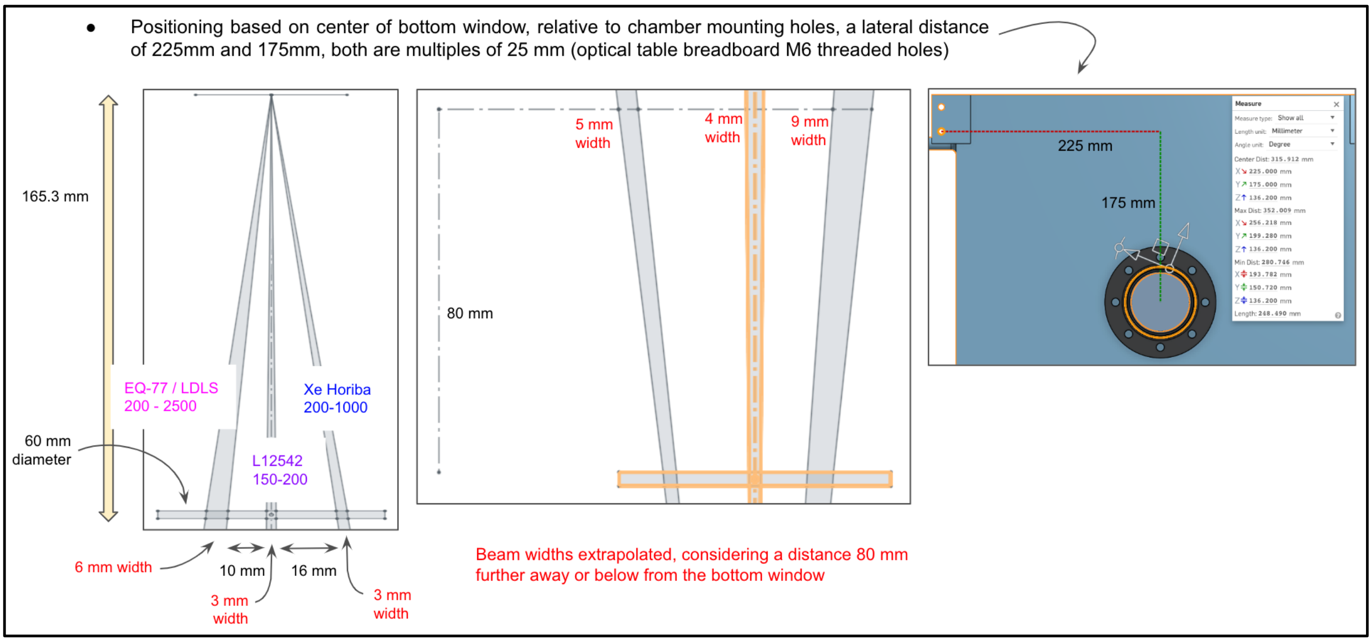

Figure 40: To design the positioning of the collimating lens to fibre, a separate ray diagram was constructed to consider transmitted beam propagation. We do not consider dispersion and refraction induced by the sample. At this point, we are concerned with spatial limitations imposed by the size of the receiving lens and mounts.

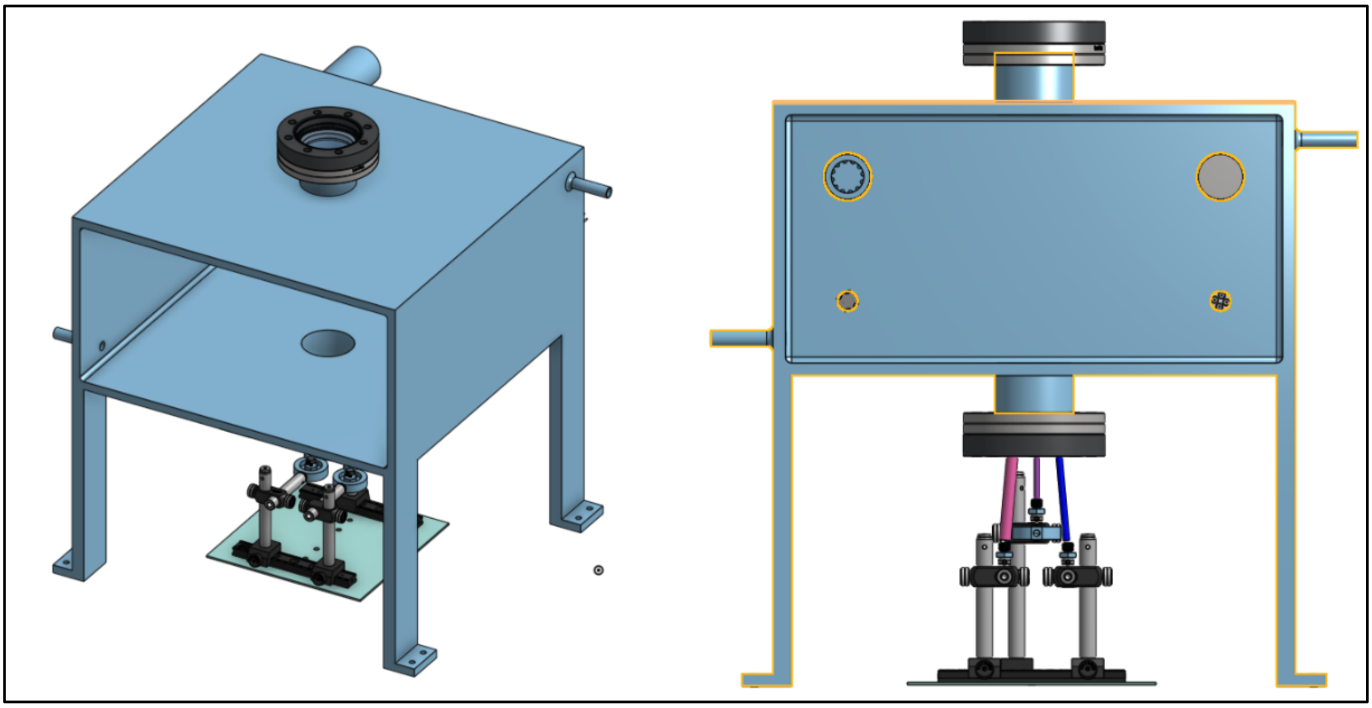

Figure 41: Optomechanics with chamber - detection of transmitted beam.

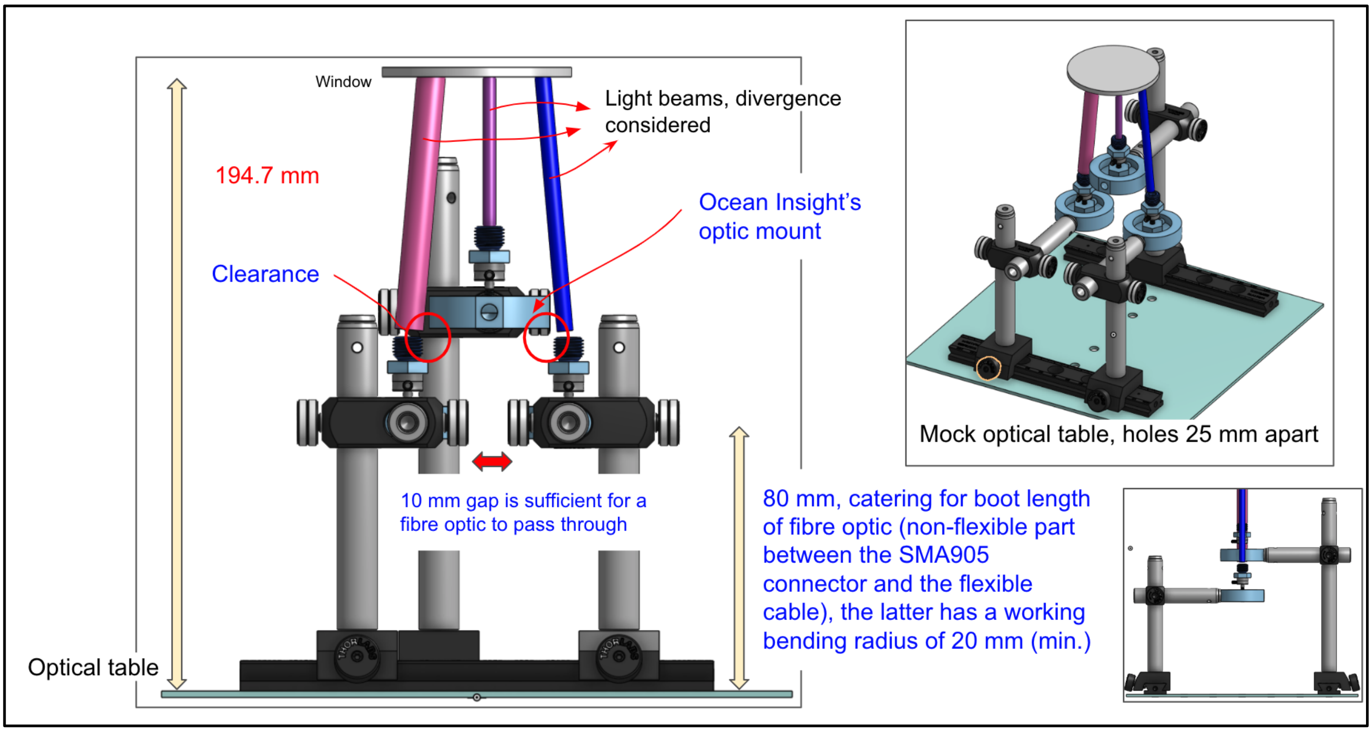

Figure 42: Two parallel dovetails will be directly mounted to the optical table. Our design allows the simultaneous monitoring of all three transmitted beams with sufficient spatial clearance. Such a requirement is unlikely to be necessary in practice, but the option exists.

We list the components required in Figure 42:

- Optical:
  - Ocean Insight - collimating lens [36]
    - 74-UV Collimating Lens
  - Ocean Insight - lens to fibre connector / fibre [37]
    - OPM-SMA Optical Mount
  - Ocean Insight - fibre [38]
    - e.g., QP115-025-XSR
    - Extreme solarization resistance UV fibre

- Mechanical: from ThorLabs
  - Optical table as the base support
  - Dovetail Optical Rails, L = 150 mm long, M6 tapped
    - RLA150/M
  - Dovetail Rail Carriers, M6 counterbore
    - RC1
  - Ø12.7 mm Stainless Steel Optical Posts - Metric, L = 100 mm / 150 mm
    - TR100/M / TR150/M
  - Right-Angle Clamp for Ø1/2" Posts, 5 mm Hex
    - RA90/M
  - Ø12.7 mm Stainless Steel Optical Posts - Metric, L = 75 mm
    - TR075/M
  - Adapter with External M6 x 1.0 Threads and External M4 x 0.7 Threads
    - AP6M4M

Ozone Generation

At this point, the design would have been mostly completed, if not for concerns of excessive ozone generation due to the interaction of UV light with the ambient O_2 in free space. The key pointers are:

(1) Oxygen generation by radiation strongly depends on lamp spectrum and power, with efficacy peaking at 160 nm.
(2) FDA limit at 50 ppb for extended exposure; natural half-life of ozone is 1-3 days
(3) Simple calculation of O3 conc. in air, e.g., 1 mg O3 / hour in a room size of 85 m3 (20 × 15 × 10 ft): Conc. = 5 ppb after one hour (10% of FDA limit, which will be exceeded in 10 hours, or overnight exp.)
(4) For reference, the 172 nm Xenon Excimer lamp is reported to generate ca. 100 mg Wh−1, easily exceeding the FDA limit by several orders of magnitude within hours, let alone with several lamps, a real hazard indeed.

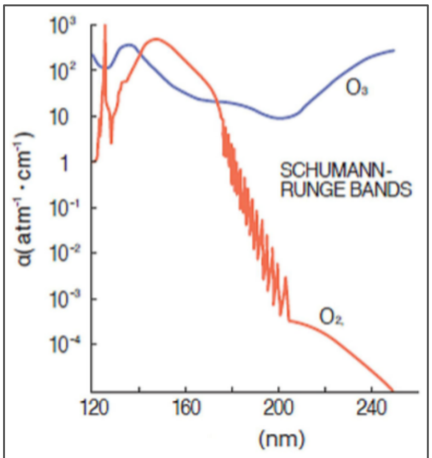

Figure 1. Wavelength dependency of oxygen absorption (6)

Reference: Claus, H. (2021). Ozone Generation by Ultraviolet Lamps†. Photochemistry and Photobiology, 97(3), 471–476. https://doi.org/10.1111/php.13391

We propose two possible solutions to this problem. In the first instance, we can design an enclosure to enclose the entire experimental setup, which is then purged with inert gas. The other option, to which a design has not yet been put forth, involves fabricating (using 3D printing for example) specially designed lens tubes that can be fitted to the path of the light beam from the D2 L12542 lamp to the top window. The former option is clearly more complex, and the remainder of the document is dedicated to this cause. We then discuss the advantages and disadvantages associated with either option.

The enclosure approach (cf. Figure 1 and Figure 42) involves constructing an acrylic or plexiglass enclosure that encapsulates the entire experimental apparatus, thereby creating a glovebox of sorts. The standard seal, which will serve as the interface between the enclosure and the optical box, as well as the chamber, will involve EPDM solid rubber cords [39], which has a 5.33mm diameter cross-section. This bears much resemblance to the AS568A-300 series, for which a standard seal based on the static O-ring groove design is designed [40].

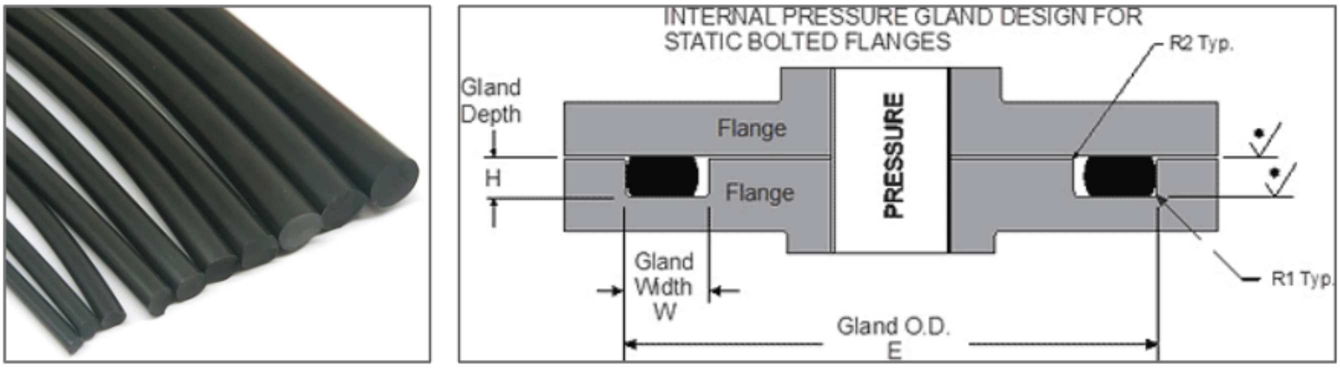

Face Seal O-Ring Gland Width and Depth Default Recomendations

AS 568A SERIES	O-RING- CROSS SECTION		GLAND WIDTH (W)		GLAND DEPTH (H)		GLAND CORNER RADII	
	NOM	TOL +/-	NOM	TOL+/-	NOM	TOL+/-	(R1)	(R2)
000	0.070	0.003	0.084	0.002	0.052	0.002	0.010	0.005
-100	0.103	0.003	0.121	0.003	0.078	0.003	0.010	0.005
-200	0.139	0.004	0.160	0.003	0.106	0.003	0.018	0.005
-300	0.210	0.005	0.240	0.003	0.164	0.004	0.028	0.005
-400	0.275	0.006	0.310	0.003	0.215	0.004	0.028	0.005

Figure 43: Our enclosure will not be circular, as in the case in O-ring applications, but for reference, the gland width we employ is ca. 20% larger than the O-ring (cross-section) diameter, and the gland depth (H) is ca. 30% smaller than the O-ring (cross-section) diameter. Therefore, we can base our design off the AS568A-300 series.

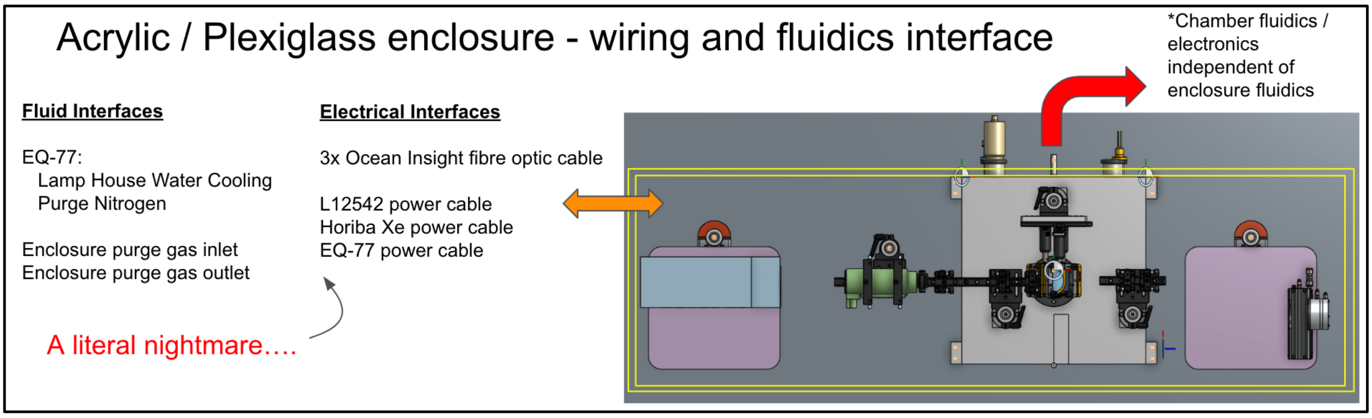

Figure 44: The next challenge is to account for a number of fluidics and electrical interfaces connected to the chamber and the light sources. For connections to the chamber, our solution is to mate the back panel of the enclosure directly to the back of the chamber (see Figure 45). For the remaining cables, we plan to drill small holes into the enclosure to allow the passage of tubes, wirings, and the occasional contraception to activate the light sources. These tiny orifices can be sealed with Blu Tack®, for which we have calculated that 0.5 grams of Blu Tack® will hold an approximate 105 g load, sufficient to withstand a differential pressure of 0.1 bar absolute for a 20 mm diameter hole. In any case, we can also afford small N_2 leaks into the atmosphere by maintaining positive pressure. This point will be brought back into focus when we consider the other solution

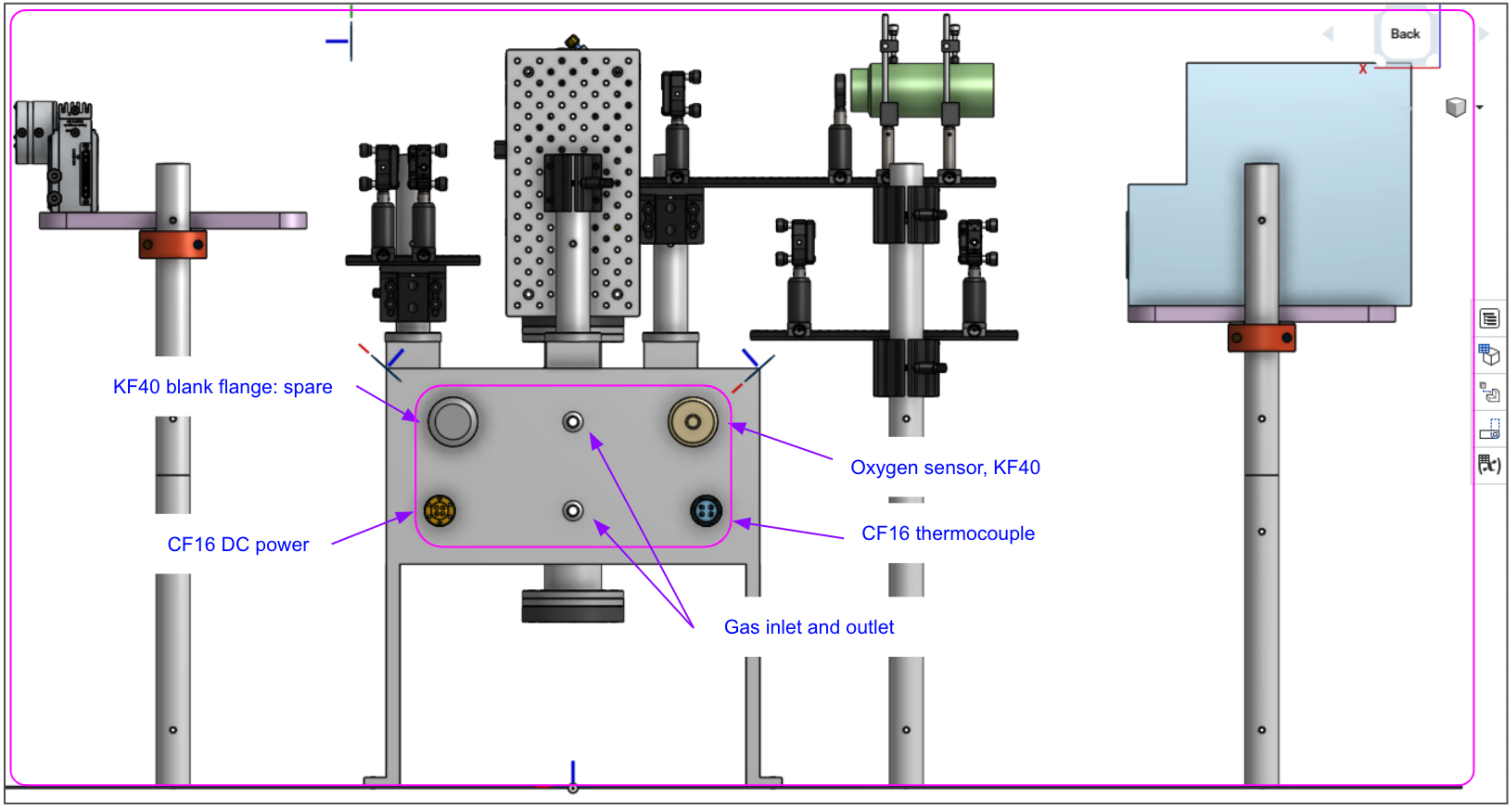

Figure 45: Modifications to the chamber were made to place all connections at the back. The flat surface of the back of the chamber can be mated to a vertical sheet of acrylic. The acrylic sheet is between the 2 pink rectangles in this diagram.

Acrylic / Plexiglass enclosure - electrical interface - some tricks

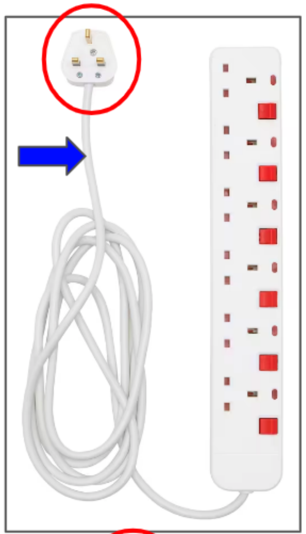

- All lamp houses and corresponding power supply / control units will be located in the enclosure as well
- An extension cable will be used to provide all power within the enclosure; we can separate the wiring by unscrewing the “head” (red circle) open, if not, we will cut the the cord (blue arrow) and solder the three wires. This allows us to drastically reduce the **number and size** of orifices needed to supply power to the lamps, to just **one orifice at <= 10 mm** (recall our blue tac guesstimation…)

Electrical Interfaces		Electrical Interfaces	
3x Ocean Insight fibre optic cable	→	3x Ocean Insight fibre optic cable	3 x 10 mm circular orifices
L12542 power cable Horiba Xe power cable EQ-77 power cable		1 x power cable	1 x 10 mm circular orifice
		3x switches for the lamp controllers	3 x 10 mm circular orifices

<u>What about ignition switches?</u>

- Lamp controllers usually have the option of electrical interfacing, e.g., using RS232 serial communication, so we could in principle control it using a computer connected via (again) some electrical wiring
- However, looking at where the switches are on the lamp controller, I propose a vastly simpler solution of positioning the lamp controllers near the side of the enclosure, and using a small circular cutout large enough for your index finger or Allen key to fit through and hit the switch.
- You can even duct tape a (very) small plastic bag to serve as an improvised “glovebox glove”.
- In any case, we can once again reduce to an **orifice at <= 10 mm** diameter.

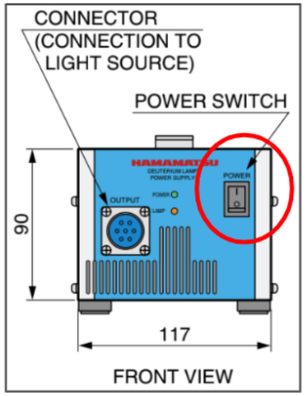

Figure 46: We document a number of tricks to resolve the electrical interface problem (part 1).

Acrylic / Plexiglass enclosure - fluidics interface - more tricks

- Since we have our extension cable providing power, we could in principle have our water tank and water pump inside the enclosure for cooling the EQ-77 lamp housing, allowing all the fluidics and fittings to be housed within the enclosure.
- QN: If the EQ-77 is housed in a nitrogen dominant atmosphere, could we do away with pressurized nitrogen purging?

"Regarding the purging with pressurized nitrogen, it is still recommended to do it for the first time before deploying it into the glovebox, but if not, it should be still fine as the glovebox will be with 1 atm pressure nitrogen eventually."

Verdict: In any case, we shall provide two ports (see below, right most in purple) in case we want to route some piping through.

Fluid Interfaces

EQ-77:
Lamp House Water Cooling
Purge Nitrogen

Enclosure purge gas inlet
Enclosure purge gas outlet

Fluid Interfaces

EQ-77:
~~Lamp House Water Cooling~~
~~Purge Nitrogen~~

Enclosure purge gas inlet
Enclosure purge gas outlet

Provisions for fluid interfaces

2 x 1/2 in. Female ISO Parallel Thread

2 x 1/2 in. Female ISO Parallel Thread

Stainless Steel Swagelok Tube Fitting, Male Connector, 1/2 in. Tube OD x 1/2 in. Male ISO Parallel Thread
Part #: SS-810-1-8RP

½" tube

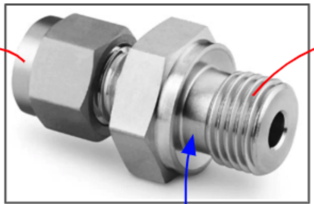

Into the acrylic block
Why parallel thread?
- The thread does not bear the brunt of the pressure, which is the job of the O-ring (blue arrow). The thread just guides and positions the fitting.

Stainless Steel Pipe Fitting, Pipe Plug, 1/2 in. Male ISO Parallel Thread, Straight Shoulder
Part #: SS-8-P-RS

When not in use, use a plug to provide a proper seal, an alternative to duct tape / blue tac.

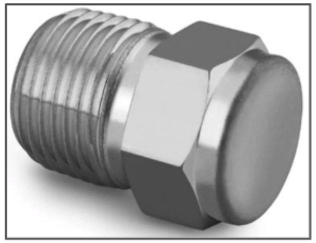

Figure 47: We document a number of tricks to resolve the electrical interface problem (part 2).

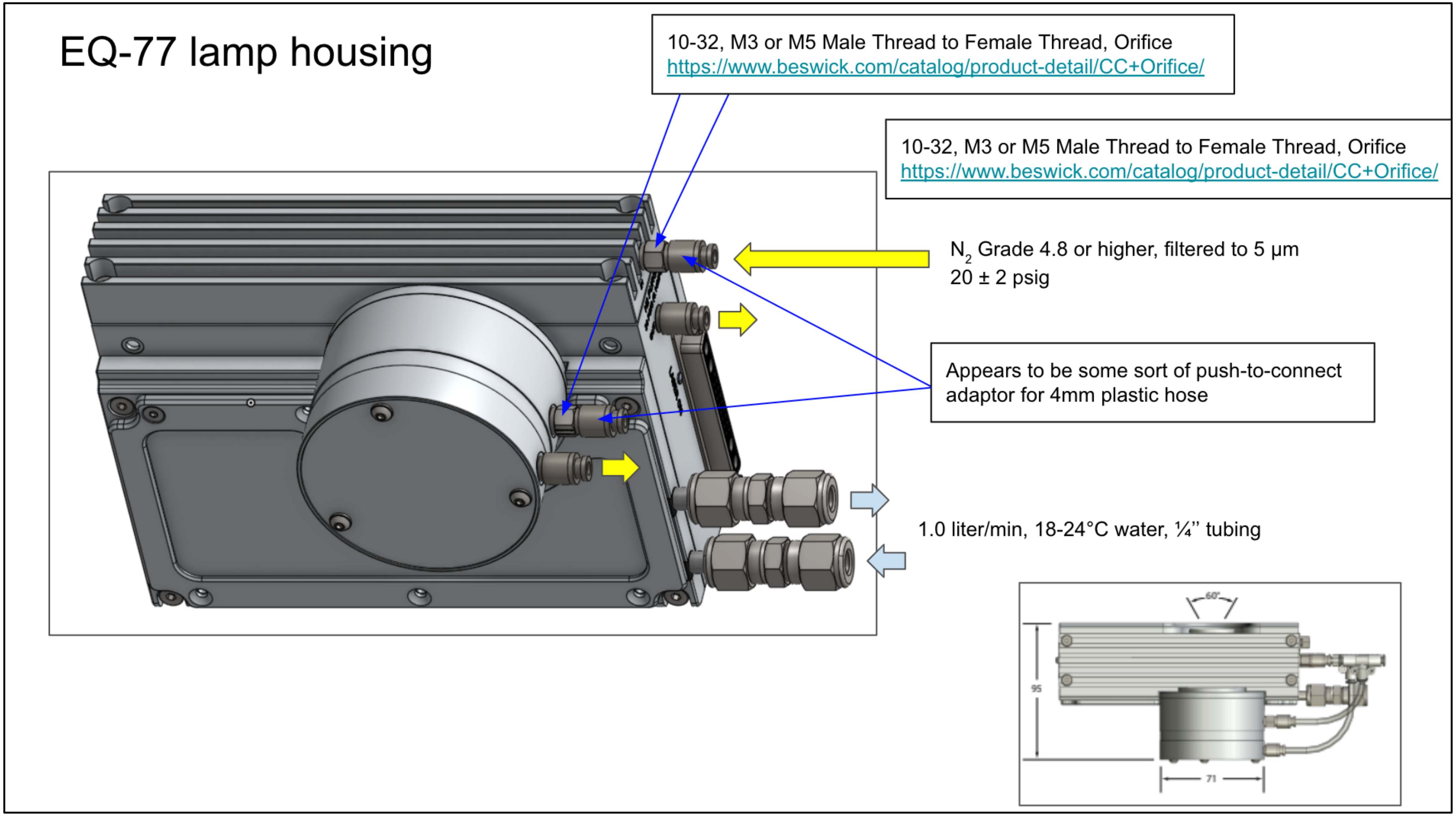

Figure 48: Details concerning the EQ-77, which requires active nitrogen purging. Of course, if the lamp is already housed in an inert atmosphere, there is no need for additional purging.

Miscellaneous pointers

- Recommend the use of tube inserts to prevent plastic tubing from collapsing when used in conjunction with metallic compression fittings

- The securing of the acrylic enclosure to the optical table, chamber back surface and the top piece of the enclosure will be achieved using **through holes**, **fasteners (nut and bolt)** as well as **plastic washers**.

Specifications	Features
Product Code:	760LISS1/2X3/8
Body Material:	Stainless Steel 316
OD Size:	1/2″
ID Size:	3/8″

Tube Insert

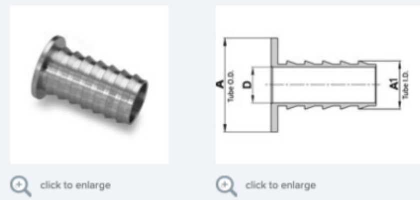

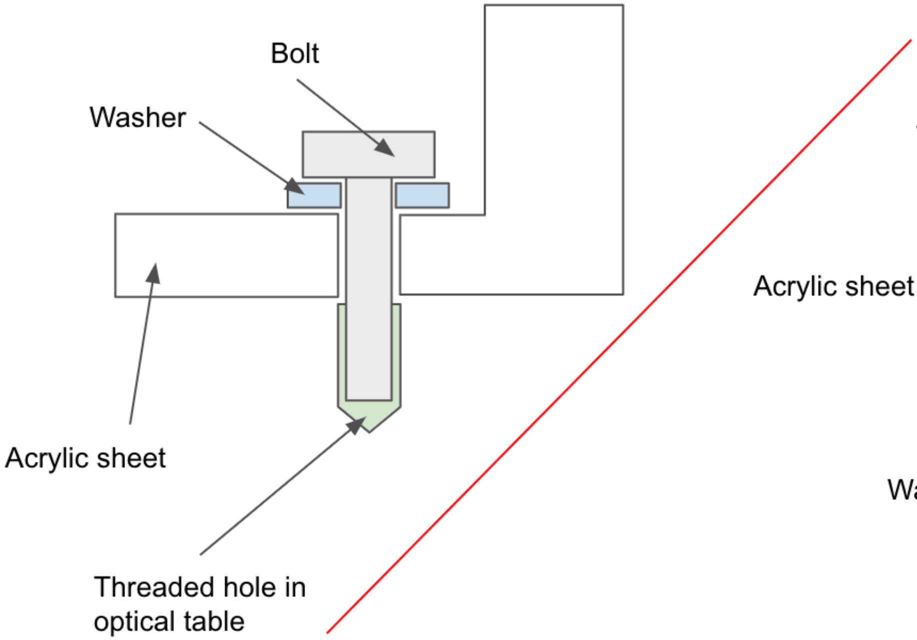

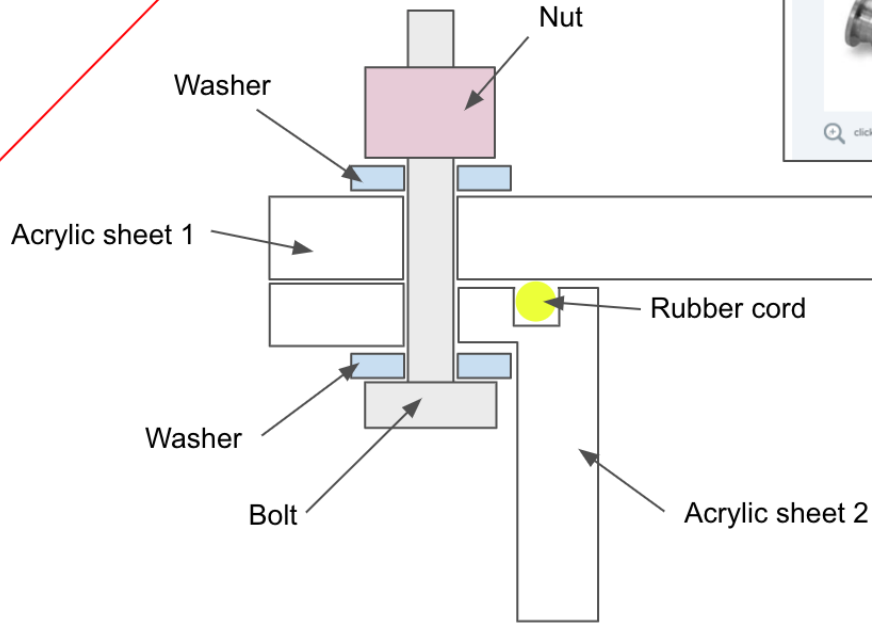

Figure 49: A small note on how we envision the acrylic enclosure to be fastened together and with the optical table. We are particularly wary about the metallic fasteners damaging the plastic sheets, so we introduce washers.

Acrylic / Plexiglass enclosure - general design

With a useable internal volume of approx. 1.6 m (L) x 0.5 m (W) x 0.9 m (H), and 5 mm thickness (with structural reinforcements in the form of ribs etc.), the full structure will weight 40 kg, ca. 20 + 20 kg

XE25C11/M <- all needs to be contained in that volume.

Crucially, considering how one side of the enclosure will be attached to the back of the chamber, with a cutout for the electrical and fluidic interface (for the chamber), it will not be possible to remove the enclosure without having to disconnect those connections, thereby interrupting the experiment.

We want to have the option to remove the enclosure (or at least part of it) without having to open and vent the chamber.

The solution is to split the enclosure halfway along the vertical into two parts (right diagram):

- Typical human has height ~1.7 m, ape index ~1, shoulder width ~0.4 m → length of one arm ~65 cm
- The bottom chunk will be fixed to the optical table, with all the ports and holes etc. for the interfacing
- The top chunk will be mated to the bottom chunk using the same method of O-ring and fasteners.

To remove the top chunk with sufficient clearance over the optics, require **< 1.4 m** clearance **above** the optical table (itself **0.91 m**).

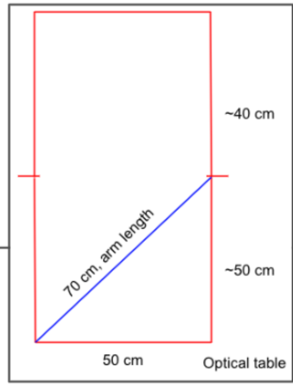

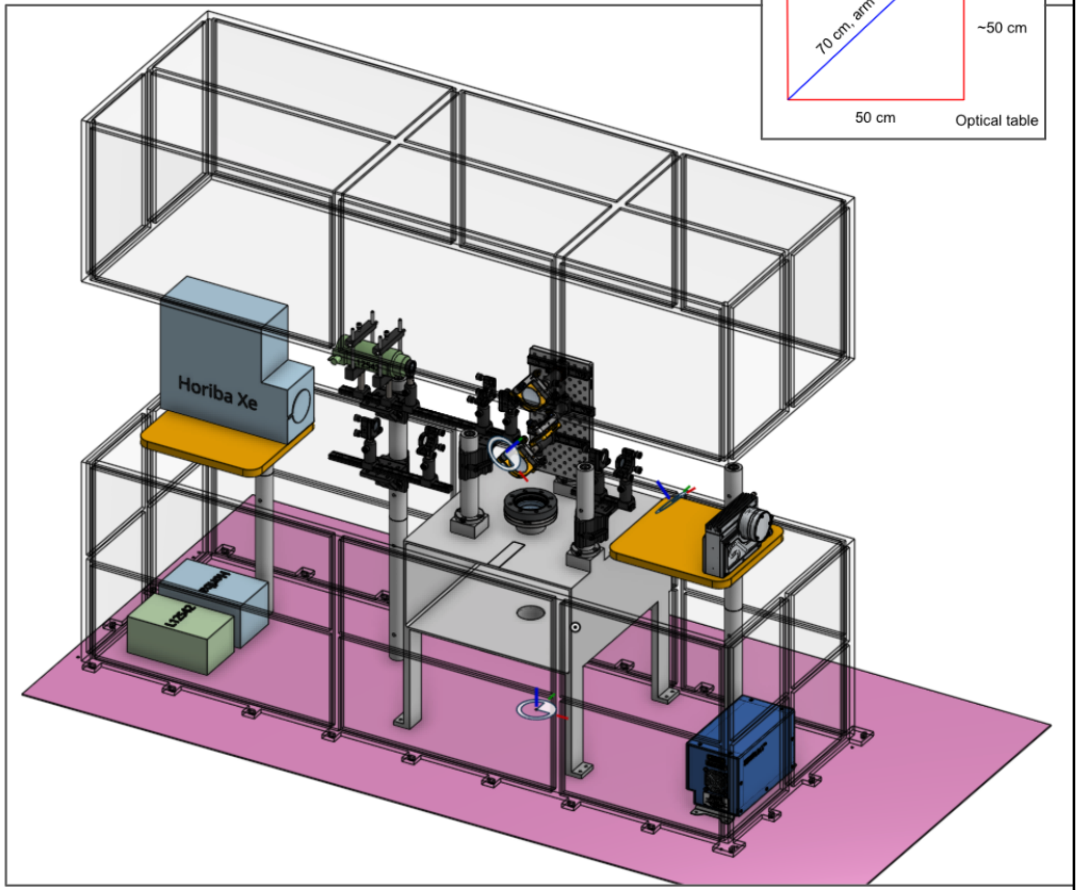

Figure 50: At some point, we consider splitting the acrylic enclosure, which will be of no trivial weight, into two parts. The lower segment will be secured to the optical table most of the time, while the upper portion will only be introduced after successfully setting up the experimental apparatus and beam alignment. We perform simple calculations to ensure a person can reach all parts of the set up.

Acrylic / Plexiglass enclosure - comments and considerations

In some ways, a rudimentary (albeit cheaper) “glove box”

Acrylic over polycarbonate: cost and UV resistance

Might want to consider installing a ceiling crane to help with lifting the chamber (ca. 50 kg), and greatly aid with the removal of the top chunk of the enclosure… just a thought

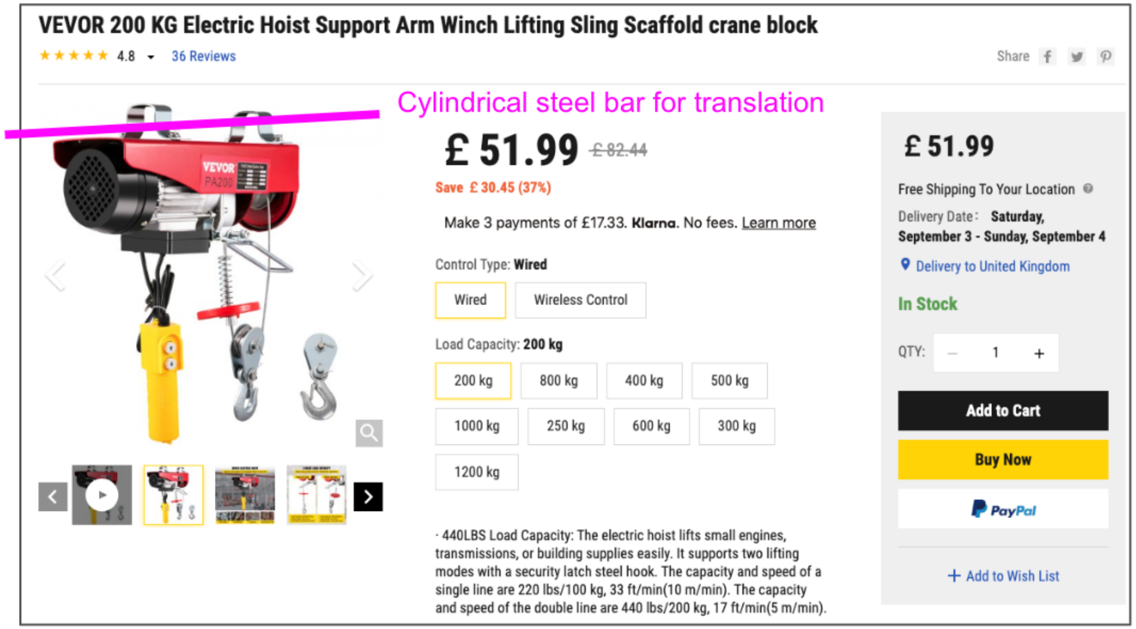

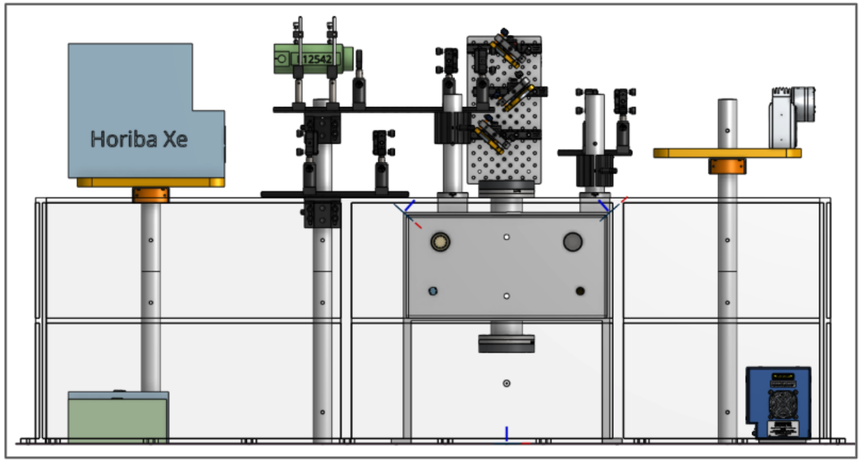

What about the option of opening the chamber door without having to remove the lower chunk of the enclosure…?

We can talk about this in person in the lab…

Figure 51: The fancy option of using a mechanised motor to assist the manoeuvring of the acrylic enclosure exists.

Comments

At this point, the reader would agree that the first option is particularly complex and costly. This is expected since we were essentially designing a glove box, which would be particularly useful if we needed to create an isolated secondary atmosphere surrounding the chamber during experimental runs.

The second option requires active inert gas purging, meaning nitrogen gas will constantly be released into the atmosphere. Concerns over ventilation problems in the lab (a relatively small room) prompted us to look into the first option.

However, our latest understanding is that StarLab V2 will be hosted in a lab with sufficient ventilation. Our calculations show that the rate of nitrogen outgassing (from purging the EQ-77 and estimations for the lens tubes) should be well below the limitations imposed by the lab ventilation capabilities. As such, we suggest revisiting option 2 and developing the concept into a functioning design.

Most likely, the design will employ two separate contraptions. The first will be a box-like acrylic enclosure with cutouts to accommodate the dovetail rails, which will be placed on top of the chamber to enclose the vertical breadboard and associated optical components. The second will be a tube placed between the first and second lenses associated with the light beam.

Unavoidably, both structures will have open geometries to accommodate various optical components in the way, and will have provisions to connect fittings for the nitrogen purge line. As mentioned, the nitrogen gas will be vented into the atmosphere.

Undoubtedly, this option will be cheaper than the full enclosure solution, and we can forget the nightmares associated with the interfacing of the electrical and fluidics subsystems with the chamber and light sources. Nevertheless, additional cost will be incurred in the significantly higher amounts of purging gas, and the need for several oxygen and ozone monitors in the lab for safety purposes.

We are inclined to proceed with the development of the second option.

Conclusion

In short, we have developed a full solution for an experimental stellar simulator to study prebiotic chemical reactions under various planetary atmospheres. We have also compiled a list of tasks that we recommend should be completed in good time:

(1) Concerning simulations performed on the manipulation of the light beams, we recommend the use of more sophisticated software like Zeemax Optics to verify our results. We emphasise the goal is not to reach an extremely high level of accuracy and fidelity, since additional unforeseen inaccuracies and errors are likely to occur in practice. Rather, we wish to place an upper bound on the size of the errors expected, and ensure our optical sub-system is well designed to handle these errors.

Our underlying concept has been to collimate all the beams before reflection by the prism / mirror and irradiation. We have assumed negligible Rayleigh or Tyndall scattering, i.e., sample is a solution rather than colloid. Moreover, any collimated beam, typically modelled as a Guassian beam, will still diverge. We suggest investigating the extent and effects of divergence.

Other particularly concerning considerations include chromatic aberration and refraction caused by curved the watch glass.

(2) We suggest rechecking the calculations made on the power of the light beams to better constrain the amount of sample heating, as well as for comparisons with the damage threshold imposed by the use of mirrors. Concurrently, the effects of dispersion and aberration (as in point 1) caused by the use of prisms rather than mirrors should be properly investigated.

(3) Perform design work on the second option proposed to mitigate effects of ozone generation.

(4) TECs have been proposed as a somewhat novel or unusual method to provide sample cooling. It also requires dedicated code development to actively monitor incoming data from the thermocouples, as well as controlling when to turn the TEC on or off via the RS485 protocol. We suggest testing this prior to its implementation in the chamber, which will also serve as an excellent opportunity to test the RS485 protocol.

(5) Calculations to do with ozone generation and release of nitrogen purge gas into the lab should have been already done. It will be good to have them handy, or get a cross-check to ensure they are correct.

References

1. Rimmer, P. B., Thompson, S. J., Xu, J., Russell, D. A., Green, N. J., Ritson, D. J., ... & Queloz, D. P. (2021). Timescales for prebiotic photochemistry under realistic surface ultraviolet conditions. Astrobiology, 21(9), 1099-1120.

2. https://github.com/KingLam26/StarLab

3. https://drive.google.com/drive/folders/1gmvrPs8zTq7zmStlXmTwW9f-aqXrO_0U

4. https://cad.onshape.com/documents?nodeId=628cd256867cab2c3432aea6&resourceType=resourceuserowner

5. https://www.onshape.com/en/education/#form-container

6. https://lairdthermal.com/products/thermoelectric-cooler-modules/peltier-annular-series/SH14-125-06-L1-W4.5

7. https://www.thorlabs.com/newgrouppage9.cfm?objectgroup_id=4982

8. https://www.mollier-diagram.com/

9. https://www.engineeringtoolbox.com/evaporation-water-surface-d_690.html

10. https://pyserial.readthedocs.io/en/latest/#

11. http://hamamatsu.com.cn/UserFiles/DownFile/Product/L11798_L11799_TLSZ1014E04.pdf

12. https://www.newport.com/n/deuterium-lamp-spectral-irradiance-data

13. https://www.energetiq.com/extreme-high-brightness-laser-driven-light-source-eq-77-ldls

14. https://www.horiba.com/int/products/detail/action/show/Product/powerarc-1601/

15. https://www.thorlabs.com/newgrouppage9.cfm?objectgroup_id=12393

16. https://www.edmundoptics.eu/p/50mm-diameter-vacuum-uv-enhanced-mirror/3368/

17. https://www.edmundoptics.co.uk/knowledge-center/application-notes/optics/metallic-mirror-coatings/

18. https://www.crystran.co.uk/optical-materials/calcium-fluoride-caf2

    Similar links for other materials, on the same website.

19. https://www.edmundoptics.eu/p/50mm-diameter-vacuum-uv-enhanced-mirror/3368/

20. https://www.edmundoptics.eu/p/50508mm-diameter-kinematic-mount-3-screws/15652/

21. https://www.edmundoptics.co.uk/knowledge-center/application-notes/optics/metallic-mirror-coatings/

22. https://cad.onshape.com/documents/5c26b577b30458294b471740/w/cbcf8d603b35ae2592f8994e/e/930943aede826a8dd0c88ae6, FiniteBeamv5.

23. https://www.thorlabs.com/newgrouppage9.cfm?objectgroup_ID=30

24. https://www.thorlabs.com/newgrouppage9.cfm?objectgroup_id=2952

25. https://www.thorlabs.com/newgrouppage9.cfm?objectgroup_id=1268

26. https://www.thorlabs.com/newgrouppage9.cfm?objectgroup_id=1266

27. https://www.thorlabs.com/newgrouppage9.cfm?objectgroup_id=1313

28. https://www.thorlabs.com/newgrouppage9.cfm?objectgroup_id=1313

29. https://www.thorlabs.com/newgrouppage9.cfm?objectgroup_id=1310

30. https://www.thorlabs.com/newgrouppage9.cfm?objectgroup_id=169

31. https://www.thorlabs.com/newgrouppage9.cfm?objectgroup_id=1861

32. https://www.thorlabs.com/thorproduct.cfm?partnumber=T1020Q

33. https://www.thorlabs.com/newgrouppage9.cfm?objectgroup_id=8425

34. https://www.thorlabs.com/newgrouppage9.cfm?objectgroup_id=1420

35. https://www.thorlabs.com/NewGroupPage9.cfm?ObjectGroup_ID=8295

36. https://www.oceaninsight.com/products/sampling-accessories/free-space-optics/collimating-lenses/74-uv/?qty=1

37. https://www.oceaninsight.com/products/sampling-accessories/free-space-optics/lens-holders--mounts/opm-sma/?qty=1

38. https://www.oceaninsight.com/products/fibers-and-probes/fibers/patch-cords/qp115-025-xsr/?qty=1

39. https://therubbercompany.com/extrusions-profiles/solid-sponge-rubber-cords/epdm-solid-rubber-cord

40. https://www.allorings.com/o-ring-groove-design-static-face-seal

Appendix

Proposed Experiment

Ferrocyanide is a powerful catalyst for a variety of prebiotic chemical reactions [1] and is itself a reactant in the production of nitroprusside, a precursor for prebiotic non-enzymatic activating agents [2]. Ferrocyanide has been proposed as a target molecule for the Perseverance Rover on Mars, to assess past habitability and potential for origins of life on the Martian surface [3]. However, given its strong UV absorbance [4] and instability at high temperature and low hydrogen cyanide concentrations [5], it is unclear whether the lifetime of ferrocyanide is compatible with the prebiotic scenarios that include it, let alone whether it can survive long enough to be detected by the Perseverance rover.

In simulating the light of the active young sun, StarLab will be used to irradiate aqueous chemical samples of ferrocyanide. A variety of geochemical conditions for the ferrocyanide will be approximated by varying temperature, pH, salinity, and with varying concentrations of phosphate, carbonate, sulphate and sulfite, nitrate and nitrite. The lifetime of the ferrocyanide will be measured using UV-Vis spectroscopy as a function of these conditions.

Ultimately, these lifetimes will provide insight into the prebiotic plausibility of ferrocyanide, within a geochemical context, as well as the potential for ferrocyanide to survive on ancient Mars.